# THE IMMUNOCYTOCHEMICAL AND ELECTROPHORETIC LOCALISATION OF AFLATOXIN $B_1$-BINDING PROTEINS IN ISOLATED LIVER MITOCHONDRIA

**BY**

**GARETH RAMAN**

*BSc., BSc. (Hons.), (UDW)*

**Submitted in partial fulfilment of the requirements**
**for the degree of M. Med. Sc.**
**in the**
**Department of Physiology, Faculty of Medicine**
**University of Natal, Durban**

**1998**

# ABSTRACT

**Mitochondria** perform functions which are central to the life of most eukaryotic cells. These organelles can be considered the ultimate energy power house of a living cell. The role of mitochondria in cancer phenotype remains a fertile area of research. Several carcinogens are known to enter the mitochondria, resulting in impaired functioning and altered structure. **Aflatoxin $B_1$** ($AFB_1$) a primary type I mycotoxin elaborated by *Aspergillus flavus* and *Aspergillus parasiticus*, is carcinogenic for a wide species range. The epoxide is capable of binding to nucleic acids and proteins, resulting in induced mutations, cellular toxicity, and eventually carcinogenesis.

Approximately 250 000 deaths occur annually in both China and Africa due to patients presenting with Hepatocellular Carcinoma (HCC). The causative agents being $AFB_1$-ingestion via contaminated foods and feeds, and the Hepatitis B Virus infection. The toxin has a multifaceted mode of attack, capable of being activated to a highly reactive and carcinogenic derivative, the $AFB_1$-8,9-epoxide, via the cytochrome $P_{450}$ enzyme system of the microsomes, endoplasmic reticulum and also the **mitochondria**. The epoxide is capable of binding to nucleic acids and proteins, resulting in the formation of covalent adducts. The repeated occurrence of gold labelled toxin within mitochondria from hepatomas of patients presenting with HCC suggested that these organelles were direct sites of toxin binding.

**Despite observations that mitochondria appear as direct and perhaps preferential targets for attack by $AFB_1$, the actual *in vivo* immunolocalisation and characterisation of bound $AFB_1$ within liver mitochondria has not been reported previously.**

**In addition the role of $AFB_1$-protein binding within mitochondria was investigated to determine the mode of action of the toxin, within the mitochondrial system.**

Liver sections from rats treated with a single lethal dose of $AFB_1$, showed distinct ultrastructural abnormalities viz. large nuclei, increased heterochromatin, and swollen mitochondria. Immunocytochemistry revealed for the first time, the selective localisation of conjugated gold labelled toxin within the mitochondria. Toxin was found in the intracristal and peripheral spaces and frequently within the mitochondrial matrix. The mitochondria isolated from treated rats revealed significant alterations and damage to the mitochondrial membranes. The cristae were also markedly swollen with the associated clearing of the mitochondrial matrix.

Western blot immunoassays revealed the presence of five $AFB_1$-bound proteins (150kDa, 50kDa, 25kDa, 18kDa, 14kDa) in the inner mitochondrial fraction of isolated mitochondria. High pressure liquid chromatography also revealed that a significant proportion (84%) of an initial dose of toxin, was absorbed by mitochondrial protein. This study is the first to show the presence of specific mitochondrial proteins involved in toxin binding. In addition, the presence of toxin within the mitochondria and the specific binding to inner mitochondrial proteins suggest that the toxin specifically targets the electron transport chain and hence effects ATP production.

**This study conclusively indicates that mitochondria are direct targets for attack by $AFB_1$ during experimental carcinogenesis. Mitochondria therefore play an important role in $AFB_1$-mediated carcinogenesis.**

# DEDICATION

## To my Lord and Saviour Jesus Christ

Knowledge comes from learning, but wisdom comes from you
You are the ultimate Healer, my Refuge and my Strength.

# PREFACE

This study represents the original work by the author and has not been submitted in any form to another University. The use of work by others has been duly acknowledged in the text.

The research described in this study was carried out in the Department of Physiology, Faculty of Medicine, University of Natal, Durban, under the supervision of Mr A.A. Chuturgoon and Professor M.F. Dutton.

**G.P. RAMAN**

# ACKNOWLEDGEMENTS

I would like to thank :

- **My Parents**, for providing me with the tools of perseverance, sacrifice, and understanding. For all you have done for me, during this year, and throughout time and for your love, I am eternally grateful.
- **Gresham and Petronella Raman,** you mean the world to me and I always appreciate and love you. Thank you for always being there.
- **The Mellon Foundation**, for providing me with a subsistence bursary, you have indeed made this thesis possible.
- **Prof. M.F. Dutton** for the FRD Grant Holders' Masters Bursary, and for his support as co-supervisor of this study.
- **Mr Anil Chuturgoon**, who has furthered an independence in myself. I am always grateful for your immense understanding and support during this study. For allowing me to go beyond, giving me the freedom of time, and for your excellent research ideas and motivations that have in effect allowed this study to occur.
- **Dr D. York and Ms N. Padayachi,** you have indeed been instrumental in this thesis reaching its finality. For your unparalleled expertise in gel electrophoresis and western blotting, and for your patience and support, I will always be grateful. I wish to also thank the entire Department of Molecular Virology, for you have been hospitable and patient with my presence in your laboratories.
- **Ms D Pillay**, for being my friend and for all your help. **Ms S Moodley** for her constant help in the laboratory.
- **Mr M Wagner** for his expertise in High Pressure Liquid Chromatography, and for giving me the unconditional use of his office and computer. You were indeed a friend.
- **The Electron Microscope Unit (UND)** and **Ms S Bux** for help with microscopy.
- **Ms Nikki Coumi**, you have truly kept me going, through all the difficult times I have encountered. I am always thankful for your friendship and help.
- **Mrs Marie Hurley** you are a pillar, strengthened on the word. I am always grateful for your constant help, prayers and support.
- **Pastor Clive Gopaul - Asherville Christian Church and School of Prayer,** for all your support and prayers...always.

# PAPERS AND PRESENTATIONS

## INTERNATIONAL PAPER

**Raman GP**, Chuturgoon AA, Dutton MF. Mitochondrial proteins sensitive to Aflatoxin $B_1$. Mycotox '98-**Toulouse, France. Revede Medicine Veterinaire**, 1998: 122

## NATIONAL PAPER

**G.P. Raman**, M.F. Dutton, S. Bux, A.A. Chuturgoon. Aflatoxin $B_1$ metabolism in the mitochondrion. **Electron Microscopy Society of Southern Africa - Proceedings 1997**; 20: 102.

## ORAL PRESENTATIONS

**Gareth P. Raman**, Anil Chuturgoon, Shamin Bux, Sathiakanthi Moodley, Michael Dutton. The immunocytochemical and electrophoretic localisation of Aflatoxin $B_1$-binding proteins in rat liver mitochondria. **South African Society of Biochemistry and Molecular Biology, Fourteenth conference, Grahamstown**, January 1997.

**G.P. Raman**, A. Chuturgoon, S. Bux, M. Dutton. Immunodetection of Aflatoxin $B_1$-binding proteins in rat liver mitochondria. **National Cancer `97 Annual Conference**, Cape Town, January 1997.

**G.P. Raman**, A.A. Chuturgoon, S. Bux, M.F. Dutton. Aflatoxin $B_1$-binding mitochondrial proteins : An immunocytochemical and electrophoretic study. **Faculty Research Day, Faculty of Medicine**, University of Natal, Durban, September 1997..

**G.P. Raman**, M.F. Dutton, S. Bux, A.A. Chuturgoon. Do mitochondria have specific proteins that bind Aflatoxin $B_1$. **Joint Kwa-Zulu Natal Biochemistry and Microbiology Symposium**, Durban, October 1997.

**G.P. Raman**, M.F. Dutton, S. Bux, A.A. Chuturgoon. Aflatoxin $B_1$ metabolism in the mitochondrion. **Electron Microscopy Society of Southern Africa - Proceedings 1997**; 27: 102.

## POSTER PRESENTATIONS

S. Moodley, S.Bux, **G.P. Raman**, M.F. Dutton, A. Chuturgoon. Ultrastructure of Aflatoxin $B_1$ treated rat, liver, kidney and spleen. . **National Cancer `97 Annual Conference**, Cape Town, January 1997.

# AWARDS AND SCHOLARSHIPS

**United States Mellon Foundation Academic Subsistence Award** : 1996, 1997.

**BEST PAPER** : **Joint Kwa-Zulu Natal Biochemistry and Microbiology Symposium**, Durban, October 1997. Prize sponsored by Boehringer Mannheim.

**UNITED STATES OF AMERICA FULBRIGHT SCHOLARSHIP** :
Awarded for a **PhD** in Environmental Health Hazards, USA.

Nominated for the **FOGARTY INTERNATIONAL TRAINING GRANT**, which supports research and training of South African students at the School of Public Health, Department of Environmental and Industrial Health, **University of Michigan, USA.**

# ABBREVIATIONS

| | |
|---|---|
| **ADP** | Adenine Diphosphate |
| **$AFB_1$** | Aflatoxin $B_1$ |
| **AFBO** | Aflatoxin-8,9-epoxide |
| **ATP** | Adenine Triphosphate |
| **BSA** | Bovine Serum Albumin |
| **C** | Cytoplasm |
| **CC** | Cytoplasmic Clearing |
| **$CHCL_3$** | Chloroform |
| **CoA** | Coenzyme A |
| **CoQ** | Coenzyme Q |
| **$CoQH_2$** | Ubiquinol |
| **CSIR** | Centre for Scientific and Industrial Research |
| **cyt** | Cytochrome |
| **Da** | Dalton |
| **DAB** | Diaminobenzidine |
| **DMSO** | Dimethyl Sulphoxide |
| **DNA** | Deoxyribonucleic Acid |
| **DVA** | Derivatising Agent |
| **EDTA** | Ethylenedimethyltetraacetic Acid |
| **ER** | Endoplasmic Reticulum |
| **EtOH** | Ethanol |
| **FAD** | Flavin Adenine Dinucleotide |
| **$FADH_2$** | Flavin Adenine Dinucleotide dihydrogen |
| **FAPY** | Formamidopyrimidine |
| **FMN** | Flavin Mononucleotide |
| **$FMNH_2$** | Flavin Mononucleotide Dihydrogen |
| **GIP** | General Insertion Protein |

| | |
|---|---|
| **GTP** | Guanine Triphosphate |
| **HBV** | Hepatitus B Virus |
| **HCC** | Hepatocellular Carcinoma |
| **HPLC** | High Pressure Liquid Chromatography |
| **hsp** | heat shock protein |
| **IARC** | International Agency for Research on Cancer |
| **ICC** | Immunocytochemistry |
| **IHC** | Immunohistochemistry |
| **IM** | Inner Membrane |
| **ip** | Intraperitoneal |
| **ISOM** | Isolation Medium |
| **kDa** | Kilodalton |
| **KOH** | Potassium hydroxide |
| **M** | Mitochondria |
| **MIM** | Mitochondrial Inner Membrane |
| **MM** | Mitochondrial Matrix |
| **MOM** | Mitochondrial Outer Membrane |
| **mtDNA** | Mitochondrial Deoxyribonucleic Acid |
| **mtRNA** | Mitochondrial Ribonucleic Acid |
| **N** | Nucleus |
| **NAD** | Nicotinamide Adenine Dinucleotide |
| **NADH** | Nicotinamide Adenine Dinucleotide (reduced) |
| **NGS** | Normal Goat Serum |
| **NM** | Nuclear Membrane |
| **NU** | Nucleolus |
| **OM** | Outer Membrane |
| **P** | Paracrystalline inclusions |
| **PAGE** | Polyacrylamide Gel Electrophoresis |
| **PBS** | Phosphate Buffered Saline |
| **RNA** | Ribonucleic acid |

| | |
|---|---|
| **SDS** | Sodium Dodecyl Sulphate |
| **SMP's** | Sub-Mitochondrial Particles |
| **TEM** | Transmission Electron Microscopy |
| **TEMED** | Tetramethylethylenediamine |
| **TFA** | Trifluoroacetic Acid |
| **TMPD** | Tetramethyl p-phenylenediamine |
| **tRNA** | Tranfer Ribonucleic Acid |

# LIST OF TABLES

# LIST OF FIGURES

**Chapter 4**

# TABLE OF CONTENTS

# CHAPTER 1
# INTRODUCTION

Every living organism lives its' life with an adequate means of assuring survival. Their individual protective mechanisms that inherently support survival are often complex and scientifically elegant. The consequences however, of the action of one organism on the environment, and on others in the same biome, even though unintentional, may have adverse and often severely deleterious and hazardous effects.

Aflatoxin $B_1$ ($AFB_1$) is a carcinogenic secondary metabolite elaborated by pathogenic fungi such as *Aspergillus flavus* and *Aspergillus parasiticus*, fungi that are ubiquitous, and commonly found on poorly stored foods and feeds. Aflatoxin $B_1$ synthesis has no obvious physiological role in primary growth and metabolism of the organism and therefore it is considered a "secondary" process (Malik, 1982). To date, no biological role for aflatoxin $B_1$ in the ecological survival of the fungal organism has been confirmed. However, since $AFB_1$ is toxic to certain potential competitor microbes in the ecosystem (Detroy *et al.*, 1971), a survival benefit to the producing fungi is implied.

Based on its potent teratogenecity, mutagenecity, carcinogenecity and wide-spread occurrence in foods and feeds, the International Agency for Research on Cancer (IARC) has classified $AFB_1$ as a Primary Type I carcinogen in humans and animals.

Society as we know it, has advanced to such extents that man has adequately found measures to protect against winds, floods, storms and fires. He has even created light and electricity to cook, to warm and to insulate, to cool, refrigerate and preserve. Yet despite these advances in technologies, the majority of the world does not yet have access to them.

Aflatoxin $B_1$ is thus a major public health concern, especially in poorly developed countries and areas, where long term food storage is often inadequate, and where high temperatures and humidity stimulate the growth of fungal moulds. Dietary contamination of foods with $AFB_1$ will inevitably result in several adverse human and animal health effects.

Despite intensive research on aflatoxin $B_1$ (at least 4000 research articles) that have described exposure, toxic effects, and mechanisms of action, its exact role in toxin mediated carcinogenesis is still largely unknown.

The united efforts of researchers from a broad research field, with culminated ideas from disciplines like molecular biology, biochemistry, physiology, microbiology, botany and basic science, are indeed necessary for a more coherent picture of this carcinogen and its mode of action in human and animal systems.

## 1.1 Objectives

Aflatoxin $B_1$, the most potent and carcinogenic of all mycotoxins was selected for this study. Recent studies at the Mycotoxin Research Unit (University of Natal) have shown the presence of $AFB_1$ in the liver tissues from patients presenting with Hepatocellular Carcinoma (HCC) at King Edward VIII Hospital, Durban. Biopsies taken from hepatomas from these patients, revealed the presence of toxin in several organelles, including the nucleus, endoplasmic reticulum and mitochondria. The repeated occurrence of $AFB_1$-gold labelled conjugates within the liver mitochondria from these patients, observed in our laboratories, suggested that these organelles were principle sites of toxin binding.

With these observations in hand, the effect of the toxin on rat liver tissues, isolated mitochondria and sub-mitochondrial particles was examined. In addition, the ultrastructural changes in isolated mitochondria, during $AFB_1$ toxicity was examined. The transport of $AFB_1$ within the liver and into the mitochondria was investigated, with particular interest in $AFB_1$-binding mitochondrial proteins that may be involved in $AFB_1$ mediated toxicity in the liver.

CHAPTER 2

# LITERATURE REVIEW

## 2.1 INTRODUCTION

"Microscopic, unassuming, and insignificant ", these are the words that could often describe the rather troublesome and inconvenient presence of pathogenic fungi such as *Aspergillus flavus* and *A. parasiticus*. Deadly cytotoxic killers that prey silently on thousands of ignorant, and innocent people and animals, all over the world. These are the mycotoxins, a group of highly toxic, carcinogenic and mutagenic metabolites elaborated by fungi such as *A. flavus* and *A parasiticus*.

These compounds result in toxicity to humans and to a variety of other animal species, when contaminated food supplies are ingested. Since the discovery of these molecules in 1960, as the result of acute toxicity of poultry from contaminated food supplies, and their subsequent evaluation as carcinogens to rodents (Lancaster *et al.*, 1961), aflatoxins have been internationally recognised as potent environmental toxicants and carcinogens to many species (IARC, 1976, 1987; WHO, 1979, Newborne and Butler, 1969). These widely disseminated environmental carcinogens cause liver parenchymal tumours as well as tumours at several other organ sites including the colon (Wogan and Newborne, 1967), glandular stomach (Butler and Barnes, 1966) and kidney (Epstein *et al.*, 1969). Although several aflatoxin metabolites and congeners have been tested for their carcinogenecity, aflatoxin $B_1$ ($AFB_1$) is the most potent (Hsieh *et al.*, 1984).

Aflatoxin $B_1$ is a procarcinogen that must be activated metabolically to the $AFB_1$-8,9-epoxide (AFBO), the putative ultimate carcinogen. Garner *et al.*, (1972) were the first to show that metabolic activation of aflatoxin was necessary for mutagenic activity. Indeed, the bioactivation of $AFB_1$ has been demonstrated as a necessary step in the most dramatic of its toxic and carcinogenic effects. Figure 2.1 shows the biotransformation pathways for $AFB_1$.

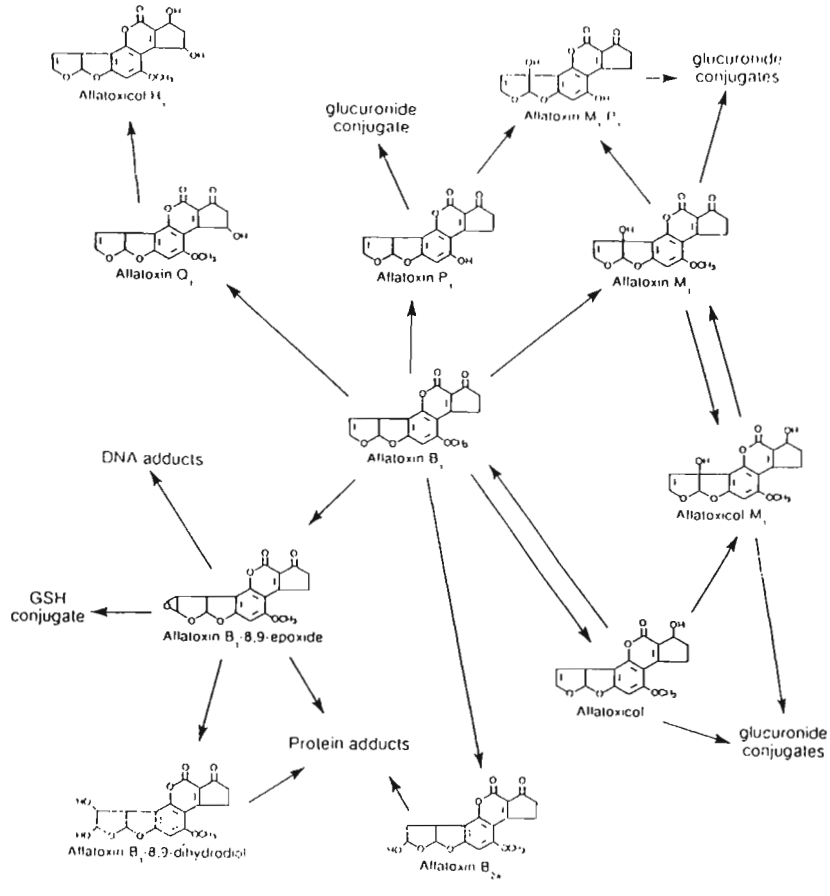


**Figure 2.1** **Biotransformation pathways for Aflatoxin $B_1$ (Eaton and Groopman, 1994).**

In addition to the recognised pathways of aflatoxin bioactivation, metabolic detoxification of aflatoxins and their reactive metabolites have also been demonstrated. An important detoxification mechanism involves the conjugation of the reactive epoxides with gluthathione (GSH). The conjugation of GSH is an important reaction in determining the susceptibility of different species to the toxic effects of $AFB_1$ (Hayes *et al.*, 1991).

This conjugation reaction is mediated by cytosolic glutathione *S*-transferase (Ramsdell and Eaton, 1990). A most striking species difference in GSH conjugation of $AFB_1$-8,9-epoxide has been observed in the mouse and the rat (Quinn *et al.*, 1990). Although the mouse has a very high microsomal $AFB_1$ epoxidation activity (Monroe and Eaton, 1987), the species is very resistant to $AFB_1$ induction of tumours. The very high level of glutathione *S*-transferase activity toward AFBO in the mouse appears to be the basis of its own resistance.

As shown schematically in Figure 2.2, the fate of $AFB_1$ is dependent on the relative activity of several biotransformation pathways, in addition to other factors such as DNA repair rates. The amount of the mycotoxin that is going to exert carcinogenic or toxic effects will depend on the amount converted to various metabolites, as well as on the biological activity of those metabolites.

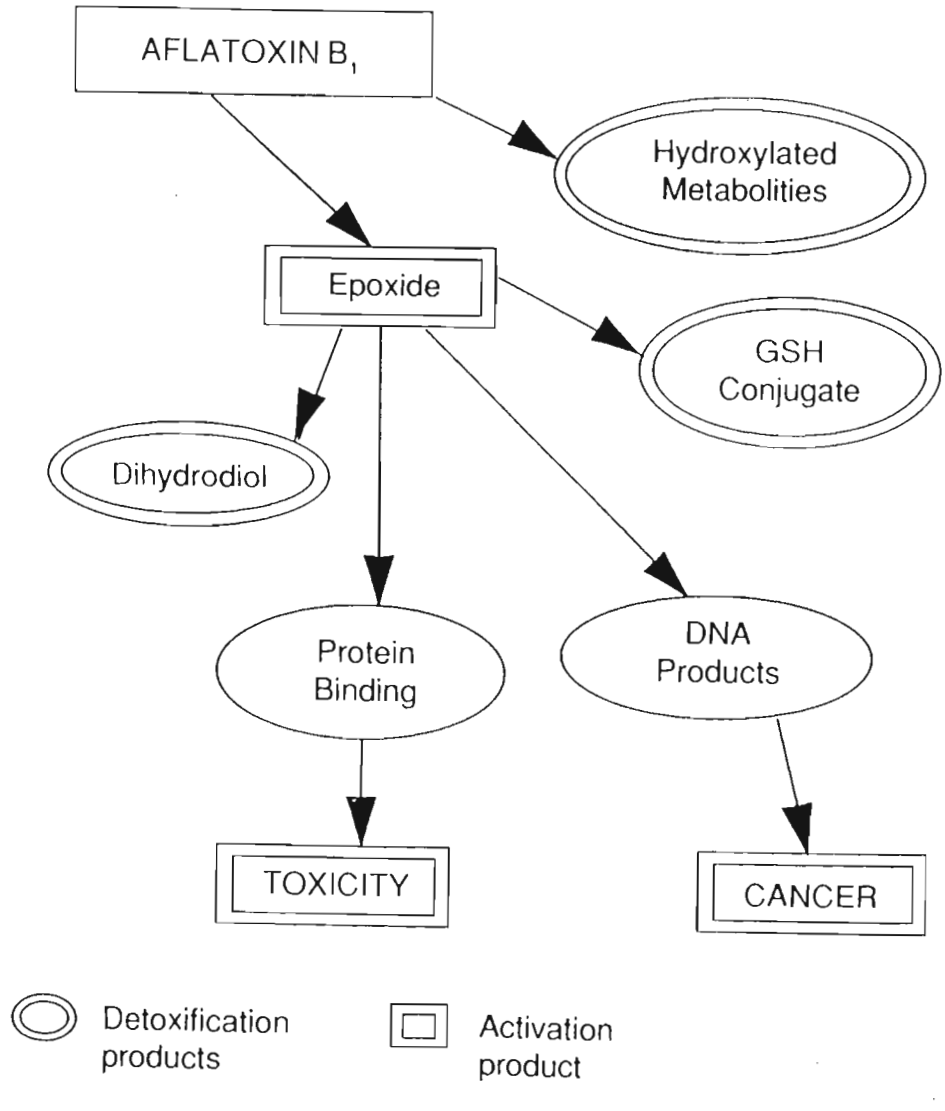


**Figure 2.2** **Schematic representation of the role of various biotransformation pathways in the disposition, toxicity, and carcinogenecity of aflatoxin $B_1$ (Eaton and Groopman, 1994).**

## 2.2 ABSORPTION AND BIOLOGICAL ACTIVITY OF AFLATOXIN $B_1$

Aflatoxin $B_1$ is a relatively low molecular weight, lipophilic molecule, suggesting its efficient absorption after ingestion (Eaton and Groopman, 1994). Wogan et al. (1967) reported no significant difference in the excretion and distribution of radioactivity after either oral or intraperitoneal (ip.) administration of [$^{14}$C]$AFB_1$ in male Fischer rats (125g). This implied that absorption after oral exposure was complete.

Aflatoxin $B_1$ appeared to be absorbed rapidly from the small intestine into the mesenteric venous blood. In an experiment with Wistar rats, Kumagai (1989) injected [$^{3}$H]$AFB_1$, directly into the stomach and into various sites of the small intestine of rats and measured radioactivity in the bile after 30 minutes. The results indicated that the site of absorption was the small intestine, the duodenum being the most efficient absorption site. From the intestine, $AFB_1$ apparently enters the liver through the hepatic portal blood supply (Wilson *et al.*, 1985). The toxin was concentrated heavily in the liver, not only after oral administration but after intravenous and ip. dosing as well. This occurs because of the high permeability of the hepatocyte membrane for $AFB_1$, and its active metabolism and subsequent covalent binding with hepatic macromolecules (Eaton and Groopman, 1994).

According to several authors, most of the $AFB_1$ retained in the liver, several hours after dosing, was bound irreversibly to tissue macromolecules. Holeski *et al.*, (1987) found that 2 hours after $AFB_1$ administration (0.25 mg/kg, ip.), 15% remained in the liver. Of the radioactivity in the liver, 12% constituted polar metabolites, 3% nonpolar metabolites, and 70% covalently bound adducts. Wong and Hsieh (1980) reported that 100 hours after [$^{14}$C]$AFB_1$ dosing, 6.5% of the administered dose was retained in the rat liver.

### 2.2.1 Acute Hepatotoxicity of Aflatoxins

It is now apparent that the principal target organ in susceptible mammalian, avian and fish species is the liver. Acute structural and functional damage to the liver, as a result of $AFB_1$ toxicity, has been reproduced experimentally in most laboratory animals and in several domestic animal species. Numerous outbreaks of human acute aflatoxicosis involving liver failure and gastrointestinal bleeding have occurred in Southeast Asia and Africa (Massey *et al.*, 1995).

Further, extensive studies in a large population of mainland Chinese has confirmed significant exposure to aflatoxin $B_1$, and a relationship of this exposure to liver cancer seems likely (Yeh *et al.*, 1989). Such exposure is associated with a high incidence of hepatocellular carcinoma, but the extent to which concomitant hepatitis B virus (HBV) infection is involved is not known. It is however estimated that approximately 250,000 deaths occur annually in certain parts of China and sub-Saharan Africa due to hepatocellular carcinoma (Kensler *et al.*, 1994).

The major contributors to this high rate of hepatocellular carcinoma included both aflatoxin ingestion and HBV infection. Evidence of acute aflatoxicosis has also been reported from Taiwan and Uganda (Shank, 1981) and is characterised by vomiting, abdominal pain, pulmonary edema, fatty infiltration and necrosis of the liver. An outbreak of aflatoxin poisoning in western India was also described (Shank, 1981), arising from the consumption of heavily mouldy corn. Specimens analysed showed 6-16mg $AFB_1$/kg corn. Of the nearly 400 patients examined, over 100 fatalities occurred. Liver specimens revealed marked parenchymal cell necrosis and extensive bile duct proliferation, lesions that are often seen in experimental animals after acute aflatoxin exposure.

### 2.2.2 Role of Aflatoxin-DNA adducts in the cancer process

Aflatoxin $B_1$ reacts *in vivo* with the DNA in target cells to give primarily *trans*-8,9-dihydro-8-($N^7$-guanyl)-9-hydroxyaflatoxin $B_1$ (Figure 2.3), (Bailey, 1994). The presence of a positive charge on the imidazole portion of the initial $N^7$-guanyl adduct (Figure 2.3), gives rise to a ring-opened formamidopyrimidine (FAPY) derivative with some distinct chromatographic behaviour (Croy and Wogan, 1981). Accumulation of this derivative is time dependent, nonenzymatic, and of some potential biological importance, because of its apparent persistence in DNA. Aflatoxin-DNA adduction is far greater in the liver than in other organs. The level of liver DNA adduction per unit $AFB_1$ dosage generally correlates with species susceptibility (Cole *et al.*, 1988).

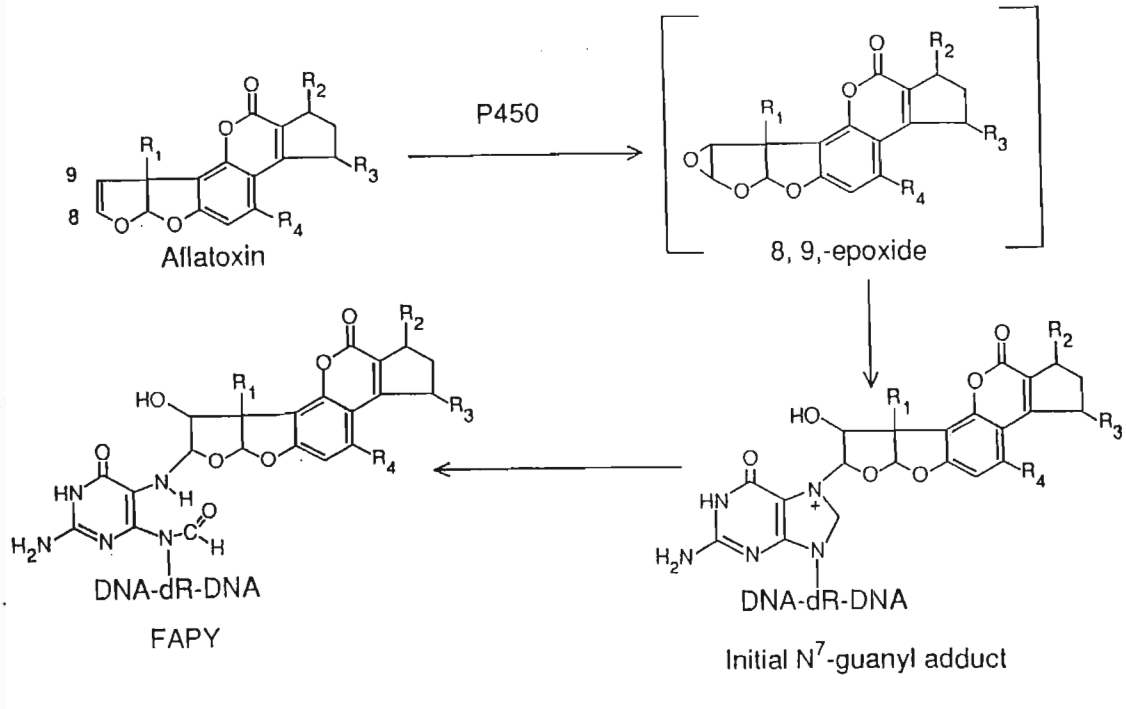


**Figure 2.3** **Metabolic pathway leading to DNA adduction and formation of FAPY adducts for aflatoxin $B_1$. $R_1$ = H, $R_2$ = O, $R_3$ = H, $R_4$ = $OCH_3$ (Bailey 1994).**

### 2.2.3 Interaction with Proteins

The binding of aflatoxins to proteins has received a great deal of attention. Proteins that bind aflatoxins reversibly may act as reservoirs of the toxin, prolonging toxin exposure, or they may serve as carriers in the transport of reactive metabolites (Mclean and Dutton, 1995). Mainigi and co-workers (1977) described several aflatoxin-protein complexes present in the liver cytosol during $AFB_1$ induced hepatocarcinogenesis. Histones, nuclear non-histone proteins, albumin, and several other unknown proteins are reported as $AFB_1$-binding proteins (Iwaki *et al.*, 1993).

However the roles of these proteins in $AFB_1$ mediated carcinogenesis and toxicity are largely unknown. There is evidence that some $AFB_1$ molecules become cytoplasmically bound to molecules destined for the nucleus (Mclean and Dutton, 1995, Ch'ih *et al.*, 1993). These researchers have classified these proteins as specific cytoplasmic binding proteins. It is proposed that $AFB_1$, on entering the cell, is translocated in a non-covalently bound form (by these cytoplasmic binding proteins) to microsomes for activation by microsomal enzymes, to form the highly reactive 8,9-epoxide.

The majority of the epoxide is detoxified and rapidly removed from the cell as water-soluble polar metabolites. A portion of the activated $AFB_1$ is translocated to various subcellular sites where covalent bonding occurs, first to cellular macromolecules like the rough endoplasmic reticulum, and then later to the nucleus, and finally to the mitochondrion (Mclean and Dutton 1995).

## 2.3 AFLATOXIN $B_1$ IN THE MITOCHONDRION

The presence of $AFB_1$ within liver mitochondria has been well documented (Wu *et al.*, 1984, Niranjan *et al.*, 1986, Obidoa, 1986). The actual *in vivo* disposition of the toxin in human and animal liver, however, has not yet been deduced. At acute aflatoxin exposure levels, inhibition of cellular energy production is a major metabolic effect (Mclean and Dutton, 1995).

### 2.3.1 The Mitochondrion

Mitochondria are respiratory organelles that constitute about 20% of the cytoplasmic volume of liver cells (Hinke, 1994). Their primary function is electron transport, linked to adenine triphosphate (ATP) synthesis (oxidative phosphorylation). Mitochondria can be considered the ultimate power house of a cell, and contain the enzymes of the tricarboxylic acid cycle, fatty acid oxidation, and oxidative phosphorylation (Table 1). Other functions in liver cells include parts of the urea cycle, gluconeogenesis, fatty acid synthesis pathways, and the regulation of intracellular calcium ion concentrations (Hinke, 1994).

**Table 1. Location of liver mitochondrial enzymes (Hinke, 1994)**

## Outer membrane

Monomine oxidase
Cytochrome $b_5$ reductase
Cytochrome $b_5$
Kynurenine hydroxylase
Pore protein
Phospholipase $A_2$
Lysophosphatidate acyltransferase
Glycerophosphate acyltransferase
Acyl CoA synthetase

## Intermembrane space

Adenylate kinase
Nucleosidediphosphate kinase
DNAse I
Sulphite-cytochrome c reductase
D-Xylulose reductase
Cytochrome c

## Inner membrane

$F_0F_1$ ATPase (ATP synthase)
NADH-CoQ reductase (complex I)
Succinate-CoQ reductase (complex II)
Glycerol-3-phosphate-CoQ reductase
Electron transferring-flavoprotein CoQ reductase
Choline-CoQ reductase
Proline-CoQ reductase
$CoQH_2$-cytochrome c reductase (complex III)
Cytochrome c
Cytochrome c oxidase
3-hydroxybutyrate dehyrogenase
Transhydrofenase
Inorganic pyrophosphatase
Carnitine palmitoyltransferase

***Transporters for the following substrates:***

ATP-ADP antiport
Phosphate-OH antiport
Tricarboxylate-malate antiport
Pyruvate-OH antiport
Glutamate-OH antiport
Glutamate-aspartate antiport
α-Ketoglutarate-malate antiport
L-Ornithine-proton antiport
Citrulline uniport
Acyl carnitine-carnitine antiport
Calcium ion uniport
Calcium-proton antiport
Sodium, potassium-proton antiport

## Matrix

***Tricarboxylic acid cycle***

Pyruvate dehydrogenase
Citrate synthase
Aconitate hydratase
Isocitrate dehydrogenase
α-Ketoglutarate dehydrogenase
Succinyl-CoA synthetase
Fumarate hydratase
Malate dehydogenase

***Urea cycle enzymes***

Carbomyl-phosphate synthase
Ornithine carbamoyltransferase

***Fatty acid oxidation***

Acetyl-CoA synthetase
Acyl-CoA synthetase
Acyl-CoA dehydrogenase
Enoyl-CoA hydratase
Enoyl-CoA isomerase
3-Hydroxyacyl-CoA dehydrogenase
Acetyl-CoA acetyl transferase
Acetyl-CoA acyl transferase
Electron-transferring flavoprotein

***Other matrix enzymes***

Fatty acid elongation system
Aspartate aminotransferase
Aldehyde dehydrogenase
Dimethylglycine dehydrogenase
Sarcosine dehyrogenase
Glutamate dehydrogenase
Hydroxymethylglutaryl-CoA lyase
Hydroxymethylglutaryl-CoA synthase
Nucleosidediphosphate kinase
Phosphoenolpyruvate carboxikinase
Pyruvate carboxylase
Aminoacyl-tRNA synthetases
DNA polymerase
Elongation factors
Polyriboadenylate polymerase
RNA polymerase
Ribosomes
Propionyl-CoA carboxylase
Methylmalonyl-CoA Mutase
Methylmalonyl-CoA racemase

### *2.3.1.1 Basic Structure*

The apparent structure of mitochondria *in situ.* revealed by thin sectioning depends on the type of cell in which the mitochondria occur, and on the physiological state of the cell. Within these limits, all mitochondria can be referred to by a general pattern.

Each mitochondrion consists of a limiting or outer membrane within which is a peripheral inner membrane, which in turn, encloses an inner space called the matrix. The matrix is rich in protein and also contains DNA and RNA. In a great number of cell types, the mitochondrial matrix exhibits rounded electron-dense granules rich in cations such as calcium and magnesium (Munn, 1974, Hinke, 1994). Lying in the matrix are a variable number of membranous structures called cristae, which appear either free, or as invaginations of the inner membrane (Figure 2.4). Most often , the cristae contain a space known as the intracristal space. There is also a space between the outer and inner membrane, known as the peripheral or intermembrane space (Figure 2.4).

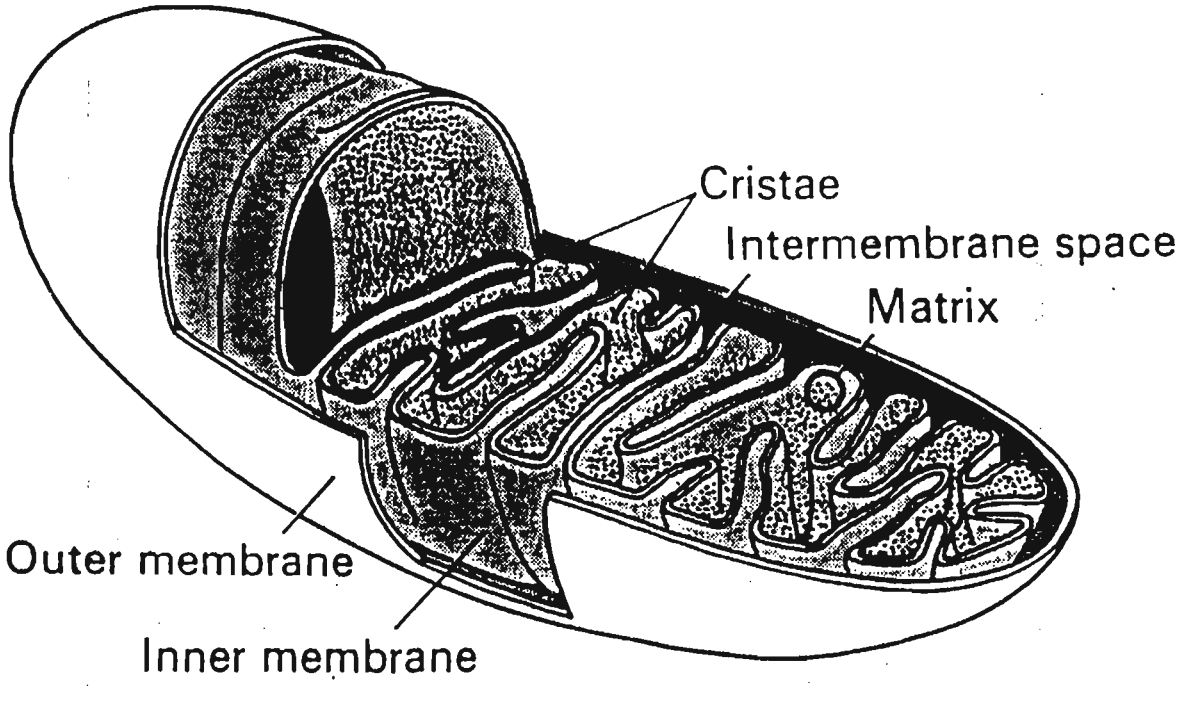


**Figure 2.4** **Diagrammatic representation of a section through a mitochondrion (Munn, 1974).**

The inner membrane from rat liver can be separated from the outer membrane by treatment with digitonin, which breaks up the latter because it contains cholesterol. The resulting inner membrane may be intact, in which case it is known as a mitoplast, or inner membrane fragments may result, called sub-mitochondrial particles (SMP's).

Electron microscopy reveals numerous knobs (arrows) attached to the outside surface of the inner membrane. These knobs have been identified as a complex of proteins with ATP synthase activity (Figure 2.5).

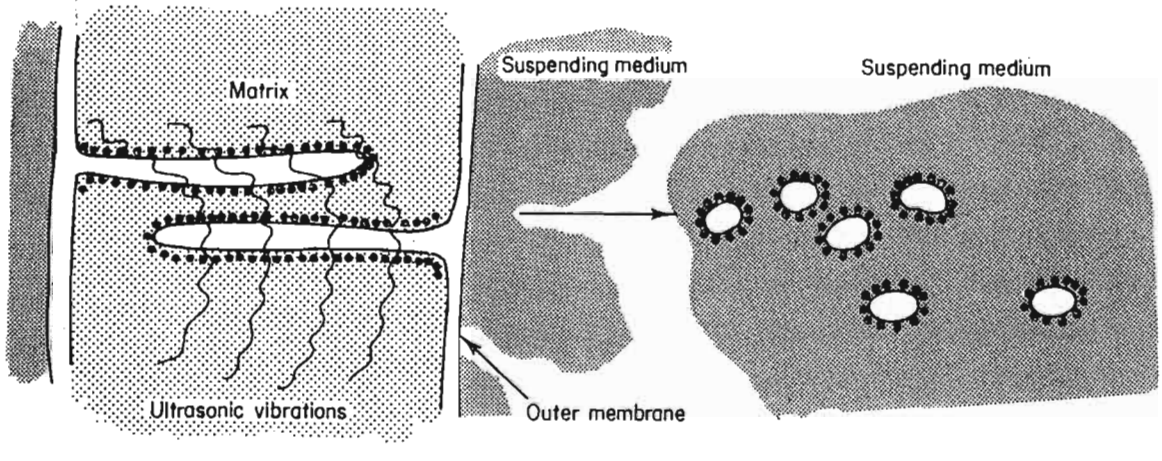


**Figure 2.5** **Formation of submitochondrial particles by disruption of the cristal membrane. The outer membrane and inner boundary membrane are also disrupted, thus releasing the submitochondrial particles into the suspending medium (Munn, 1974).**

### *2.3.1.2 Protein composition*

Quantitatively, the most important component of mitochondria is water. Water is absent from only certain small regions inside some proteins and membranes. The bulk of the dry mass of mitochondria is composed of protein. Schnaitman and Greenawalt (1968) have calculated that the matrix of rat liver mitochondria contain 67% of the total mitochondrial protein, the intracristal and peripheral spaces 6.3%, and the inner and outer membrane 21.3% and 4% respectively. According to Munn (1974), the proteins of the inner membrane of rat liver mitochondria can be resolved into at least 23 components; both the inner and outer membranes contain major proteins in the range of 50-70,000 Da, however, no individual proteins account for more than 10-15% of the total. The bulk of the protein generally represent enzymes (Table 1).

### *2.3.1.3 Lipids, metal ions, nucleotides and other anions*

The lipid content of mitochondria from different organs varies substantially, but in all cases phospholipid accounts for over 75% of the total. The most commonly encounted phospholipids are phosphatidylcholine and phosphotidylethanolamine. The lipid composition of rat liver mitochondria is listed in Table 2.

**Table 2. Lipids of rat liver mitochondria (Munn, 1974).**

| LIPIDS | INNER MEMBRANE | OUTER MEMBRANE | MATRIX |
|---|---|---|---|
| Total phospholipid as % of phospholipid plus protein | 25.4 | 37.4 | 1.4 |
| Molar ratio cholesterol: phospholipid | 1:53 | 1:9 | 1:12 |
| ***Phospholipids as % total*** | | | |
| Phosphatidylcholine | 39.2 | 59.0 | 35.6 |
| Phosphatidylethanolamine | 34.4 | 20.3 | 44.2 |
| phosphatidic acid + cardiolipin | 13.7 | 6.3 | 9.1 |
| Phosphatidylinositol | 6.6 | 4.8 | 4.3 |
| Lysophosphatidylcholine | 3.1 | 3.4 | 2.0 |
| sphingomyelin + phosphatidylserine | 3.4 | 7.5 | 4.8 |

Rat liver mitochondria contain several metal ions including potassium (83-160 nmoles/mg protein), magnesium (20-50 nmoles/mg protein), sodium (3-75 nmoles/mg protein) and calcium (10-33 nmoles/mg protein). Smaller amounts of zinc, iron, manganese and copper have also been reported (Munn, 1974). Mitochondria from a variety of organs in the rat have been shown to contain adenine nucleotides, and relatively smaller amounts of guanine, cytidine and uridine nucleotides. Other anions found in mitochondria include 2-glycerophosphate, phosphoenolpyruvate, citrate, malate, and sulphate (Munn, 1974).

### 2.3.2 Import of proteins into various sub-mitochondrial compartments

More than 90% of all mitochondrial proteins are coded for by the nucleus (Hartl *et al.*, 1989; Hay *et al.*, 1984, Hartl and Neupert, 1989). These proteins are synthesised as precusor proteins on free cytosolic polysomes and are post-translationally imported into one of the four submitochondrial compartments, viz., the outer membrane, the intermembrane space, the inner membrane and the matrix. Experiments conducted in several laboratories have given us a basic understanding of how mitochondria integrate the many proteins synthesised in the cytosol (Hay *et al.*, 1984, Pon *et al.* 1989, Hinke, 1994, Hartl and Neupert, 1989).

Incorporation of cytoplasmically synthesised proteins into mitochondria can be divided conceptually into five steps (Hay *et al.*, 1984).

1) Synthesis of the polypeptide itself, usually a larger precursor.
2) Recognition and binding of the precursor to the mitochondrial surface.
3) Translocation of the precursor across or into one or both mitochondrial membranes, depending on the final suborganellar localisation of the protein.
4) Cleavage and/or other covalent modification (processing of the polypeptide chain to the mature protein).
5) Assembly of subunits to functional holoenzymes, which in some cases involves an association with mitochondrially made subunits.

### *2.3.2.1 Binding of precursors to specific receptors of the outer membrane*

Several lines of evidence suggest that proteinaceous receptors at the surface of mitochondria are involved in specific recognition of precursor proteins. According to Hay *et al.*, (1984), if import of a mitochondrial protein is mediated by a receptor, then this receptor should :

a) be exposed at the cytoplasmic face of the outer membrane, so that it is accessible both to newly synthesised precursors, and to factors which modify the receptor-precursor interaction.

b) bind precursors even when their subsequent translocation and/or assembly is prevented.

c) satisfy rapid and reversible binding, receptor-ligand interactions.

d) serve an obligate role in the import pathway.

Our current knowledge of precursor protein binding and recognition, involves at least four different classes of import receptors, i.e., for porin, the ADP/ATP carrier, $F_1$ ATPase subunit β and cytochrome *c*. These receptor sites are protease accessible and converse at a common membrane insertion site, referred to as a general insertion protein (GIP) in the outer membrane. Pfaller *et al.*, (1988) believe that GIP facilitates membrane insertion. Proteins of the matrix, inner membrane and intermembrane space (e.g. $F_1$ ATPase subunit β, ADP/ATP carrier and cytochrome $b_2$ respectively) are directed into translocation sites between the outer and inner membranes ( Hartl and Neupert, 1989).

Morphologically described translocation contact sites between outer and inner membranes have been known for a number of years (Moynagh, 1995). Schleyer and Neupert (1985) used several immunological techniques to accumulate precursor proteins in translocation contact sites, thus experimentally demonstrating their importance in protein translocation.

Pfanner *et al.*, (1987) showed that the transport of precursor proteins occurred through a hydrophilic membrane, since translocation intermediates spanning the contact sites, were easily extractable with hydrophilic perturbants, such as urea. Import into the mitochondrial matrix and inner membrane, unlike import into or across the outer membrane, requires an electrochemical potential across the inner membrane (Hay *et al.*, 1984).

Completion of the translocation into the inner membrane or matrix however, is independent of membrane potential, but dependent on the presence of nucleoside triphosphates, which according to Hart and Neupert (1989), appear to be required for the unfolding of precursor portions still outside the mitochondrion.

#### *2.3.2.2 Proteolytic processing of translocated mitochondrial precursors*

During or shortly after their translocation, many mitochondrial precusor proteins undergo some form of covalent modification. According to Hay *et al.*, (1984) the most frequent modification is proteolysis. Mitochondrial precusor proteins with amino-terminal presequences undergo either one or two separate proteolytic cleavages during their maturation. The first occurs in the matrix, and is mediated by a neutral, chelator-sensitive protease.

This enzyme has been shown to be highly active at neutral pH, and is strongly inhibited by a variety of chelating agents, including EDTA and GTP. The enzyme was also insensitive to serine protease inhibitors, small polypeptide protease inhibitors, and sulfhydrol-modifying agents such as iodoacetamide (Hay *et al.*, 1984). Bohni *et al.*, (1983) and McAda and Douglass (1982) used partially purified preparations of the enzyme to determine its substrate specificity, as well as some physical characteristics.

These workers found that in the crude submitochondrial extract, the partially purified enzyme shows a narrow substrate specificity. Five mitochondrial precursors have been reported to be cleaved to their mature intramitochondrial forms in two discrete steps. The first cleavage, mediated by matrix protease yields a form of each protein which migrates electrophoretically between the precusor and the mature forms (Hay *et al.*, 1984).

These intermediates appear to be firmly bound to the mitochondrial inner membrane, protruding into the intermembrane space. The second cleavage, converts these intermediates to their mature forms. This takes place on the outer surface of the inner membrane.

#### *2.3.2.3 Assembly of processed proteins into functional units*

The final step in the import pathway is the assembly of cytoplasmically made polypeptides into functional forms within the mitochondrion. As yet, no research has directly demonstrated the proper assembly of newly imported subunits into complex forms in the mitochondrion. Mitochondrial protein import involves a process with more variations than one might anticipate. The entire process however, can be summarised in Figure 2.6.

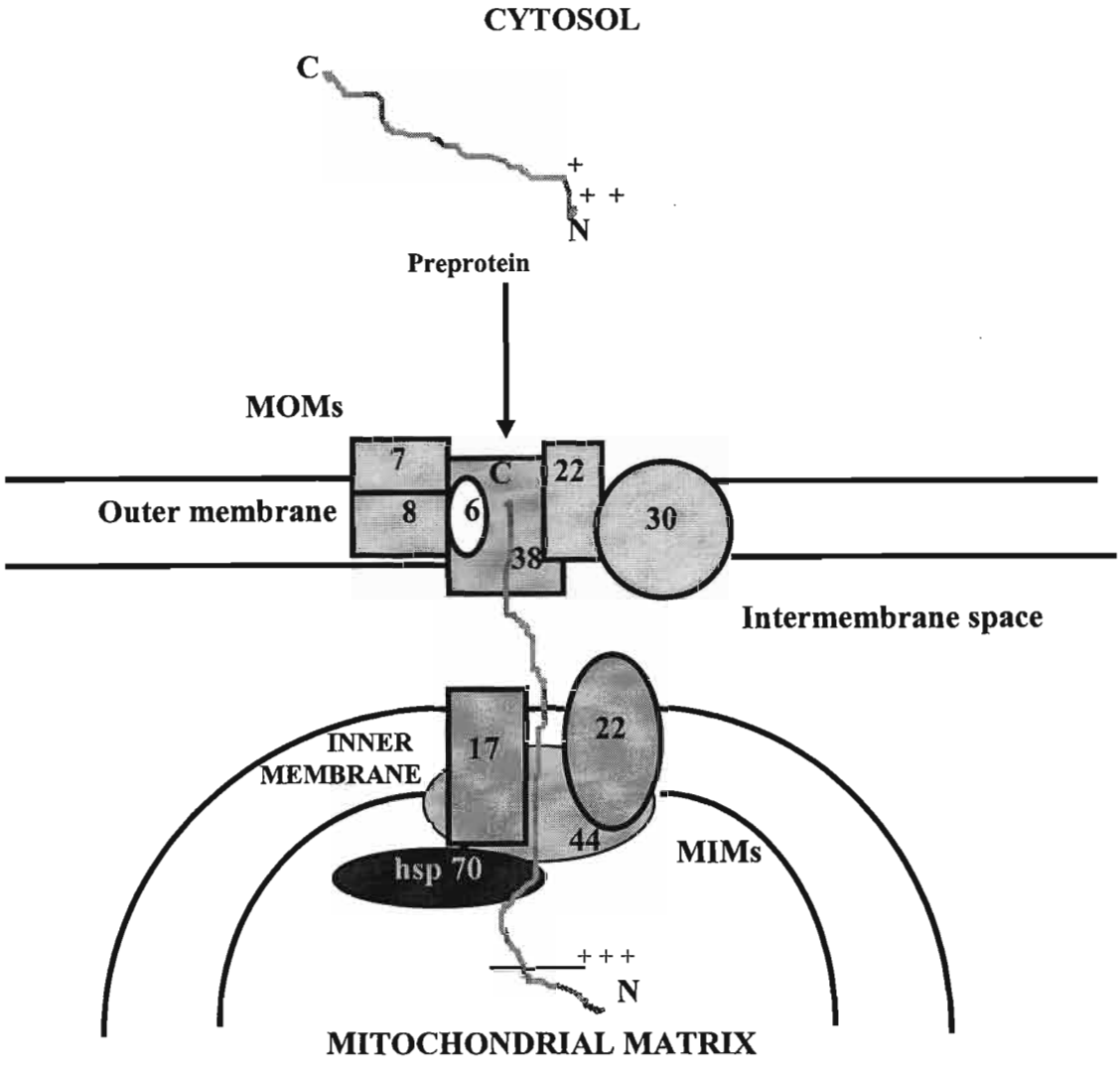


**Figure 2.6** **Pathway for import of proteins into mitochondria**
MIM, mitochondrial inner membrane protein; MOM, mitochondrial outer membrane protein. The numbers represent the molecular weights of each protein (adapted from Moynagh, 1995).

Basically, mitochondrially targeted proteins are synthesised on cytosolic ribosomes as preproteins which possess positively charged signal sequences at their N-termini. These preproteins are guided by cytosolic chaperones and mitochondrial outer membrane receptors to the outer membrane translocation complex, which is present in contact site regions. This hetero-oligomeric complex spans the outer membrane and may form a translocation pore.

Several polypeptide subunits of the complex have been identified. These include mitochondrial outer membrane proteins MOM38, MOM7, MOM8, MOM22, MOM30, where the numbers represent the molecular mass of each subunit (Figure 2.6). It is presumed that these subunits form a translocation channel which serves to receive incoming preproteins from the outer membrane receptors, and subsequently to guide preproteins to an adjacent mitochondrial inner membrane import complex (Moynagh, 1995). In addition the mitochondrial inner membrane proteins MIM17 and MIM23 behave as integral proteins of the mitochondrial inner membrane and may form the preprotein translocation channel of the inner membrane.

A third protein, MIM44 is an essential component of the inner membrane import machinery. It seems to be a peripheral membrane protein on the mitochondrial matrix side but is firmly associated with the inner membrane by interaction with integral membrane proteins (either MIM17 or MIM23), (Figure 2.6). Heat-shock protein (hsp70) in the mitochondrial matrix also binds to preprotein in transit. A significant portion of hsp70 is reversibly associated with MIM44. It has been proposed that the two proteins function in close co-operation to drive protein import through the inner membrane into the mitochondrial matrix (Figure 2.6).

### 2.3.3 Components of the Electron Transport Chain

The *electron transport chain* or *respiratory chain* in mitochondria forms the means by which electrons, from the reduced electron carriers of intermediatary metabolism, are channelled to oxygen and protons to yield $H_2O$. The main components of the chain are as follows :

**$NAD^+$ / NADH**

*The electron-transport reaction for the $NAD^+$ / NADH conjugate redox pair is :*

$$NAD^+ + H^+ + 2e^- \longrightarrow NADH$$

**In effect, electrons are transported as *hydride* ions ($H^-$), which are *formally* equivalent to ($H^+$+2$e^-$).**

**Flavin Nucleotides**

*The electron-transport reactions for FAD and FMN are :*

$$FAD + 2H^+ + 2e^- \longrightarrow FADH_2$$

$$FMN + 2H^+ + 2e^- \longrightarrow FMNH_2$$

**Electrons are effectively transported as H atoms by these nucleotides [H ≡ ($H^+$ + $e^-$)]**
**These carriers transfer electrons into the electron-transport chain independently of and bypassing the $NAD^+$ / NADH couple.**

**Coenzyme Q**

Coenzyme Q (alternatively known as ubiquinone or CoQ) is a benzoquinone derivative with a long hydrocarban side chain made up of repeating isoprene units (Figure 2.7). The molecule undergoes a ($2H^+ + 2e^-$) reduction to form $CoQH_2$ (alternatively known as ubiquinol).

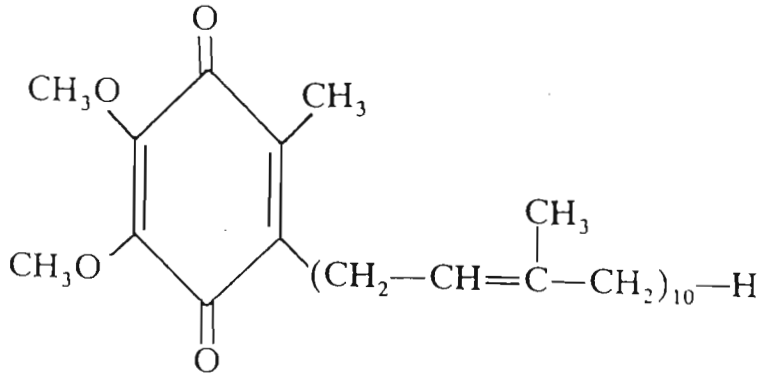


**Figure 2.7** **The form of CoQ in mammalian mitochondria (Kushel and Ralston, 1988).**

## Cytochromes

The cytochromes are a family of proteins containing prosthetic haem groups. Mitochondria contain three classes of cytochromes viz. a, b, and c, which have haem groups of different structures (Figure 2.8).

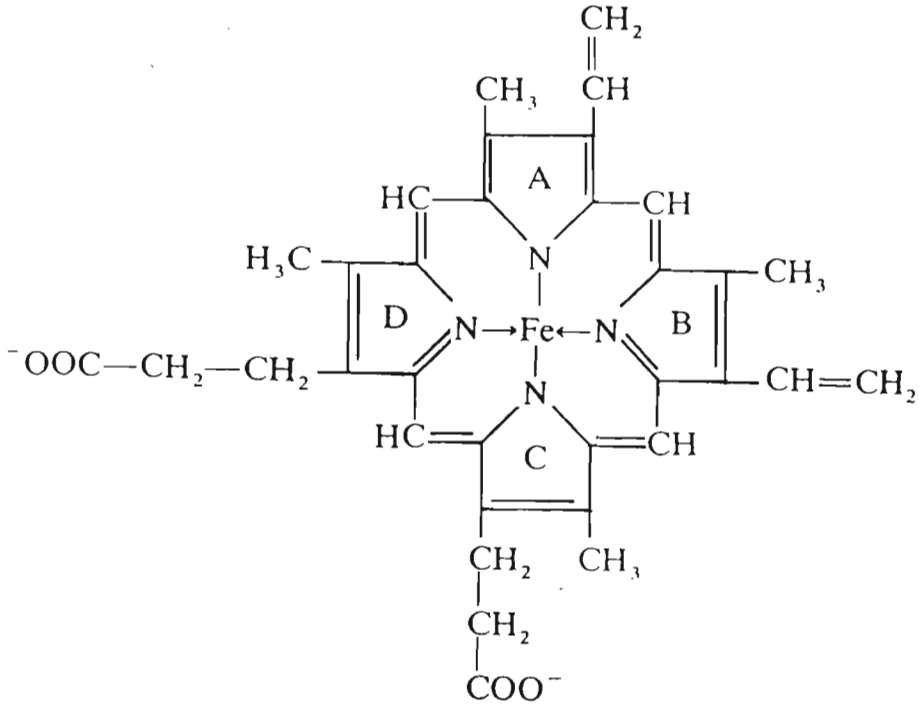


**Figure 2.8** **The general cyclic tetrapyrrole structure of a haem ring.** In cytochromes *c* and $c_1$, the hemering is covalently attached to the protein via *thioether bonds*, formed by the reaction of the*vinyl* groups (-CH=$CH_2$) on pyrrole rings A and B and cysteine residues of the protein. These thioether bonds are absent in cytochrome *b*. In cytochromes *a* and $a_3$, the vinyl group on the ring A is replaced by a hydrocarbon chain, and the methyl group on ring D is replaced by a formyl ( -CHO) group. In addition, cytochromes *a* and $a_3$ contain bound Cu ions. (Kushel and Ralston, 1988).

**Iron-Sulphur Proteins**

The electron-transport chain contains a number of iron-sulphur proteins (also known as non heme iron proteins. The iron atoms are bound to the proteins via cysteine - S - groups and sulphide ions (Figure 2.9). These proteins mediate electron transport by direct electron transfer.

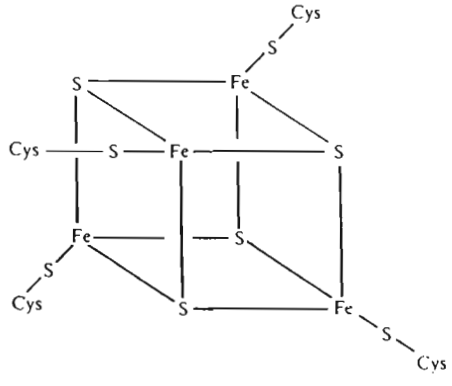


**Figure 2.9** **Schematic representation of an iron-sulphur protein (Kushel and Ralston, 1988).**

### *2.3.3.1 Organization of the electron-transport chain*

The electron-transport chain is composed of four complexes listed in Table 3. The pattern of electron transfer within these complexes is illustrated in Figure 2.10.

**Table 3. Complexes of the electron transport chain.**

| Complex | Enzymatic Function | Functional Components |
|---|---|---|
| I | NADH/CoQ oxidoreductase | FMN; FE-S clusters |
| II | Succinate/CoQ oxidoreductase | FAD; Fe-S clusters |
| III | CoQ - cytochrome *c* oxidoreductase | Cytochromes b, cytochrome $c_1$; Fe-S clusters |
| IV | Cytochrome *c* oxidase | Cytochromes *a* and $a_3$ |

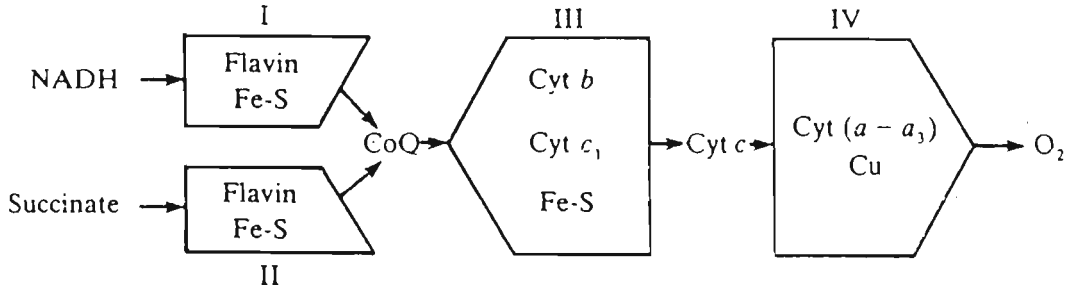


**Figure 2.10** **Schematic organisation of the electron-transport chain in mitochondria (Kushel and Ralston, 1988).**

### 2.3.4 Hepatic Mitochondrial Cytochrome P-450 system - Distinctive features of Cytochrome P-450 involved in the activation of Aflatoxin $B_1$

In addition to their primary role in electron transfer and oxidative phosphorylation, mammalian mitochondria also carry out several metabolic functions. One of these specialised functions is steroid hydroxylation by a unique mitochondrially located Cytochrome P-450 (Cyt $P_{450}$) in various steroidogenic tissues. There is now compelling evidence for the existence of multiple forms of Cyt $P_{450}$ in mammalian liver (Niranjan *et al.*, 1984). In mammalian liver, these Cyt $P_{450}$ - linked monooxygenases are compartmentalised in the microsomal fraction, in the nuclei, and in the mitochondria (Raney *et al.*, 1992, Liu and Massey, 1992).

The microsomal Cyt $P_{450}$ is involved in the oxidation of a number of physiologically important metabolites. The physiological and metabolic significance of Cyt $P_{450}$ reported to occur in the hepatic nuclear fraction, remains unclear. The Cyt $P_{450}$ - linked monooxygenase activity of hepatic mitochondria appears to play an important role in bile acid synthesis and vitamin $D_3$ metabolism. Niranjan *et al.*, (1984) showed that intact rat liver mitoplasts and submitochondrial fractions possess a unique Cyt $P_{450}$ type monooxygenase system for the activation of $AFB_1$ into it highly reactive, electrophilic epoxide, which can then covalently bind to DNA, RNA and proteins.

## 2.4 THE EFFECTS OF $AFB_1$ ON OXIDATIVE PHOSPHORYLATION AND ELECTRON TRANSPORT

The *in vitro* and *in vivo* effects of $AFB_1$ on oxidative phosphorylation and electron transport have been investigated (Ramachandra *et al.*, 1975, Bai *et al.*, 1977, Niranjan and Avadhani, 1980). Aflatoxin $B_1$ is known to inhibit respiration, uncouple phosphorylation and affect ATPase activity.

Liver mitochondrial injury is indeed one of the dominant features of aflatoxin toxicity. Doherty and Cambell (1973) reported that in rats, an oral dose of 0.45mg pure $AFB_1$/kg body weight inhibited both oxygen consumption and phosphorylation, after 24 hours of administering the toxin. According to Svoboda *et al.*, (1966) respiration returned to normal after 72 hours, but not the phosphorylation. Clifford and Rees (1967) however, observed no changes in respiration or P:O ratios in rats, even up to 24 hours after administration of 7 mg $AFB_1$/ kg body weight.

Ramachandra *et al.*, (1975) reported inhibition of respiration in rat liver mitochondria by about 50-70% in the presence of $AFB_1$ at concentrations of $1 \times 10^{-4}$ M and $3 \times 10^{-4}$ M respectively. They showed that aflatoxins have two distinct effects on mitochondrial function, as uncouplers at lower concentrations and as inhibitors at higher concentrations. Aflatoxin $B_1$ acted as an uncoupler at a concentration of $1 \times 10^{-6}$ M and at a concentration of $1 \times 10^{-4}$ M, $AFB_1$ inhibited electron transport. Aflatoxin $B_1$ has been shown to inhibit electron transport between cytochrome b (Cyt b) and cytochrome c (Cyt c) or cytochrome $c_1$ (Cyt $c_1$). Bai *et al.*, (1977) investigated the effect of a single $LD_{50}$ dose of $AFB_1$ on cytochrome oxidase, NADH oxidase, succinate dehydrogenase, α-glycerophosphate dehydrogenase, fumarase, isocitrate dehyrogenase and malate dehydrogenase of rat liver and kidney mitochondria, 48 hrs after administering the $AFB_1$.

Aflatoxin $B_1$ inhibited all of the enzymes, with the exception of α-glycerophosphate dehydrogenase. The low levels of these mitochondrial enzymes during aflatoxin toxicity, observed in these studies, could point to mitochondrial injury after administration of the toxin.

Aflatoxins have also been reported to induce decreases in certain mitochondrial dehydrogenases and electron transfer catalysts in ducklings and chickens (Obidoa and Siddiqui, 1978). These researchers investigated the effects of $AFB_1$ on electron transport and oxidative phosphorylation in the guinea fowl (*Numida meleagris* Pearl.) hepatic mitochondria. The addition of different concentrations of $AFB_1$ to guinea fowl liver mitochondria was shown to inhibit oxygen consumption.

A complete interruption of oxygen uptake was observed when succinate was the respiratory substrate at an $AFB_1$ concentration of $3.3 \times 10^{-6}$ M. Succinate is an FAD-dependent substrate which donates its electrons specifically to CoQ, and thus bypasses the first phosphorylation coupling site in its oxidation pathway. Obidoa and Siddiqui (1978) effectively showed that although succinate oxidation is inhibited by $AFB_1$, the major point of inhibition was not at the dehydrogenase site, since tetramethyl *p*-phenylenediamine (TMPD) used in the study, significantly overcomes the effect. The compound (TMPD) is known to shunt electrons between Cyt b and Cyt c, thereby forestalling phosphorylation at the second uncoupling site.

These results suggested that the possible site of action of $AFB_1$ on the respiratory chain was the second crossover point. These authors suggested that any differences in the effect of $AFB_1$ on guinea fowl liver mitochondrial respiration and that of rat liver, may be attributed to inherent species differences, since the study revealed that $AFB_1$ inhibition of guinea fowl liver mitochondrial respiration is not localised at coupling site II, but may also involve inhibition around site I (Figure 2.10). These findings further explained a greater susceptibility of avian species to aflatoxin toxicity.

## 2.5 THE EFFECTS OF AFLATOXIN $B_1$ ON PROTEIN, RNA AND DNA SYNTHESIS

### 2.5.1 DNA synthesis

The interaction between $AFB_1$ and the DNA of their target organs appears to be a reaction of great consequence in the oncogenic response. Specifically, several reports show that acute and chronic carcinogen administration of $AFB_1$ inhibits mitochondrial DNA (mtDNA) synthesis (Wogan,1969).

On the basis of uptake of thymidine-$^3$H and autoradiography, De Recondo *et al.*, (1965) demonstrated that $AFB_1$ inhibited 65 % of DNA synthesis after 1 hour and 95 % after 12 hours in rats. They further demonstrated with *in vivo* techniques that the enzymes responsible for general DNA synthesis (phosphokinases, polymerases, and native DNA-activating factor) remained fully active in $AFB_1$ treated animals. In view of these results, it was assumed that $AFB_1$ acts directly on the mtDNA molecule, and inhibits its ability to act as a primer for DNA synthesis.

Friedman *et al.* (1978) also investigated the acute and subchronic effects of $AFB_1$ on the *in vitro* incorporation of thymidine-$^3$H into mtDNA. However, their experiments involved mouse liver mitochondria. Aflatoxin $B_1$ was found to induce a 50 % decrease in mtDNA synthesis acutely, with a 50 % decrease in the synthesis of high molecular weight mtDNA. Subchronic administration of $AFB_1$ also resulted in inhibition of mtDNA synthesis by 54 %. Results also showed that $AFB_1$ not only affected an inhibition of mtDNA synthesis, but also significantly reduced the primer activity of DNA isolated in the presence of the toxin.

In a general context, the results of these experiments indicate that an early effect of $AFB_1$ in rat liver is the suppression of DNA synthesis, and further that this action is a consequence of the interaction of the toxin with DNA.

According to current knowledge, a hypothesis has evolved concerning the mechanisms by which aflatoxins interfere with cellular activities viz. protein synthesis, DNA and RNA synthesis. The interaction of aflatoxin $B_1$ with DNA is thought to be the initial and critical event in the response. This interaction is expected to interfere with DNA transcription. Hence, failure of DNA transcription would impair both DNA and RNA synthesis, given that the polymerases responsible for the respective syntheses would also be inhibited. Consequently, impaired transcription would also inhibit protein synthesis.

### 2.5.2 RNA synthesis

Administration of $AFB_1$ to rats results in rapid and dramatic inhibition of the RNA precursor incorporation into nuclear RNA (Wogan, 1969). Lafarge *et al.* (1969) found that precursor incorporation into nuclear RNA was significantly inhibited within 30 minutes after $AFB_1$ administration. This inhibition was still evident 12 hours after dosing. They also showed a marked decrease in the nuclear content of RNA during the 12 hour period. The total cellular content of RNA and of DNA, however, was unaffected by the treatment.

The marked suppression of precursor incorporation into nuclear RNA and decrease in the content of nuclear RNA caused by $AFB_1$ has been reported by a number of investigators, who have studied the responses by different experimental approaches. The marked decrease in nuclear RNA following $AFB_1$ treatment, have led researchers to determine its effect on RNA polymerase, the enzyme responsible for DNA-directed RNA synthesis.

Gelboin *et al.*, (1966) determined the activity of RNA polymerase in liver cell nuclei isolated at intervals from 15 minutes to 24 hours after dosing with $AFB_1$. They reported a 60% inhibition as early as 15 minutes, which further persisted up to 2 hours. The $AFB_1$ dose used in these experiments (1mg/kg body weight) was well below the lethal dose (6mg/kg body weight) in the rat. Subsequently, it has been shown that larger doses (5mg/kg) of $AFB_1$ produced an inhibition of RNA polymerase activity that persisted for several days after dosing.

### 2.5.3 Protein synthesis

Various biochemical studies using liver slices and isolated liver nuclei have shown that $AFB_1$ administration leads to a pronounced inhibition of DNA and RNA synthesis. It should therefore be anticipated that protein synthesis should be inhibited under the same experimental conditions. Inhibition of protein synthesis has been demonstrated in rat liver preparations exposed *in vitro* to $AFB_1$. However, when studied *in vivo*, the toxin has been shown to inhibit the synthesis of only a few specific proteins, (inducible enzymes), (Wogan *et al.*, 1969). The total liver protein synthesis, however appeared to be largely unaffected by the compound.

Bhat *et al.*, (1982) designed experiments to determine the *in vivo* effects of a single (6mg/kg body weight) dose of $AFB_1$ on rat liver mitochondrial transcription and translation processes. With the use of intact hepatocytes, and also a highly selective mitoplast system for incorporation, they observed that both mitochondrial transcription and translation activities are inhibited progressively, even after 24 hrs of carcinogen administration.

Most mitochondrially translated proteins are coded for by the mitochondrial genome. The observed inhibition of mitochondrial translation products may therefore be due to the direct attack of $AFB_1$ on the mitochondrial genetic system (Niranjan *et al.*, 1986). Emeh *et al.*, (1981) investigated the effects of $AFB_1$ on hepatic transcription and translation during early stages of $AFB_1$ carcinogenesis. Their results indicated a characteristic inhibition of both heterogeneous nuclear RNA and cytoplasmic protein synthesis, of about 90 % during the initial 3-9 hours after $AFB_1$ administration, although a rapid recovery in these biosynthetic processes occurred between 12-24 hours after toxin administration.

In addition, their results showed that about 3-4 hours after *in vivo* administration of $AFB_1$, over 60 % of the carcinogen in the hepatic tissue or in isolated hepatocytes, was present in a covalently bound form. This level steadily declined to reach an undetectable level at 24 hours, suggesting that the observed recovery in translation/transcription activities may be dependent upon or related to the repair process.

Contrary to this, Backer and Weinstein (1980) showed that the level of another carcinogen, Benzopyrene in the mitochondrial genome remained nearly constant even up to 24 hours after toxin administration. This is possibly due to the lack of repair in the mitochondrial genetic system. Hence the *in vivo* administration of $AFB_1$ may lead to a prolonged inhibition of mitochondrial biosynthetic activities. These observations confirm and extend the view, that mitochondria are direct targets for attack by $AFB_1$.

## 2.6 AFLATOXIN $B_1$ BINDING TO MITOCHONDRIAL PROTEINS

The role of mitochondria in the production and maintenance of cancer phenotype has been a subject of argument ever since the pioneer work of Warburg (1930), which showed fundamental changes in the metabolic patterns of tumour tissues. A number of studies have demonstrated altered mitochondrial content (Cederbaum *et al.*, 1976, Howatson and Ham, 1955), structure and function (Feo *et al.*, 1973, Hackenbrock *et al.*, 1971, White *et al.*, 1974) in a variety of tumour cells. It has been shown that mitochondria from tumour cells have altered ultrastructural organisation, membrane composition, abnormal ion transport, and altered biochemical properties.

Bhat *et al.*, (1982) and Niranjan *et al.*, (1984) have clearly shown the presence of a unique monooxygenase system in the mitochondria, which can activate $AFB_1$ into the highly carcinogenic, electrophilic epoxide (AFBO). The activated epoxide has been shown to bind covalently to mtDNA, RNA and protein. The transport mechanism, however, for the distribution of $AFB_1$ within liver tissues has not been elucidated. Extensive studies have been carried out on $AFB_1$-protein binding as a means of toxin transport. Several studies concerning the distribution of $AFB_1$ in blood have shown that the toxin binds to serum albumin, and is carried by the blood cells and other plasma proteins (Sabbioni *et al.*, 1987).

Despite observations that the epoxide binds to proteins within the mitochondria, the actual *in vivo* disposition, characterisation and immunolocalisation of $AFB_1$-binding proteins in liver mitochondria have not been elucidated.

## 2.7 THE EFFECTS OF AFLATOXIN $B_1$ ON THE ULTRASTRUCTURE OF RAT LIVER TISSUES, ISOLATED MITOCHONDRIA AND SUB-MITOCHONDRIAL PARTICLES.

Several mycotoxicologists have used light and electron microscopy to assess effects of toxins within cell systems and experimental animals. The morphological and biochemical lesions caused by $AFB_1$ toxicity in animals appears to be exclusively in the liver (Massey *et al.*, 1995). Several histological changes (characteristic of aflatoxicosis) including haemorrhage, hepatic necrosis and bile duct proliferation have been observed, primarily within this organ (Heathcote and Hibbert, 1978; Newberne and Wogan, 1968).

At the light microscopic level, Clifford and Rees (1967) and Theron (1965) showed that rats and ducklings exhibit periportal necrosis and bile duct proliferation. Microscopic lesions associated with aflatoxicosis vary with species, duration of exposure, amount of toxin consumed, and quality of feed (Clifford and Rees, 1967; Vesonder *et al.*, 1991; Theron, 1965).

At the ultrastructural level, Svoboda *et al.*, (1966) showed gross cellular alterations and indicated that $AFB_1$ interferes with DNA synthesis in hepatoma cells of rats fed $AFB_1$-contaminated feed, by altering the structure of the nucleolus. The ultrastructural effects of $AFB_1$ on mitochondria within infected hepatocytes and liver tissues had only recently been studied. However, the role of mitochondria in cellular toxicity and cancer phenotype has been an argument of discussion ever since pioneer studies by Warburg (1930), which showed fundamental changes in the metabolic patterns of tumour tissues. Hackenbrock *et al.*, (1971) and Howatson and Ham (1955) both reported mitochondria with significantly altered ultrastructural organisation, membrane composition and altered mitochondrial function in tumour cells.

The role of mitochondria in cellular toxicity and carcinogenesis remains to be discovered. For this reason various microscopic techniques have been employed to determine the mechanism of action of $AFB_1$ and its effects on the mitochondria in liver cells. In addition, this is the first study in which immunocytochemistry has been used to specifically localise $AFB_1$ within rat liver mitochondria.

## 2.8 CONCLUSION

The specific knowledge of the chemistry, biochemistry, toxicology, and epidemiology of aflatoxins is far greater than that for any other environmentally occurring chemical carcinogen. Yet among the plethora of publications, the exact mechanism of $AFB_1$ carcinogenesis and the actual metabolic pathway leading to carcinogenesis remains unclear. Modern advances in molecular biology and biochemistry, together with basic research, only now provide research tools to explore avenues that otherwise would be quite impossible. The possible mechanism of toxin transport and the role of toxin binding to mitochondrial proteins is further emphasised in this study, as a potential factor in the metabolic fate of the toxin, and in the overall aetiology of $AFB_1$ toxicity and carcinogenesis.

# Chapter 3
# MATERIALS AND METHODS

## ETHICAL APPROVAL

***The protocol was approved by the Ethics Committee, University of Natal, Medical School, Durban.***

## 3.1 MATERIALS

### 3.1.1 Chemicals and apparatus

All chemicals were of reagent, analytical or electrophoresis grade and were obtained from one of the following sources unless otherwise stated: Sigma Chemical Co., Merck, and Boehringer Mannheim. A set of apparatus including scissors, petri dishes and centrifuge tubes were dedicated for mitochondrial use only. These were washed separately from all other glassware. All apparatus were wiped with 100% ethanol before use.

### 3.1.2 Isolation Medium

The structure of isolated mitochondria often depends on the nature of the isolation and/or suspension medium (ISOM). The composition of many buffers described in mitochondrial literature often vary according to both tissue and laboratory. Although similarities exist, it is probably true to say that the composition of buffers owes more to historical usage and personal preference than systematic study. However, certain chemicals are essential for the normal functioning of the mitochondria and these are described in Table 4.

**Table 4. Essential ingredients for mitochondrial buffers**

| Ingredient | Concentration | Rationale | Comments |
|---|---|---|---|
| Sucrose | 0.25-0.3M | Preservation of mitochondrial integrity | Most widely used osmotic agent |
| Potassium chloride | 100-150mM | Preservation of mitochondrial integrity | Not so widely used now - high ionic strength may leach out cytochrome *c* |
| EDTA | 1mM | Chelation of $Ca^{2+}$ and other divalent anions which uncouple mitochondria | Provides good respiration control |
| $Mg^{2+}$ | 5mM | Essential co-factor | Binds to ADP and ATP forming Mg-ADP and Mg-ATP complexes |
| $PO_4^{2-}$ | 5mM | Essential for ATP synthesis | Also needed for dicarboxylate transport |
| Bovine serum albumin | 1-10 mg/ml | Sequestering fatty acid and acyl-CoA's which can inhibit mitochondria. | Can also bind lipophilic inhibitors |

## 3.2 ANIMALS AND CARCINOGEN ADMINISTRATION

All experiments were carried out under aseptic conditions. Laboratory tops and benches were wiped clean using a 70% ethanol solution. In all experiments, female Wistar rats (250-300g) were used. Aflatoxin $B_1$ obtained from the Centre for Scientific and Industrial Research (CSIR), Pretoria, was dissolved in dimethyl sulphoxide (DMSO), (0.05%) and was injected intraperitoneally (ip.) at a lethal dose of 6mg $AFB_1$/kg body weight. Control rats received an equal volume of DMSO. All animals had free access to water and standard lab chow during the experiment.

After 24 hours following toxin administration, treated and untreated animals were anaethesized with ether, and sacrificed by exsanguination. Livers were immediately removed, weighed and then processed for mitochondrial isolation and electron microscopy.

## 3.3 ISOLATION OF LIVER MITOCHONDRIA AND SUB-MITOCHONDRIAL PARTICLES

Rat-liver mitochondria have long been used by researchers of mitochondrial structure and function because of the ease with which it is possible to prepare intact, pure mitochondria in high yields. The first steps in the successful isolation of largely intact mitochondria involves the rupture of the cell membrane while maintaining the structural integrity of the mitochondria. After a cell is broken, differential centrifugation may be used to separate the mitochondria from other organelles and cell debris.

Mitochondria are very easily damaged, and all necessary precautions were maintained at all times. Detergents used in washing glassware and common cations like calcium can 'uncouple' mitochondria. All buffers must therefore, be made up in double glass-distilled water. Many mitochondrial functions require mitochondrial integrity to be maintained and isotonocity of the media is usually achieved with non-ionic agents like 0.25M sucrose (Cain and Skilleter, 1987).

### 3.3.1 Mitochondrial isolation

Freshly removed rat livers (15g) were immediately placed into 30ml of ice cold ISOM, (70mM sucrose, 220mM D-Mannitol, 2.0mM Hepes buffer, 0.5mg/ml BSA, pH 7.4 using a 1% potassium hydroxide (KOH) solution just prior to use). Livers were then trimmed of fat, and placed into 60ml of fresh ISOM.

The livers were then chopped with a small scissors into minute (2mm) cubes and thoroughly washed in fresh ISOM to remove as much blood as possible. The final washing medium was free of blood. The chopped liver was then transferred to a pre-cooled glass-Teflon motorised Potter-Elvejhem homogeniser. Fresh, ice cold ISOM (2ml) was added to each gram of chopped liver. The tissue was then homogenised using six up and down strokes of the pestle rotating at 500-1000 r.p.m.

The homogenate was then filtered into a beaker, through gauze. Fresh ISOM (20ml) was then added to the filtered homogenate. The homogenate was then transferred to a centrifuge tube (50ml) and centrifuged in a Beckman J2-21 centrifuge for 10 minutes at 1000*g*. This pelleted the nucleus, red blood cells and cell debris fractions. This nuclear-debris pellet was discarded. The supernatant which contained the mitochondrial fraction was carefully decanted into a clean centrifuge tube and centrifuged at 10 000*g* for 10 minutes at 4°C. The resulting supernatant was then discarded. The mitochondria formed a soft brown pellet at the base of the centrifuge tube. The pellet also revealed an upper fluffy, light pinkish brown layer, containing broken mitochondria and microsomes. This layer was discarded. A lower layer which was white and red, comprised residual cell debris and red blood cells. This layer was also discarded. Dark brown portions of the mitochondrial pellet were discarded as it contained pelleted red blood cells.

The soft brown pellet (containing the crude mitochondrial fraction) was resuspended in 50ml of fresh ISOM using a 5mm diameter pre-cooled (4°C) glass rod, and centrifuged at 10 000*g* for 10 min. The purified pellet was then resuspended in 0.5ml of ISOM. The priority in this isolation procedure was to aim for a smaller and purer yield, than a larger one, that may be contaminated with microsomes and other debris.

### 3.3.2 Digitonin fractionation of mitochondria

The relatively recent development of techniques for separating the outer and inner membranes of liver mitochondria and the concurrent development of enzymatic markers for these membranes have permitted the overall study of submitochondrial enzyme localisation, protein function and localisation. There are two principal advantages for using fragmented mitochondria. In the first place it simplifies the system and allows certain functions to be studied in the absence of soluble components. In the second place, fragmentation overcomes the permeability barrier, imposed by mitochondrial membranes.

The techniques for separating the two membrane systems include density-gradient centrifugation following mitochondrial swelling and contraction, with controlled osmotic lysis and, treatment with digitonin in isotonic media followed by differential centrifugation (Schnaitman and Greenawalt, 1968). Of these techniques the digitonin fractionation is often the most advantageous. This procedure does not employ hypertonic density gradients and does not markedly effect the integrity of the inner mitochondrial membrane. Improvements in this technique have permitted the isolation of morphologically and biochemically intact preparations of the inner membrane-matrix fraction, which exhibits the ability to incorporate amino acids into acid-precipitable protein, and respiratory control (Greenawalt, 1974).

### *3.3.2.1 Isolation of sub-mitochondrial particles*

Stock digitonin solutions (approximately 1.2% w/v) were prepared just prior to use. Digitonin (120mg), (Sigma) was dissolved in 10ml of hot (85°C) ISOM, containing no BSA. The solution was carefully stirred on a hot plate with a magnetic stirrer, until the digitonin was completely dissolved. The solution was allowed to cool to room temperature, and then 0.1ml of a stock BSA (50mg/ml) solution was added.

The digitonin solution remains stable at 0-4°C for several hours during which time it must be used. Five millilitres of mitochondrial suspension (100mg/ml, determined by the Bradford assay, Appendix 1) was then added to a pre-cooled 20ml cylindrical vial. The vial containing the mitochondria was then surrounded by a jacket of ice, and gently stirred with a magnetic flea for 2 minutes. Five millilitres of the digitonin solution was then added and the mixture was gently stirred for 15 minutes. The digitonin-treated mitochondrial suspension (10ml) was then diluted (1:4) with fresh ISOM. The diluted suspension was stirred gently with a glass rod, and centrifuged at 10 000*g* for 10 min. The supernatant containing outer membrane and inter-membrane proteins was carefully drawn off and stored at -70°C. The pellet, designated the "crude mitoplast fraction" was diluted in 20ml of fresh ISOM and centrifuged again at the same speed for 10 min. The pellet from the second centrifugation was subsequently designated, the final mitoplast inner mitochondrial-matrix fraction or sub-mitochondrial particles (SMP's).

## 3.4 THE EFFECTS OF AFLATOXIN $B_1$ ON THE ULTRASTRUCTURE OF RAT LIVER TISSUES, ISOLATED MITOCHONDRIA AND SUB-MITOCHONDRIAL PARTICLES.

### 3.4.1 Transmission Electron Microscopy (TEM)

Freshly removed liver tissues (2g) from treated rats and untreated rats were first chopped into small (1mm) pieces with a fine blade. The tissue samples were processed according to the steps outlined in Table 5.

**Table 5. Processing of rat liver tissues for TEM**

| Step | Solution (0.5ml ) | Time |
|---|---|---|
| 1. | **Fixation**<br>Samples were fixed in 1% glutaraldehyde in 0.1M phosphate buffer, pH 7.2 | 1 hour (25°C) |
| 2. | **Buffer rinse**<br>0.1M phosphate buffer | 5 minutes |
| 3. | **Post fixation**<br>Tissues were post-fixed in 1% Osmium tetroxide | 1 hour (4°C) |
| 4. | **Buffer rinse**<br>0.1M Phosphate buffer | 10 minutes |
| 5. | **Dehydration - Graded ethanol (EtOH) series**<br>70 % ethanol<br>90 % ethanol<br>100 % ethanol<br>100 % ethanol | <br>20 minutes<br>20 minutes<br>30 minutes<br>30 minutes |
| 6. | **Ethanol : Spurr's Resin (50:50)** | 30 minutes |
| 7. | **Spurr's Resin (Full Strength)** | 1 hour (60°C) |
| 8. | **Spurr's Resin (Full Strength)**<br>Samples were embedded in gelatine drug capsules in full strength Spurr's resin | 48 hours (60°C) |

Hardened resin blocks were then removed from the gelatin drug capsules. The blocks were then trimmed with a sharp razor blade. Ultrathin sections were cut on a Reichert Ultracut microtome. Gold and silver sections were then mounted on 200-400 mesh copper and nickel grids.

Sections were then stained with 2% uranyl acetate and lead citrate according to the procedure by Reynolds (1963) and viewed with a 100S Joel Transmission electron microscope (60kV) at the Electron Microscope Unit, University of Natal.

#### *3.4.1.1 Processing of Mitochondria and Sub-mitochondrial samples*

Aqueous 1% glutaraldehyde (0.2ml) in 0.1M phosphate buffer was first placed in an eppendorf tube. One hundred and fifty microlitres of mitochondria in ISOM (30mg/ml, as determined by the Bradford Assay, Appendix 1) was then poured into the tube. The tube was then gently inverted. The mitochondria in suspension were allowed to prefix in glutaraldehyde for 1 minute. The tubes containing the pre-fixed mitochondria were then centrifuged at room temperature for 4 minutes at 15 000 *g*. The supernatant was discarded and replaced with 150µl of fresh glutaraldehyde. The mitochondrial pellet formed by centrifugation was allowed to fix in glutaraldehyde for 2 hours. After this time the pellet was gently removed from the bottom of the tube with a fine needle and washed three times with 0.25M sucrose in 0.1M phosphate buffer, pH 7.2. Samples were then stored overnight at 4°C in a fresh change of this solution. Samples were then processed according to Table 5, proceeding from Step 5.

### 3.4.2 Immunocytochemistry

In immunocytochemistry, labelled antibodies are used as reagents for the detection of specific substances or antigens *in situ*. Immunocytochemistry may therefore be defined as the identification and localisation in a biological system of any constituent or inclusion to which an antibody may be raised and marked by a visible label (Snyman, 1993).

In the present study, ICC has been employed in the identification and localisation of $AFB_1$ within liver tissues and mitochondria with the use of a polyclonal $AFB_1$ antibody. Polyclonal antibodies are normally the antibodies of choice, as they can recognise many epitopes of a single antigen (Snyman, 1993). Tissue sections are exposed to the primary antibody (anti-$AFB_1$) which is then visualised by a labelled secondary antibody (goat anti-rabbit IgG gold probe). This gold probe is a gold sphere (5-10nm in diameter).

### *3.4.2.1 Procedure*

For the immunolocalisation of $AFB_1$ within the liver tissues and isolated mitochondrial samples from treated and untreated rats, a modified post-embedding labelling technique (Polak and van Noorden, 1983) was used. Samples were processed according to Table 5, with the exception of Step 3, the post fixation in osmium was omitted. Sixty nanometer (nm) thick sections were placed on 200 mesh nickel grids. Sections were etched with 5% hydrogen peroxide (0.2ml per grid) for 3 minutes to block endogenous peroxidase activity.

The grids were then placed in a drop of distilled water and jet washed with 10ml of distilled water. The grids were then drained and dried on a fibre free paper, and incubated at room temperature in normal goat serum (NGS), (100µl per grid) for 30 minutes, to block non-specific binding sites. The grids were subsequently incubated in 20µl of primary polyclonal rabbit anti $AFB_1$ (Sigma) for 3 hours, using a working dilution of 1:100. The grids were then placed in a droplet of 50mM Tris, pH 7.2, and jet washed with the same solution, using 20ml of solution per grid.

The samples were then placed in a droplet of 50mM Tris containing 0.2 % BSA, pH 7.2, and jet washed with the same solution, using 5ml of solution per grid. The grids were then transferred to a droplet of 50mM Tris containing 1 % BSA, pH 8.2, for 5 minutes. Grids were then incubated in a droplet of IgG-gold (10µl) diluted 1:15 in Tris/BSA, pH 8.2, for 1 hour. Samples were then placed in droplets and jet washed as before using : a) 50mM Tris containing 0.2 % BSA (10ml/grid), pH 7.2, for 10 minutes; b) 50mM Tris, (5ml/grid), pH 7.2, 5 minutes and, c) distilled water (5ml/grid), 10 minutes.

The grids were then counterstained with 2 % uranyl acetate (100µl per grid) and lead citrate (100µl per grid) according to the procedure by Reynolds (1963) and viewed with a 100S Joel Transmission electron microscope (60kV).

### 3.4.3 Light Microscopy for Immunohistochemistry

#### *3.4.3.1 Tissue preparation for embedding in wax*

Small pieces (1 x 1cm) of freshly isolated rat livers (15g) from treated (6mg $AFB_1$/kg body weight) and untreated rats were immediately placed in a 10% formalin solution for 24 hours at room temperature. The liver samples were then transferred to a 50% EtOH solution for 1 hour, and then a 70% and 90% EtOH solution for 30 minutes each. The samples were then dehydrated in a 100% EtOH solution for 2 hours.

The livers slices were placed in a 50:50 EtOH (100%):Xylene (100%) solution for 30 minutes. Samples were then transferred to a 100% xylene solution for 1 hour. The livers were then placed in three changes of paraffin wax at 55°C, for 3 hours, and then overnight in a fresh change of wax at 55°C. The samples were finally embedded in fresh wax.

### 3.4.4 Immunohistochemistry (IHC)

Immunohistochemistry has proven to be a remarkable tool in aflatoxin exposure studies at the individual level. Santella *et al.*, (1993) and Hsieh *et al.*, (1984) have both shown that quantitative histochemical methods can be used to monitor exposure to Aflatoxin $B_1$ by identification and measurement of DNA adducts in liver tissues. These researchers have used indirect immunohistochemical staining to identify imidazole ring opened $AFB_1$-DNA adducts in liver sections from treated rats (2.5mg $AFB_1$/kg body weight), and human liver from patients presenting with HCC in Taiwan. Immunohistochemistry can also be used to localise toxins within liver cells at a light microscope level. Wax blocks were sectioned using a Leica RM 2025 Ultra-cut microtome (Leica Instruments, Germany). Two to five nanometer thick sections (picked on poly-L-lysine coated slides, Sigma) were used for the immunohistochemical localisation of $AFB_1$ within the liver tissues. Samples were then processed according to procedures outlined in Table 6.

The avidin-biotin complex system was selected for this study, as it is more sensitive than most other label systems for antigen detection. This methodology employs a primary antibody, a biotinylated secondary antibody, and a preformed biotinylated avidin molecule complexed with the horse-radish peroxidase complex . The immuno-substrate used was diaminobenzidine (DAB), (Figure 3.1).

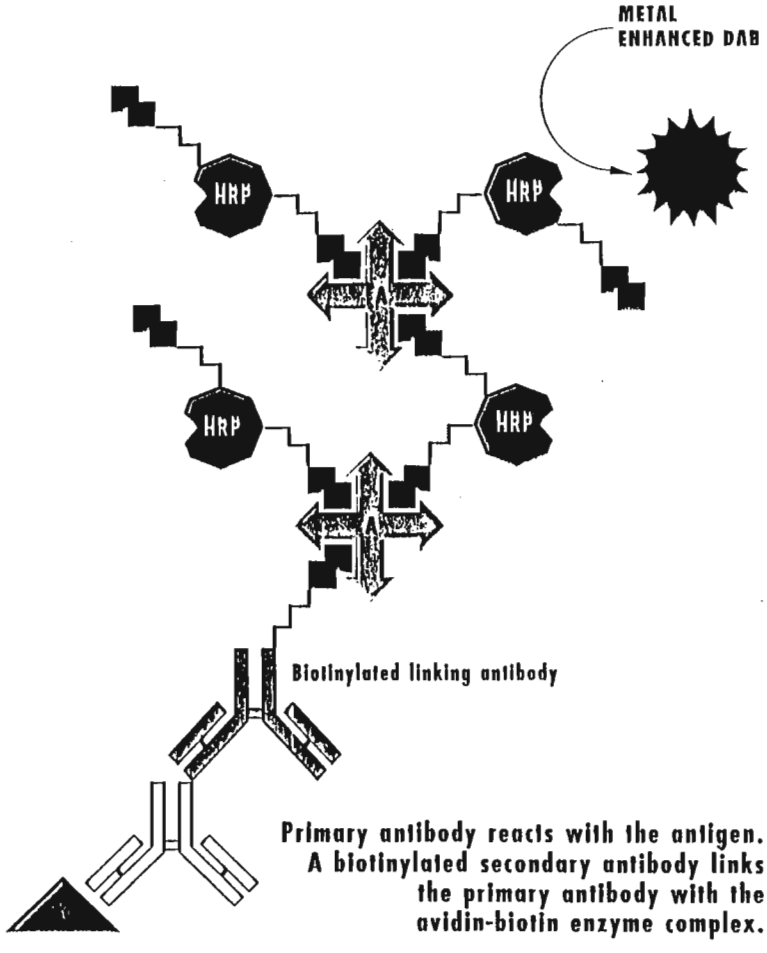


**Figure 3.1** **A schematic representation of the avidin-biotin complex labelling system (Snyman, 1993)**

**Table 6. Avidin-Biotin method for immunohistochemical localisation of Aflatoxin $B_1$**

| PROCEDURE | TIME |
|---|---|
| Dewaxing in xylene, 10ml, (x2) | 2-4 minutes |
| Dehydration 100% ethanol, 10ml, (x2) | 2-4 minutes |
| Dehydration 90% ethanol, 10ml | 2 minutes |
| Dehydration 70% ethanol, 10ml | 2 minutes |
| Repeated washing in water , 10ml | 5 minutes |
| Section delimited with delimiting pen | |
| Droplet NGS (20µl); (1:20) | 20 minutes |
| NGS drained off using fibre free paper | |
| **Droplet of polyclonal primary antibody (20µl) Rabbit-anti-$AFB_1$ (1:200)** | **3 hours** |
| Buffer wash in PBS (pH 7.4) | 5 minutes |
| **Droplet of secondary antibody (20µl) Biotinylated goat-anti-rabbit IgG (1:200)** | **30 minutes** |
| Stained with DAB | 5 minutes |
| Washed in deionised water (20ml) | 5 minutes |
| Stained with haematoxylin | 3 minutes |
| Washed in deionised water and allowed to blue (20ml) | 5 minutes |
| Mounted with coverslip using Kaiser's glycerol jelly - stored in dark until viewing | |

## 3.5 POLYACRYLAMIDE GEL ELECTROPHORESIS OF MITOCHONDRIAL PROTEINS

Polyacrylamide gel electrophoresis (PAGE) is most often the method of choice for the separation and characterisation of various biological macromolecules. Analytical electrophoresis of proteins is often carried out in polyacrylamide gels under conditions that ensure dissociation of the proteins into their individual polypeptide subunits, and that minimise aggregation.

The strongly anionic detergent sodium dodecyl sulphate (SDS) is most commonly used in combination with a reducing agent and heat, to dissociate the proteins before they are loaded on the gel. Most proteins are soluble in SDS and bind it avidly. Even the most basic proteins are converted to their acidic SDS-derivatives. The denatured polypeptides bind SDS and become negatively charged. The amount of SDS bound is almost always proportional to the molecular weight of the polypeptide and is independent of its sequence. Hence SDS-polypeptide complexes migrate through the polyacrylamide gel in accordance with the size of the polypeptide. Approximately 1.4g of detergent is bound per gram of polypeptide.

Sodium dodoecyl sulphate-polyacrylamide gel electrophoresis is often carried out with a discontinuous buffer system in which the buffer in the reservoirs is of different pH and ionic strength from the buffer used to cast the gel. The negatively charged SDS-protein derivatives are subjected to an electric current, which causes them to migrate toward the anode. After migrating through a stacking gel of high porosity, the complexes are deposited in a very thin zone on the surface of the resolving gel. Hence the discontinuous buffer system has the ability to concentrate all of the complexes in the sample into a very small volume, allowing greatly increased resolution of the gel. The sample and the stacking gel contain Tris.Cl (pH 6.8), the upper and lower buffer reservoirs contain Tris-glycine (pH 8.3), and the resolving gel contains Tris.Cl (pH 8.8).

All components of the system contain 0.1% SDS (Laemmli, 1970). Polyacrylamide gels are composed of chains of polymerised acrylamide that are cross-linked by a bifunctional agent such as *N,N'*-methylenebisacrylamide. The effective range of separation of SDS-polyacrylamide gels depends on the concentration of polyacrylamide used to cast the gel and on the amount of cross-linking. Cross-links formed from bisacrylamide add rigidity and tensile strength to the gel and form pores through which the SDS-polypeptide complexes must pass. The size of the pores decreases as the bisacrylamide:acrylamide ratio increases, reaching a minimum when the ratio is approximately 1:20. Most SDS-polyacrylamide gels are cast with a molar ratio of biscarylamide:acrylamide of 1:29. The sieving properties of the gel are determined by the size of the pores, which is a function of the absolute concentrations of acrylamide and bisacrylamide used to cast the gel.

Table 7 shows the linear range of separation obtained with the gels cast with concentration of acrylamide that range from 5% to 15%.

**Table 7. Effective range of separation of SDS-polyacrylamide gels.**

| Acrylamide[a] concentration (%) | Linear range of separation (kDa) |
|---|---|
| 15 | 12-43 |
| 10 | 16-68 |
| 7.5 | 36-70 |
| 5.0 | 57-212 |

[a]Molar ratio of bisacrylamide:acrylamide is 1:29

### 3.5.1 Procedure

Mitochondrial proteins were subjected to PAGE using a SE '250'- "Mighty Small II", Slab Gel Electrophoresis Unit (Hoefer Scientific instruments, San Franscisco), with reagents as listed in Appendix 2.

All components of the system were thoroughly cleaned with double-distilled water and dried with ethanol just before use. Two sandwiches, each constructed with a glass plate (12 x 10 cm), spacers and a notched alumina plate were mounted against a central vertical core. Two separate upper buffer chambers, each having a capacity to hold 75ml of buffer were formed when the sandwiches were clamped to the central vertical core.

The central core with the attached plate sandwiches was placed on a pre-heated (60°C) glass plate. At the same time, a 1% agarose solution was maintained at 60°C in the oven until needed. Melted agarose was then run down the edge of one spacer, into the first assembled sandwich, with a pre-heated (60°C) Pasteur pipette. The entire unit was tilted gently so as to spread the agarose evenly across the bottom of the sandwich. As the agarose hardened it formed a plug of gel that sealed the bottom of each sandwich.

In this study, 10% gels were used to resolve all protein samples analysed. All components of the gel were mixed in the order shown in Table 8.

**Table 8. Solutions for preparing resolving gels for Tris-glycine SDS-polyacrylamide gel electrophoresis**

| Solution | Component volumes (ml) per gel mold volume of | | |
|---|---|---|---|
| Components | 5ml | 10ml | 15ml |
| | | | |
| **10%** | | | |
| $H_20$ | 1.9 | 4.0 | 5.9 |
| 30% Acrylamide mix | 1.7 | 3.3 | 5.0 |
| Resolving gel buffer (pH 8.8) | 1.3 | 2.5 | 3.8 |
| 10% SDS | 0.05 | 0.1 | 0.15 |
| 10% Ammonium persulphate | 0.05 | 0.1 | 0.15 |
| TEMED | 0.002 | 0.004 | 0.006 |
| | | | |

The polymerisation initiator, ammonium persulphate and the crosslinker, N,N,N',N'-tetramethylethylenediamine (TEMED) were added just before the gel was poured. The concentration of ammonium persulphate that was used was generally higher than that used in other methods. The higher concentration eliminated the need to rid the solution of dissolved oxygen (which retards polymerisation) by degassing. The acrylamide resolving gel solution was then gently poured into the gap between the glass and alumina plates. Sufficient space was allocated for the stacking gel (the length of the teeth of the comb plus 1cm). With the use of a Pasteur pipette, the acrylamide solution was overlaid with 5ml of a resolving gel overlay solution (0.375M Tris.Cl; pH 8.8; 0.1% SDS). The overlay prevents oxygen from diffusing into the gel and inhibiting polymerisation.

The entire apparatus was left at room temperature in an undisturbed area. After gel polymerisation (30-40 minutes), the overlay was carefully poured off and the top of the gel was then thoroughly washed several times with deionised water, to effectively remove any unpolymerised acrylamide. The water was then drained off from the top of the gel with a 5ml syringe. Any remaining water was removed with the edge of a fibre free paper. The 4% stacking gel was then prepared in a disposable plastic tube. The appropriate volume of solution containing the desired amount of acrylamide for the stacking gel was prepared, using the values given in Table 9. All components of the gel were mixed in the order shown.

**Table 9. Solutions for preparing a 4% stacking gel for Tris-glycine SDS-polyacrylamide gel electrophoresis**

| Solution components | Component volumes (ml) per gel mold volume of 10ml |
|---|---|
| **4%** | |
| $H_20$ | 6.8 |
| 30% Acrylamide mix | 1.7 |
| Stacking gel buffer (pH 6.8) | 1.25 |
| 10% SDS | 0.1 |
| 10% Ammonium persulphate | 0.1 |
| TEMED | 0.01 |

The initiator and crosslinker were added just before the stacking gel was poured. Without delay, the mixture was rapidly swirled and poured directly onto the surface of the polymerised resolving gel. A clean Teflon comb that would create the desired amount of wells was immediately inserted into the stacking gel. The comb was moved slightly to avoid trapping air bubbles. Additional stacking gel solution was added to fill spaces of the comb completely. The entire apparatus was left at room temperature in an undisturbed area.

While the stacking gel was polymerising, the mitochondrial samples (200µl of isolated mitochondria in ISOM; 30mg protein/ml) were prepared by heating them to 100°C for 2 minutes in an equal volume of 2x treatment Buffer (0.125M Tris.Cl; pH 6.8; 4% SDS; 20% glycerol; 10% 2-mercaptoethanol). After heating, samples were cooled to room temperature. A sample of SDS-electrophoresis protein molecular weight markers (Boehringer Mannheim) was also denatured in the same way. The markers used included :

| | | | |
|---|---|---|---|
| 1. | α2-Macroglobulin | 170 | kDa |
| 2. | β-galactosidase | 116 | kDa |
| 3. | Fructose-6-phosphate kinase | 85.2 | kDa |
| 4. | Glutamate dehydrogenase | 55.6 | kDa |
| 5. | Aldolase | 39.2 | kDa |
| 6. | Triosephosphate isomerase | 26.6 | kDa |
| 7. | Trypsin inhibitor | 20.1 | kDa |
| 8. | Lysozyme | 14.3 | kDa |

The markers were first removed from the freezer and allowed to defrost in the refrigerator at 4°C for 1 hour. Ten microliters of each marker was then added to a clean eppendorf tube and allowed to mix. To this solution containing the eight markers, 80ml of 2x treatment buffer was added, and the solution was then heated for 2 minutes at 100°C. A small amount (10µl) of bromophenol blue (0.1%) was added to the pre-treated samples and markers. Thirty microlitres of marker solution was loaded per well on the gel. The remainder of the marker solution was stored at 4°C.

After polymerisation of the stacking gel (30-40 minutes), the Teflon comb was carefully removed. The loading wells were washed with deionised water to remove any unpolymerised acylramide. The entire central core, containing the polymerised gels was then mounted onto the electrophoresis apparatus, by simply snapping across the centre of the lower buffer chamber. Two gel well markers were secured onto the glass plates. Tris-glycine electrophoresis tank buffer (0.025M Tris; pH 8.3; 0.192M glycine; 0.1% SDS) was poured into both the top (150ml) and bottom (250ml) reservoirs, and also into all of the wells, until each well was completely filled.

Any bubbles that became trapped at the bottom of the gels were immediately removed with a bent hypodermic needle attached to a syringe. Thirty microlitres of each mitochondrial sample (30mg/ml) was loaded in a predetermined order into the bottom of the wells. The samples, including the molecular weight markers were carefully loaded with a 50µl Hamilton microlitre syringe. After each sample, the syringe was rinsed repeatedly in four sets of deionised water, twice in 100% ethanol, and twice in fresh tank buffer, to effectively clean it before the next application. The safety lid was then placed onto the unit. The electric leads were connected to the central core and also to the power supply (red to anode), (Leica Instruments). The entire apparatus was then surrounded by a jacket of ice packs. A constant current of 0.85 mA/sq.cm of gel was applied. The gels were run until the tracking dye reached the bottom of the gels (+/- 5mm from the bottom of the glass plate). The power supply was then turned off.

The gel sandwiches were then carefully removed from the central core and placed on a paper towel. The plates were carefully and gently pried apart with a spatula. The orientation of the gel was marked by cutting a corner from the bottom of the gel that was closest to the leftmost well (slot 1). Gels that were used for western immunoblotting were not marked.

One set of the gels were fixed and stained with Coomassie Blue, and the other was used to transfer proteins from the gel onto a nitro-cellulose membrane (0.45μm pore size, Millipore). The mitochondrial polypeptides separated by SDS-polyacrylamide gel electrophoresis were simultaneously fixed with methanol:glacial acetic acid and stained with Coomassie Brilliant Blue R250, a triphenylmethane textile dye.

The entire gel was immersed in 250ml of the stain solution (0.125% Coomassie Blue R250, 50% methanol, 10% acetic acid) and placed on a slowly rotating platform for 4 hours at room temperature. The stain was then carefully poured off into a dark bottle, and stored in a dark cupboard for future use. The stained gel was then soaked in a destaining solution I (Appendix 1), on a slowly rocking platform for 4 hours. The destain solution was changed at least 3-4 times during this time. The gel was then placed in a destain solution II (Appendix 1) on a rocking platform overnight. After destaining, the gel was immediately photographed, to make a permanent record. The gel was subsequently stored at 4°C in deionised water containing 20% glycerol.

## 3.6 WESTERN BLOTTING

In western blotting, electrophoretically separated components are transferred from a gel to a solid support and probed with reagents that are specific for particular sequences of amino acids. Most western blots are carried out by direct transfer of proteins from the gel to a nitro-cellulose filter. Several types of electrophoresis apparatus for western blotting are available. Older types incorporate wet blotting, where the entire apparatus is immersed in an electrophoresis transfer tank. Blotting usually takes approximately twelve hours to complete.

The newer type of apparatus, a semi-dry graphite electrode transblot apparatus (Hoefer Instruments, Germany) was used in this study. The test equipment comprised a base tray with one graphite plate secured firmly onto it, and a free, lid type graphite electrode that fitted firmly onto the base plate. The electric leads then connects to a voltage pack.

### 3.6.1 Transfer of proteins onto nitro-cellulose membranes.

When the SDS-polyacrylamide gel was approaching the end of its run, the graphite plates were carefully rinsed with distilled water. Any beads of liquid that adhered to them were wiped of with a non-absorbent tissue. Protective surgical gloves were worn throughout this experiment. Oils and secretions from the skin will prevent the transfer of proteins from the gel to the filter. In addition, proteins from the skin may also contaminate the samples. Extreme care must be taken to avoid such contamination. Six pieces of Whatman 3MM paper and one piece of nitro-cellulose filter (0.45μm pore size, Millipore) were then cut to the exact size of the SDS-polyacrylamide gel. If the filter paper is larger than the gel, the overhanging edges of the paper and filter will touch, causing a short circuit.

This will prevent the effective transfer of proteins from the gel. The nitro-cellulose filter was marked in one corner with a soft-lead pencil. The nitro-cellulose filter was then wetted briefly by floating on the surface of a tray of deionised water. The filter was allowed to wet from beneath by capillary action. After 2 minutes, the filter was completely submerged in the water for 5 minutes to displace any trapped air bubbles. The six pieces of 3MM paper were placed in a shallow tray containing 30ml of transfer buffer (39mM glycine, 48mM Tris base, 0.037% SDS, 20% methanol, pH 8.3).

Three sheets of 3MM paper, in perfect alignment were placed on the bottom electrode (the anode). The sheets were then rolled with a glass pipette to remove any trapped air bubbles. The wetted nitro-cellulose was then placed (exactly aligned) on the stack of 3MM paper. Any trapped air bubbles were then removed by rolling the sheets with a glass pipette. The SDS-polyacrylamide gel was then removed from the glass-alumina plate sandwich and transferred briefly to a tray of transfer buffer for 5 minutes. The gel was then placed exactly on top of the nitro-cellulose filter. The gel was orientated so that the mark on the filter corresponded with the bottom left-hand corner of the gel. The remaining three sheets of 3MM paper were then placed on top the gel, again in perfect alignment.

The entire stack was gently rolled with a glass pipette to remove any air bubbles. The upper electrode (the cathode) was carefully placed on top of the stack. The electrical leads were connected (red lead to the bottom electrode) and a constant current of 0.65mA/sq. cm. of gel was applied for 1.5 hours.

The entire apparatus was surrounded by a jacket of ice packs. After 1.5 hours of transfer, the current was turned off, and the leads disconnected. The stack was dissembled by gently peeling each layer off in turn. The gel was placed in tray of Coomassie blue and stained as described earlier. This allowed one to check if electrophoretic transfer was complete. The bottom left-hand corner of the filter was then cut off, as an insurance against obliteration of the pencil mark. The filter was then stained with Ponceau S.

### 3.6.2 Staining proteins immobilised on nitro-cellulose filters

The Ponceau S stain is completely compatible with all methods of immunological probing, because the stain is transient and is completely washed away during processing of the western blot. The stain does not, therefore interfere with the subsequent detection of antigens by chromogenic reactions, catalysed by antibody linked enzymes such as horseradish peroxidase.

Staining with Ponceau S is generally used to provide visual evidence that electrophoretic transfer of proteins has taken place, and to locate molecular weight markers, whose positions are then marked with pencil. Following electrophoretic transfer of mitochondrial proteins from the SDS-polyacrylamide gel to the nitro-cellulose filter, the filter was briefly allowed to float on the surface of a tray of deionised water. The filter was then transferred to a tray containing a working solution of Ponceau S stain (Appendix 1).

The filter was incubated in the stain for 10 minutes, with gentle agitation. When the protein bands became visible, the nitro-cellulose filter was washed in several changes of deionised water at room temperature. The positions of proteins used as molecular-weight standards were then marked with pencil or water-proof black ink.

### 3.6.3 Blocking binding sites for immunoglobulins on the nitro-cellulose filter

The nitro-cellulose filter was now ready for immunological probing. The blot was soaked in 30ml of 3% BSA in saline solution (0.9% NaCl/10mM Tris-HCl, pH 7.4) for 2 hours. The sections of the paper that do not contain protein were therefore blocked to prevent non-specific binding and also to reduce background staining. The blocking solution was discarded and the filter was immediately transferred to a heat sealable plastic bag.

### 3.6.4 Binding of the primary and secondary antibody to the target protein.

All western blots are probed in two stages. An unlabelled antibody specific to the target protein is first incubated with the nitro-cellulose filter in the presence of a blocking solution. The filter is then washed and incubated with a secondary reagent, anti-immunoglobulin that is either radiolabelled or coupled to an enzyme such as horseradish peroxidase. After further washing, the antigen-antibody-antibody complexes on the nitro-cellulose filter are located by autoradiography or *in situ* enzyme reactions.

In this study a target protein was not directly probed. Instead, the presence of protein-bound $AFB_1$ was targeted (Figure 3.2).

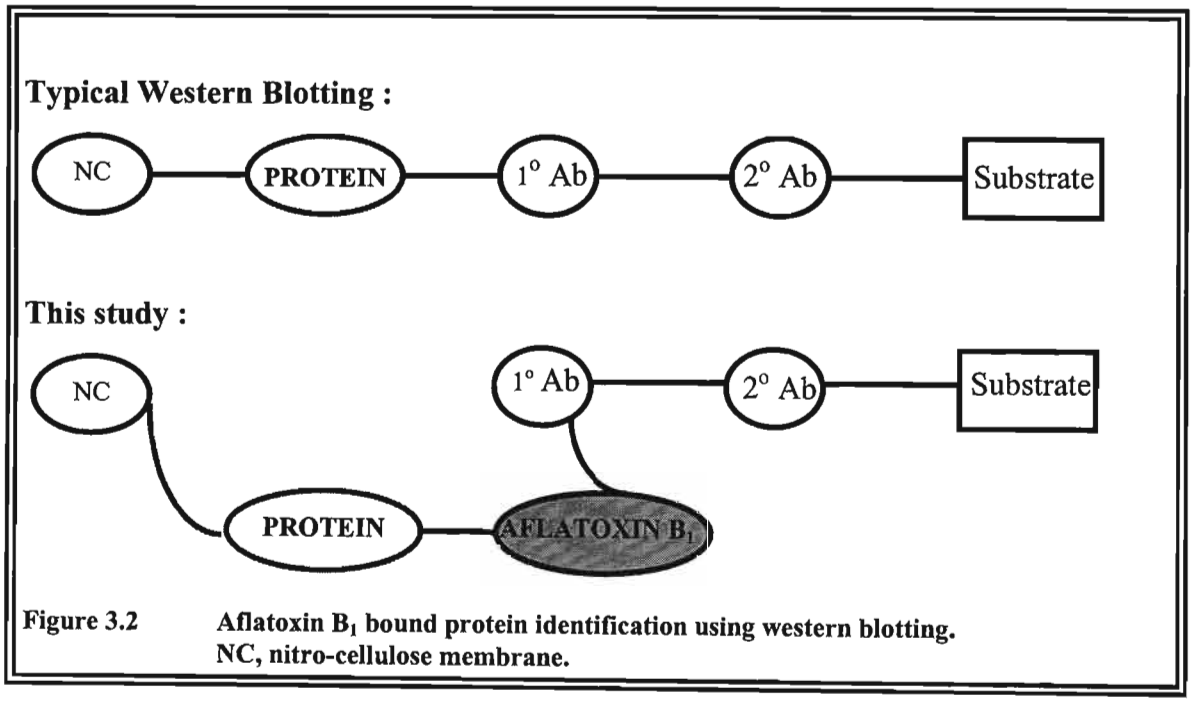


**Figure 3.2** **Aflatoxin $B_1$ bound protein identification using western blotting. NC, nitro-cellulose membrane.**

The filter was incubated at room temperature in 20µl of primary antibody (polyclonal anti-$AFB_1$, Sigma) diluted 1:10 in saline containing 3% BSA and 10% rabbit carrier serum. The sealed plastic bag was rocked on a platform shaker for 4 hours. The plastic bag was then cut open and the antibody solution discarded. The filter was thoroughly washed in five changes of saline (10 minutes each). After washing, the filter was incubated for 2 hours at room temperature with 15µl of the secondary antibody (Goat anti-rabbit antibody conjugated to horseradish peroxidase, Sigma), diluted 1:500 in saline containing 3% BSA.

### 3.6.5 Chromogenic substrate localisation of antigen-antibody-antibody complexes

The blots were then repeatedly washed in 5 changes of saline (10 minutes each) and transferred to a clean petri-dish. A solution of DAB (10ml) was then poured over the filter and gently rocked for 60 seconds (Appendix 1). The reaction was terminated as soon as the bands became visible. The blot was immediately plunged into deionised water to stop the reaction. The stained filter was washed in saline (2 minutes) and transferred to a tray of deionised water. The blot was immediately photographed for a permanent record.

## 3.7 DIRECT IMMUNODETECTION OF AFLATOXIN $B_1$ ON SDS-POLYACRYLAMIDE GELS.

Direct immunodetection of antigens on polyacrylamide gels was developed by Olden and Yamada (1970). Although western blotting is more advanced, this method was tried to confirm results produced by the western blots. We found that a higher resolution was obtained using this technique, compared with the western blots. This could be attributed to the fact that the western blot was not a typical experiment, as described earlier (Section 3.6 and Figure 3.1). The concentration of protein-bound toxin was fairly minute and would therefore be extremely difficult to locate. By direct detection on polyacrylamide gels, the possible loss of toxin during transfer was minimised. For this procedure, gels were first fixed and all the SDS removed. All steps were performed with gentle agitation using 500-1000 ml of each solution listed below. After electrophoresis, gels were fixed in 50% trichloroacetic acid for 2 hours.

They were then washed for 1 hour in 7% acetic acid, for 16 hours in 1% Triton X-100/ 7% acetic acid, for 48 hours in two changes of 0.1% Triton X-100/ 7% acetic acid, and for 24 hours in 7% acetic acid. The acetic acid was then washed out with phosphate buffered saline (PBS) for 2 hours. Following the removal of SDS, the slab gels were cut into strips with a pizza slicer, and transferred to a small container (a small plastic coverslip container was ideal). The gels were then incubated with primary and secondary antibodies in the same procedure as described for western blots in Section 3.6. Bound antibody could also be detected by increased Coomassie blue staining of an antigen band.

## 3.8 THE ABSORPTION OF AFLATOXIN $B_1$ (μg $AFB_1$/mg mitochondrial protein) BY INTACT AND VIABLE RAT LIVER MITOCHONDRIA

Several Aflatoxin $B_1$ metabolites ($AFB_1$-8,9-epoxide and $AFB_1$-8,9-dihydrodiol) are known to react with cellular macromolecules such as DNA (Swenson *et al.*, 1974), RNA (Swenson *et al.*, 1977), and proteins (Iwaki *et al.*, 1993), resulting in the formation of covalent adducts. Extensive studies have shown that $AFB_1$ can bind to several proteins including histones (Groopman *et al.*, 1980), nuclear non-histone proteins and albumin (Sabbioni *et al.*, 1987). None of these studies however have elucidated a quantitative result that indicates the amount of toxin bound by each of these proteins. Several studies however, have indicated that $AFB_1$-DNA binding is ten times greater, and $AFB_1$-rRNA twenty times greater, than $AFB_1$-protein binding (Lijinsky *et al.*, 1970; Garner and Wright, 1975). No study however has concentrated on the binding of toxin to specific mitochondrial proteins, or the amount of carcinogen bound per milligram of mitochondrial protein.

In a simple approach, this study attempts to provide a quantitative picture of the amount of toxin bound per milligram of mitochondrial protein present in the sample. All experiments were in duplicate.

### 3.8.1 Treatment of isolated mitochondria:

Mitochondria (22mg protein/ml), suspended in fresh isotonic 70mM sucrose buffer, were first incubated at 37°C for 10 minutes. To each experimental sample, 0.5μg Aflatoxin $B_1$ ($AFB_1$), per milligram mitochondrial protein (dissolved in 100μl of 0.4% DMSO) was added. The mitochondrial samples containing toxin were then incubated at 37°C for 1 hour. Control samples received an equal volume of DMSO only and were also incubated for the stipulated times. After incubation, the samples were plunged into ice, and then centrifuged at 15000g for 4 minutes, to pellet the mitochondria. The mitochondrial pellets and supernatants were gently removed and stored at -70°C for high pressure liquid chromatography (HPLC) and western blotting.

### 3.8.2 Isolation of Aflatoxin $B_1$

The pelleted mitochondria and supernatant fractions were then freeze-dried using a Virtis 8L Research Freeze Drying System. To the dried supernatant fractions which contained sucrose (designated Eppendorf 1), 500μl of chloroform ($CHCl_3$) was first added and the mixture was thoroughly vortexed.

The chloroform was then filtered through a Pasteur pipette containing sodium sulphate and glass wool, into a clean glass vial. The above procedure was repeated three times, and all the filtered chloroform was transferred to the vial. Following $CHCl_3$ extraction, 500μl of water was added to the Eppendorf 1, which contained the undissolved sucrose crystals. This would dissolve the sucrose crystals and release any toxin that may have been sequestered by the crystals. To this sucrose solution in Eppendorf 1, 500μl of $CHCl_3$ was added to effectively extract any toxin that may be present. The solution was then vortexed. The chloroform (bottom layer) was then carefully removed with a syringe and transferred to Vial A above. The above extraction was also repeated three times, by adding fresh $CHCl_3$ to the water-sucrose solution.

This procedure ensured a thorough extraction of $AFB_1$ present in the sample, hence preventing significant loss of toxin during experimental preparation. Finally, the Pasteur pipette was washed with fresh $CHCl_3$, at least twice, all of which was collected in the vial A. The $CHCl_3$ in the vial was then evaporated at 30°C in the presence of a nitrogen atmosphere and stored at 4°C.

### 3.8.3 High Pressure Liquid Chromatography

The technique of HPLC is a popular tool of research, as it enables the analysis of a variety of compounds. The methods are easily adapted for a variety of purposes including simple identification and confirmatory procedures to more complex quantitative and qualitative procedures.

Test equipment comprised a Spectro-Physics FL2000 fluorescence detector, a reverse phase column and a Millipore filter cartridge. All solvents used were of HPLC grade. The evaporated samples and standard $AFB_1$ (CSIR, Pretoria) were then derivatized. The derivatizing agent (DVA) was prepared by adding 0.15ml of $H_2O$ to 2.85ml of trifluoroacetic acid (TFA). The DVA (1.5ml), was then added to the dry extract and left to incubate at room temperature for a period of 30 minutes, in order to form hemi-acetal adducts. The extracts were once again evaporated to dryness in a nitrogen atmosphere.

The dried extracts were then reconstituted in acetonitrile to the desired concentration in g/ml. The HPLC mobile phase comprised of 10% acetonitrile, 10% 2-propanol, and 2% acetic acid. High pressure liquid chromatography was performed using a Phenomanex LC18 column with fluorescence detection at 360 nm (excitation) and 440 nm (emission). The flow rate of the mobile phase was maintained at 1.0 ml/min. All samples were injected in duplicate. Samples that were too concentrated were appropriately diluted (Figure 4.61). High pressure liquid chromatography revealed the presence of toxin within the mitochondrial pellet fraction from treated samples. The exact nature of the toxin, however, whether in free form or conjugated to protein was not elucidated by the study.

Hence, a simple dot blot of the mitochondrial pellet fraction, prior to $CHCl_3$ extraction, was used to determine if aflatoxin present in the sample was in fact protein bound. The method for the treatment of mitochondria is described earlier. The treated and untreated mitochondrial samples were first thawed on ice for 20 min. Samples were then spotted (20µl) on a strip of nitro-cellulose membrane (Figure 3.3). The membrane was allowed to dry at room temperature. The nitro-cellulose filters were then immunoprobed and stained according to the method described in section 3.6.

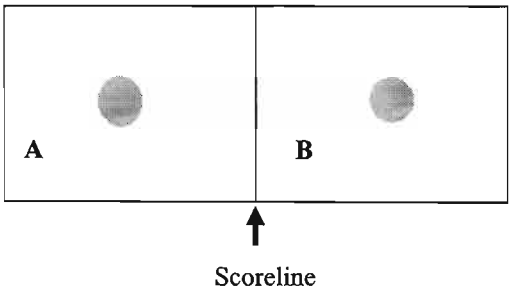


**Figure 3.3** **Diagrammatic representation of a nitro-cellulose membrane spotted with raw samples of (A) Untreated control mitochondria in sucrose (70mM) buffer (20µl); (B) Treated mitochondria, Mitochondrial pellet fraction (20µl).**

# Chapter 4
# RESULTS

## 4.1 TRANSMISSION ELECTRON MICROSCOPY

### 4.1.1 Rat liver tissues

Samples of liver tissue from treated rats showed increases of heterochromatin in the peripheral and scattered cells of several nuclei; the nucleolus showed distinct micro-segregation (Figure 4.1). Untreated rat liver tissues however, revealed nuclei that contained a single nucleolus with peripheral heterochromatin and regular profiles of the nuclear membrane (Figure 4.2). Mitochondria in both treated and untreated tissues were numerous. Cristae were well developed and the mitochondrial membranes largely intact.

Several mitochondria in the experimental tissues exhibited distorted and elongated forms (Figure 4.3; 4.4) as compared to control samples which were well rounded and regular in shape (Figure 4.2).

### 4.1.2 Isolated Mitochondria

Isolated mitochondria from the livers of untreated rats showed distinct, well rounded and relatively even sized mitochondria (Figure 4.5; 4.6). The outer and inner membranes were clearly discernible and the cristae were also distinct (Figure 4.5; 4.6). The control samples also exhibited minimal mitochondrial division. Mitochondria from experimental samples however revealed several grossly swollen giant mitochondria (Figure 4.7). In addition, these samples showed high incidence of regular mitochondrial division (Figure 4.8).

Several mitochondria in treated samples revealed an extension of the outer membrane, to exhibit a budding type of mitochondrial division (Figure 4.9). Several mitochondria isolated from treated rats revealed a distinct separation of membrane components; the outer membrane appeared to be separated from a condensed and granular matrix (Figure 4.10).

### 4.1.3 Isolated Sub-Mitochondrial Particles (SMP's) - Inner membrane fraction

Control samples indicated fully expanded circular forms with most of the inner membrane largely intact and with numerous minute circular particles extending from the base of the inner membrane (Figure 4.11). In addition numerous paracrystalline filaments were observed in the control samples as compared to experimental samples (Figure 4.12).

Experimental samples however, showed great disruptions in inner membrane integrity (Figure 4.13). There was also an abundance of damaged fibrillar and membranous material present (Figures 4.13; 4.14). The numerous particles found in the control samples (Figure 4.11) were hardly present in the experimental samples (Figures 4.13; 4.14).

## 4.2 IMMUNOCYTOCHEMISTRY

### 4.2.1 Rat liver tissues

Conjugated gold labelled $AFB_1$ was successfully located in several organelles within the liver tissues from treated rats. Label was found within several mitochondria and also closely associated with the mitochondrial membranes and matrices (Figure 4.15; 4.16; 4.17). Bound toxin was also localised in the nucleus and along the nuclear membrane (Figure 4.18), in the nucleolus and bordering its membranes (Figure 4.19), in areas of cytoplasmic clearing (Figure 4.20) and also within the endoplasmic reticulum and along its membranes (Figure 4.21).

### 4.2.2 Isolated Mitochondria and Sub-mitochondrial particles from treated and untreated rats

Immunogold-labelling of $AFB_1$ was specific within the experimental mitochondrial samples (Figure 4.22). Method controls for isolated mitochondria and SMP's did not reveal the presence of bound toxin. In most cases, experimental samples revealed label scattered throughout the mitochondrial matrix which remained finely granular (Figure 4.23). Cristae were not easily visible. Label was also found near the mitochondrial membranes (Figure 4.23). Label was frequently found within dividing mitochondria (Figure 4.24) and along the membrane of division (Figure 4.25).

Toxin was often found within the inter-membrane space and also in the areas of the outer membrane (Figure 4.25). No label was found in the control samples (Figure 4.26). No label was located in isolated SMP's from untreated rats (Figure 4.27). The particles were well rounded, the inner membrane was largely intact and there appeared to be an abundance of particles extending from the base of the membranes in the control samples (4.27). Experimental fractions showed the presence of $AFB_1$ in close proximity to damaged membranous fractions (Figure 4.28) and in definite association with the inner membrane (Figure 4.29). Conjugated gold label was also found within paracrystalline filaments in the treated samples (Figure 4.30). Method controls were very specific, no label was found in both control SMP samples (Figure 4.31) and also in the treated SMP samples (Figure 4.32).

### 4.2.3 Isolated mitochondria in 70mM sucrose - Treated with $AFB_1$ (0.5µg $AFB_1$/mg mitochondrial protein).

The mitochondria suspended in 70mM sucrose assumed an orthodox conformation. The matrix was finely granular and the cristae hardly visible (Figures 4.33). The mitochondria were generally oval to spherical in shape. Bound toxin was located in most mitochondria from samples treated with a single dose of toxin (0.5µg $AFB_1$/mg mitochondrial protein).

Toxin was often found within the mitochondrial matrix and within the intermembrane fraction (Figure 4.34). Label was also found closely associated with both the outer and inner membranes within budding mitochondria (Figures 4.35). Toxin was also found within mitochondria where matrix clearing appeared to be occurring (Figure 4.36). Bound toxin was also located in areas of distinct membrane damage or breaks, with the associated swelling of cristae and matrix clearing, particularly in areas of localised toxin (Figure 4.37). The appearance of toxin in treated samples appeared to damage the membranes of several mitochondria, allowing the extrusion of the mitochondrial matrix (Figure 4.38). Sub-mitochondrial samples isolated in 70mM sucrOse showed no label in control samples (Figure 4.39). Toxin was localised within treated SMP's (Figure 4.40) and also closely associated with the inner mitochondrial membrane fragments (Figure 4.41).

### 4.2.4 Isolated mitochondria in 250mM sucrose - Treated with $AFB_1$ (0.5µg $AFB_1$/mg mitochondrial protein)

The mitochondria suspended in 250mM sucrose revealed a distinct change in ultrastructure, from the orthodox conformation to a highly configured form (Figure 4.42). The cristae were easily visible (Figure 4.42; 4.43). The inner and outer membrane components were also easily discernible (Figure 4.43). Immunocytochemistry revealed the presence of bound toxin within the mitochondrial matrix and cristae of treated mitochondrial samples (Figures 4.44). Several mitochondria showed distinct membrane breaks and membranous damage, with the associated clearing of mitochondrial matrices, particularly in areas of localised toxin (Figure 4.45).

Bound toxin was also located in areas of the outer membrane, where the membrane appeared to be dissolved, and with the associated swelling of the cristae in that region (Figure 4.46). Figure 4.47 also shows a mass of labelled toxin at the outer membrane region of the mitochondria. Label was also located within distorted mitochondria, which displayed swollen cristae (Figure 4.48). No toxin was found in the control-untreated mitochondrial samples (Figure 4.42).

## 4.3 LIGHT MICROSCOPY - IMMUNOHISTOCHEMISTRY

The presence of the chromagen, diaminobenzidine (DAB), was successfully located in liver tissues from treated rats. No stain was found in the untreated samples (Figure 4.49) or the method controls (Figure 4.50). In the first experimental sample, examined 30 minutes after injection, toxin was located within the cytoplasm of infected cells (Figure 4.51). Stain was also found bordering the cell membranes (Figure 4.51). After 2 hours a large amount of toxin was found within the cells. The entire cytoplasm appeared to be infiltrated with toxin. The nuclei however remained largely uncontaminated (Figure 4.52).

In the 24 hour samples the stain was found within the cytoplasm and also within the nuclei. Several cells showed distinct membrane damage and associated cytoplasmic clearing (Figure 4.53).

## 4.4 POLYACRYLAMIDE GEL ELECTROPHORESIS

### 4.4.1 Mitochondrial protein and rat serum albumin concentrations in untreated and treated rats

Protein concentrations were determined using the Bradford Assay (1976), (Appendix 1). Rats were sacrificed 24 hours after toxin administration.

**Table 10.** **Absorbance (595 nm) and protein content (mg/ml) of unknown mitochondrial samples isolated from rat liver (15g), (E = experimental mitochondria, C= control mitochondria), and in rat serum albumin (5ml).**

| Sample | ABS (595 nm) | | Mean | Protein Content (mg/ml) |
|---|---|---|---|---|
| No. | 1 | 2 | | |
| $E_1$ | 0.525 | 0.500 | 0.512 | 25.00 |
| $C_1$ | 0.272 | 0.310 | 0.291 | 14.55 |
| $E_2$ | 0.523 | 0.520 | 0.521 | 24.00 |
| $C_2$ | 0.267 | 0.317 | 0.292 | 14.60 |
| | | | | |
| Serum Albumin C | 0.354 | 0.398 | 0.376 | 18.80 |
| Serum Albumin E | 0.562 | 0.689 | 0.625 | 31.25 |

**Percentage increase in protein concentration between control and experimental samples :**
Mitochondrial protein increased by 41.8% following toxin treatment.
Rat serum albumin increased by 40% in treated animals.

Inverted light density - images of the polyacrylamide gels also confirmed an increase in protein concentration established by the Bradford assay above. Protein staining was more dense in the experimental fractions of both experimental mitochondria and SMP's isolated from the same part of the rat liver (15g), (Figures 4.54b, c and 4.55b, c).

This was not as easily visible in the normal Coomassie blue stained gels (Figures 4.54a & 4.55a). Rat serum albumin samples from treated and untreated rats also revealed a higher concentration of albumin in the experimental sample (Figure 4.56).

### 4.4.2 Protein profiles of rat liver mitochondrial and sub-mitochondrial fractions

Mitochondrial fractions were repeatedly resolved on polyacrylamide gels to first establish a constant result. The experimental fractions were first diluted 1:40 so that the bands could be easily resolved. The fractions obtained from different rats were all identical, indicating that the extraction procedures were correct and constant (Figure 4.57). The mitochondrial proteins that were resolved were in the molecular weight range of 10-200 kDa. There were no significant differences between protein patterns from mitochondria isolated from the livers of untreated and treated rats (Figure 4.57; lanes 2 and 3 respectively). In addition, there were no differences in protein profiles between control mitochondria and mitochondria that were treated with toxin (Figure 4.57; lanes 4 and 5 respectively).

The isolated sub-mitochondrial fraction showed a lower number of proteins than the mitochondrial crude samples (Figure 4.58). The proteins that were not resolved included the outer membrane proteins and the inter-membrane fraction proteins. There were no significant differences between protein patterns of SMP's isolated from untreated and treated rats (Figure 4.58).

## 4.5 WESTERN BLOTTING

The diaminobenzidine chromagen was rather difficult to use, resulting in rapid background staining and at the same time, extremely rapid fading in the presence of light, particularly during the few minutes of photographing. Given the different nature of the western blot procedure and the minute concentration of toxin bound to a particular protein in a single band of the gel, the staining was indeed faint and at times was only discernible to a trained eye. Nevertheless, the specificity of binding was determined by repeated trials, taking extreme caution to maintain all laboratory conditions exactly the same during each trial. Basic factors like temperature differences, unnecessary vibrations and irregular shaking all seemed to effect the staining reaction.

The western-immunoblots of the inner mitochondrial-matrix fraction (Figure 4.58) from treated rats revealed the presence of 5 $AFB_1$-bound protein fragments in the following molecular weight range (154kDa, 50kDa, 25kDa, 18kDa, 14kDa), (Figure 4.59).

## 4.6 DIRECT IMMUNODETECTION ON POLYACRYLAMIDE GELS

The presence of $AFB_1$-bound proteins in the inner mitochondrial membrane-matrix fraction (Figure 4.58) was further confirmed by this technique, which in this instance provided a more visible result as the immunolocalisation was directly on the gel.

The results confirmed the presence of the same 5 $AFB_1$-bound protein fragments in the same molecular weight range (154kDa, 50kDA, 25kDA, 18kDA, 14kDA), (Figure 4.60).

## 4.7 HIGH PRESSURE LIQUID CHROMATOGRAPHY

High pressure liquid chromatography revealed the presence of toxin in both the supernatant and mitochondrial fraction. With the use of a 5.5µg $AFB_1$ standard (>80% fluorescence), fluorescence chromatograms revealed the presence of toxin in the supernatant sucrose buffer fraction at 7% fluorescence (0.3µg.ml$^{-1}$ peak) and in the treated mitochondrial pellet fraction at 70% (4.6µg.ml$^{-1}$ peak), (Figure 4.61).

**Initial Dose = 5.5µg $AFB_1$/mg mitochondrial protein present in sample**

| | | |
|---|---|---|
| Percentage HPLC recovery | = | 89 % |
| Amount of toxin internalised by mitochondria | = | 84 % |
| Amount of toxin in supernatant | = | 5.4 % |

These results suggest that approximately 84% of the initial dose was internalised by the mitochondria, indicating that approximately 4.6µg of $AFB_1$ was internalised by every milligram of mitochondrial protein present in the sample.

**"Internalised"** is the operative word, because although HPLC revealed the presence of toxin within the mitochondrial fraction analysed, the exact nature of the toxin within this fraction, whether protein bound or not, needed to be elucidated.

For this, a simple dot blot of the HPLC mitochondrial fraction was used against untreated control mitochondria (Figure 4.33). The results indicated that the toxin within the HPLC fraction analysed was in fact protein bound (Figure 4.62).

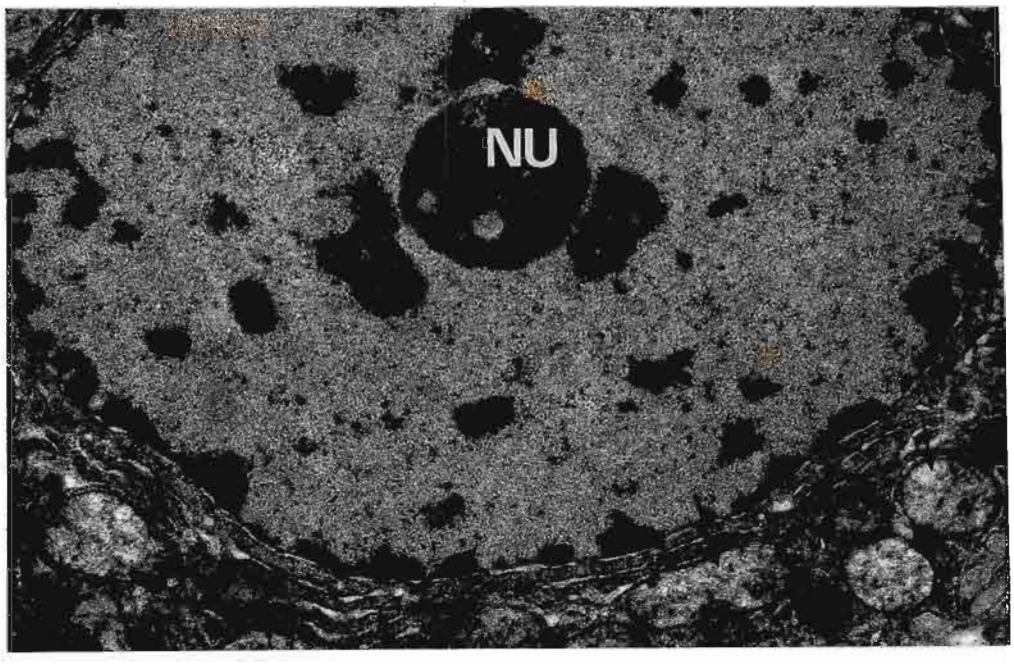


Figure 4.1 Liver from rats treated with a single dose of toxin (6mg $AFB_1$/kg body weight). Chromatin segregation is evident, the nucleolus (NU) showing distinct microsegregation. Mitochondria (arrows) are swollen and show distinct clearing of martices, X8000.

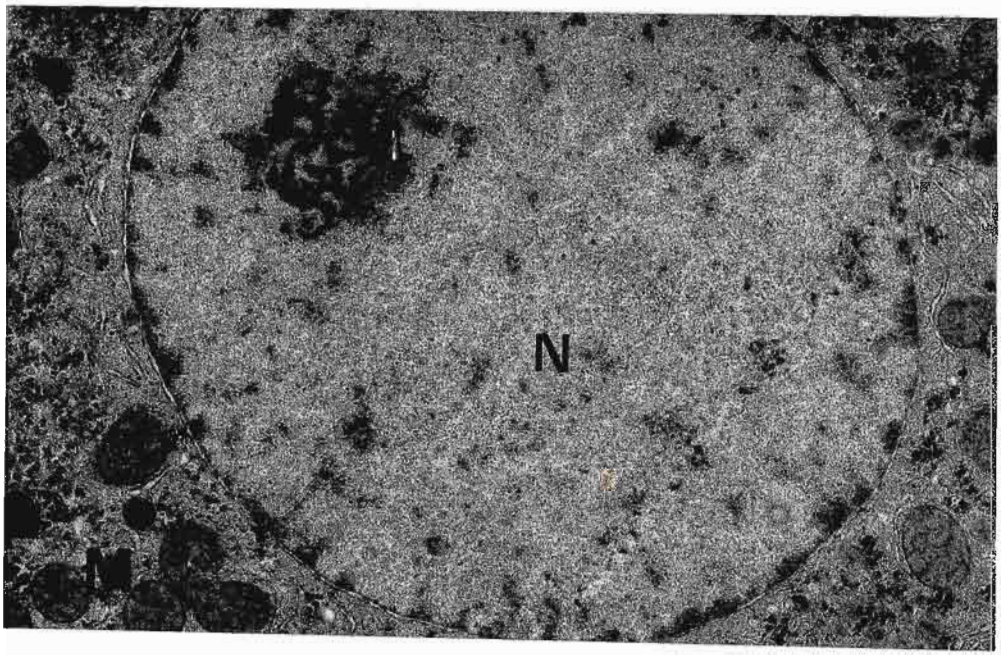


Figure 4.2 Liver from control-untreated rats. The nucleus (N) contains a single compact nucleolus showing peripheral heterochromatin and regular profiles of the nuclear membrane, X6000.

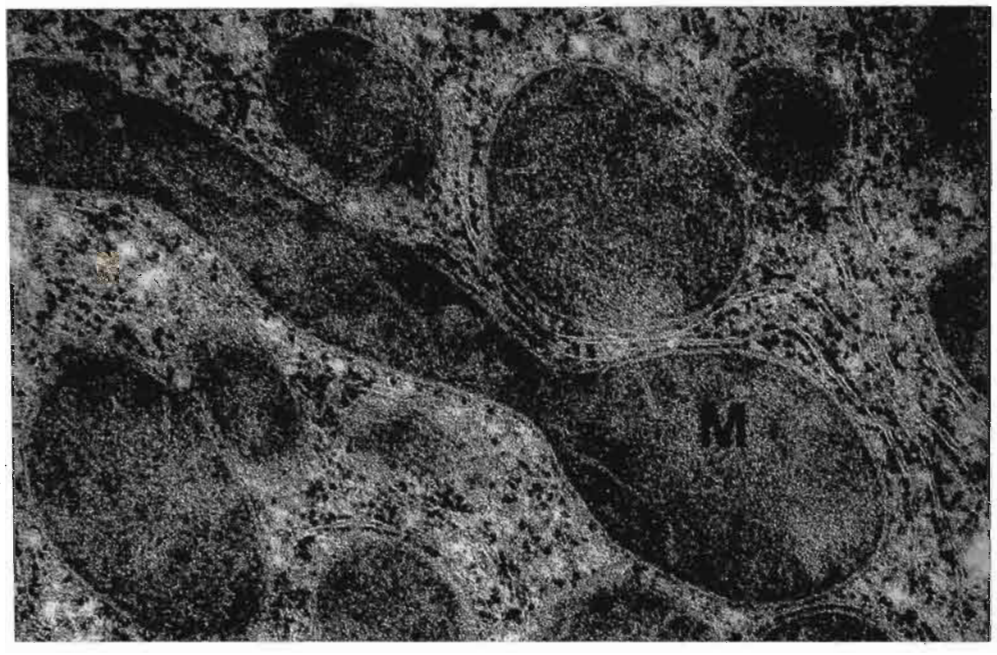


Figure 4.3 Liver tissue from a toxin treated rat showing a distorted and enlarged mtiochondrion (M), X30 000.


Figure 4.4 Liver tissue from a toxin treated rat showing an elongated mitochondrion (M), X 12 000.


Figure 4.5 Electron micrograph of isolated mitochondria from untreated rats. The inner and outer membrane (arrows) and cristae (C) are discernible, X15 000.

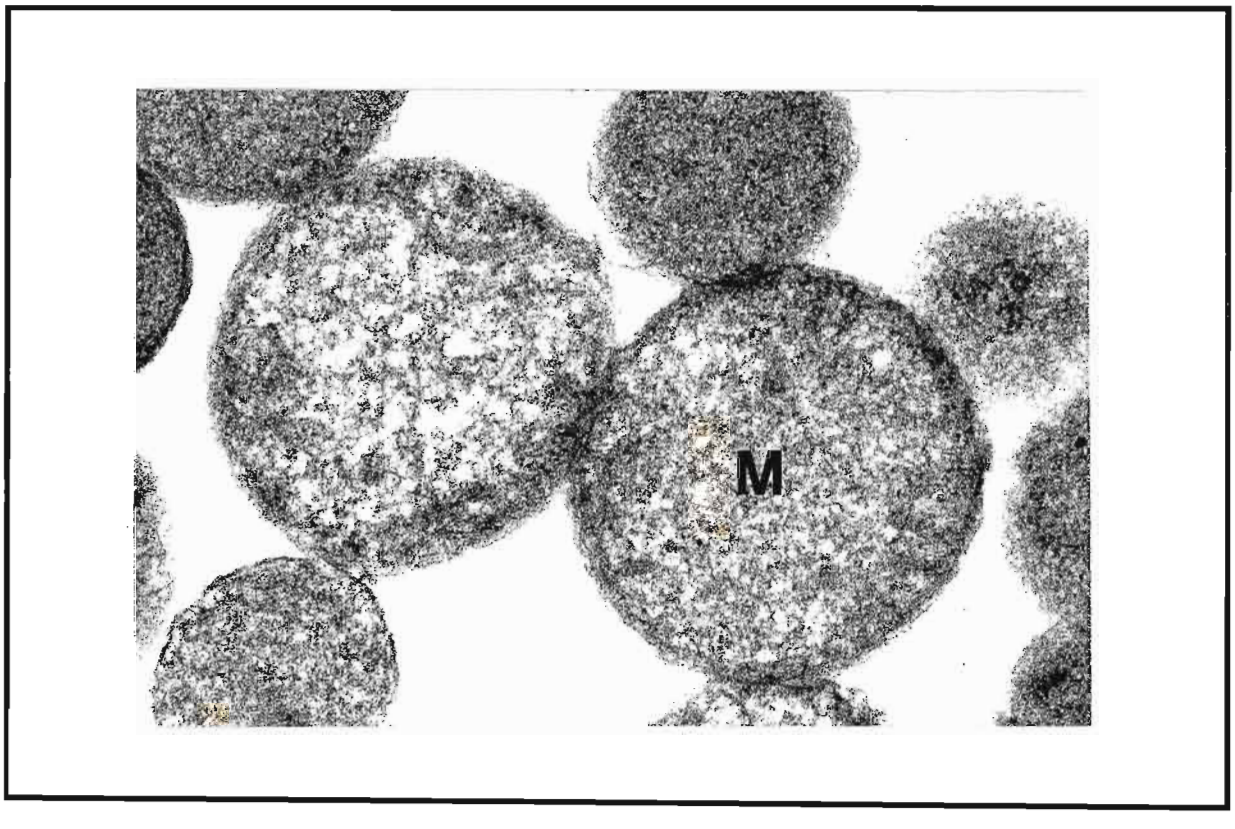


Figure 4.6 Electron micrograph of isolated mitochondria from untreated rats. The mitochondria (M) are well rounded and are of even size, X30 000.

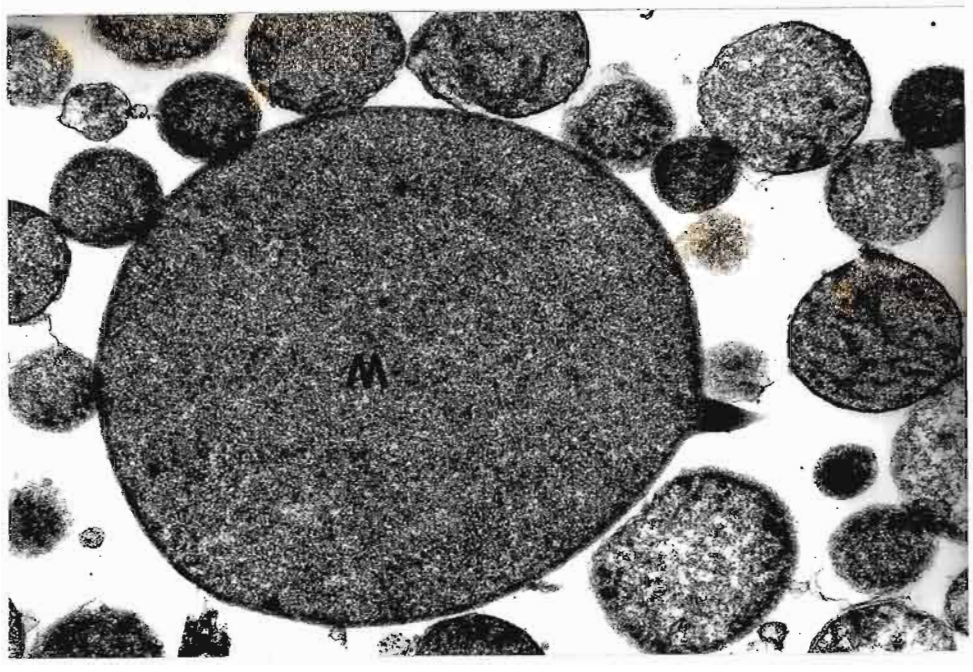


Figure 4.7 A solitary grossly swollen giant mitochondria (M) is seen among numerous normal-looking mitochondria isolated from the liver of a toxin treated rat, X10 000.

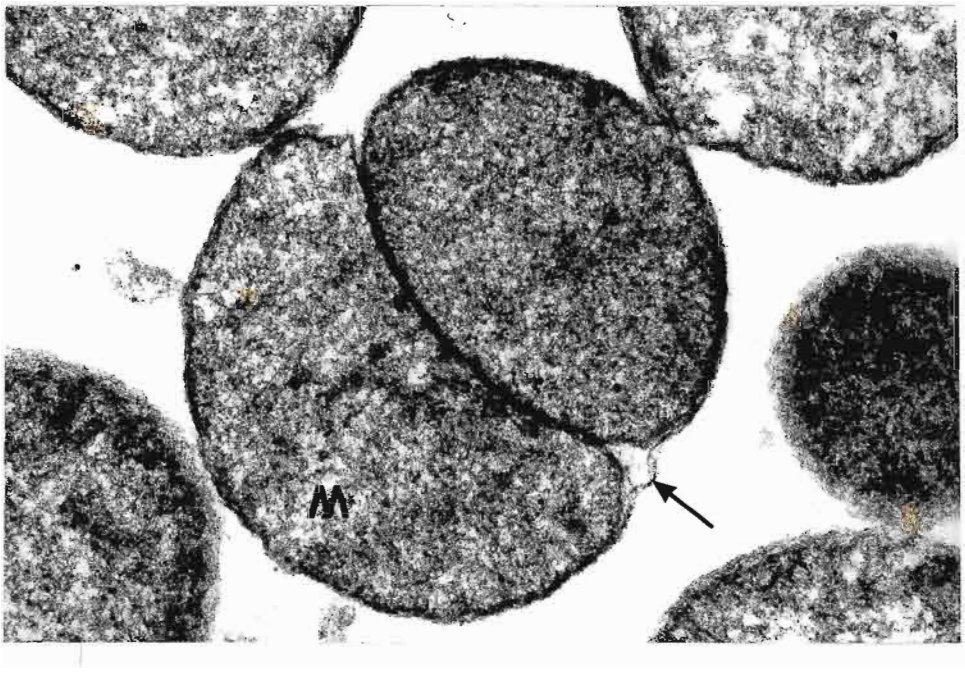


Figure 4.8 Isolated liver mitochondria from a toxin treated rat showing a dividing mitochondrion (M). The division appears as a continuation of the outer membrane (arrow), X30 000.

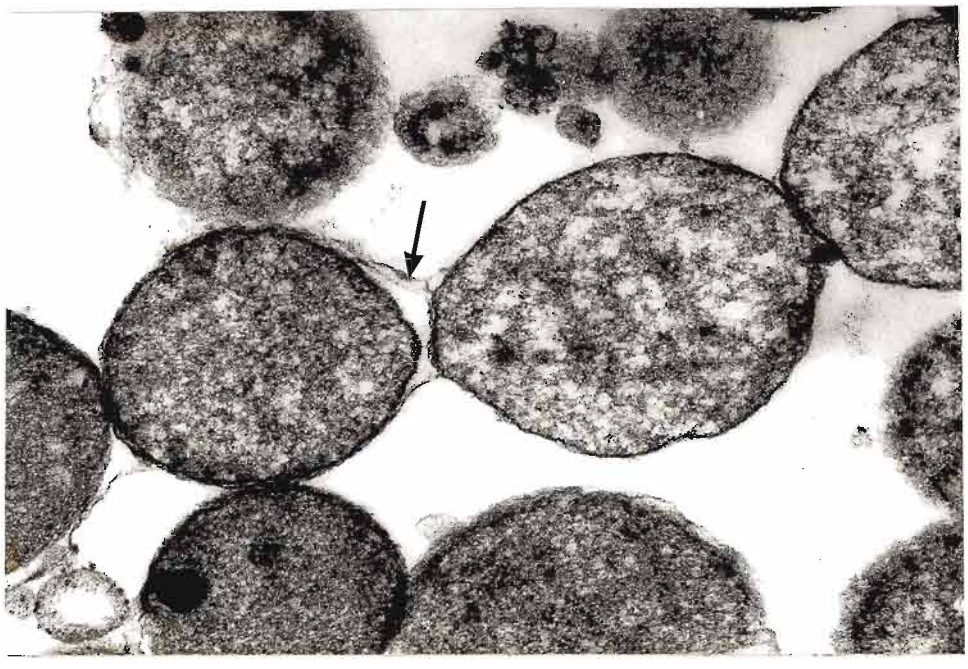

Figure 4.9 Isolated rat liver mitochondria displaying a budding type of division. The outer membrane (arrow) is continuous with all dividing mitochondria, X15 000.

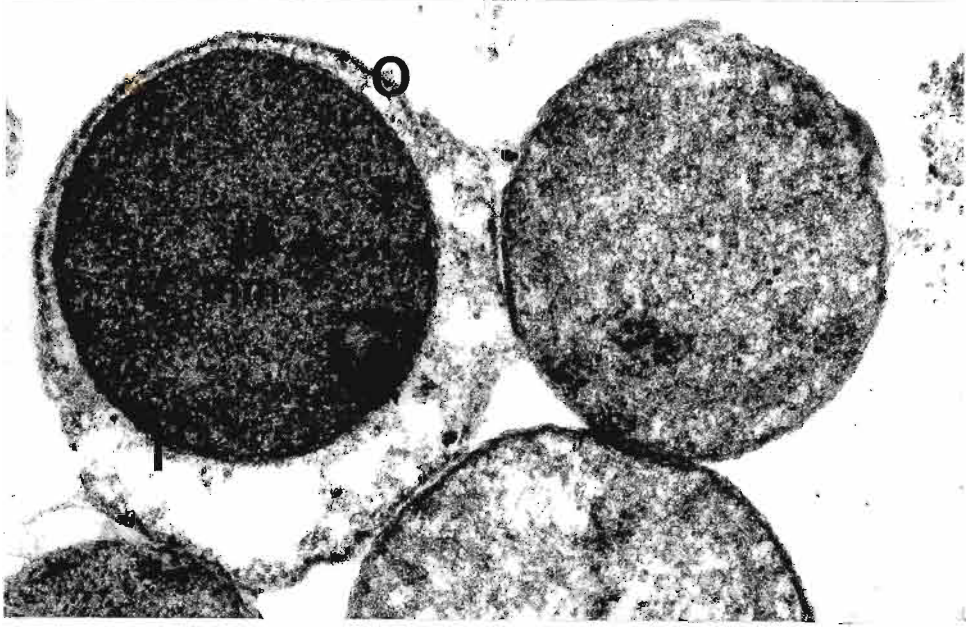


Figure 4.10 Isolated liver mitochondria from treated rats showing a mitochondrion with a condensed and granular matrix (MM). The inner (I) and outer (O) membrane are separated, X30 000.

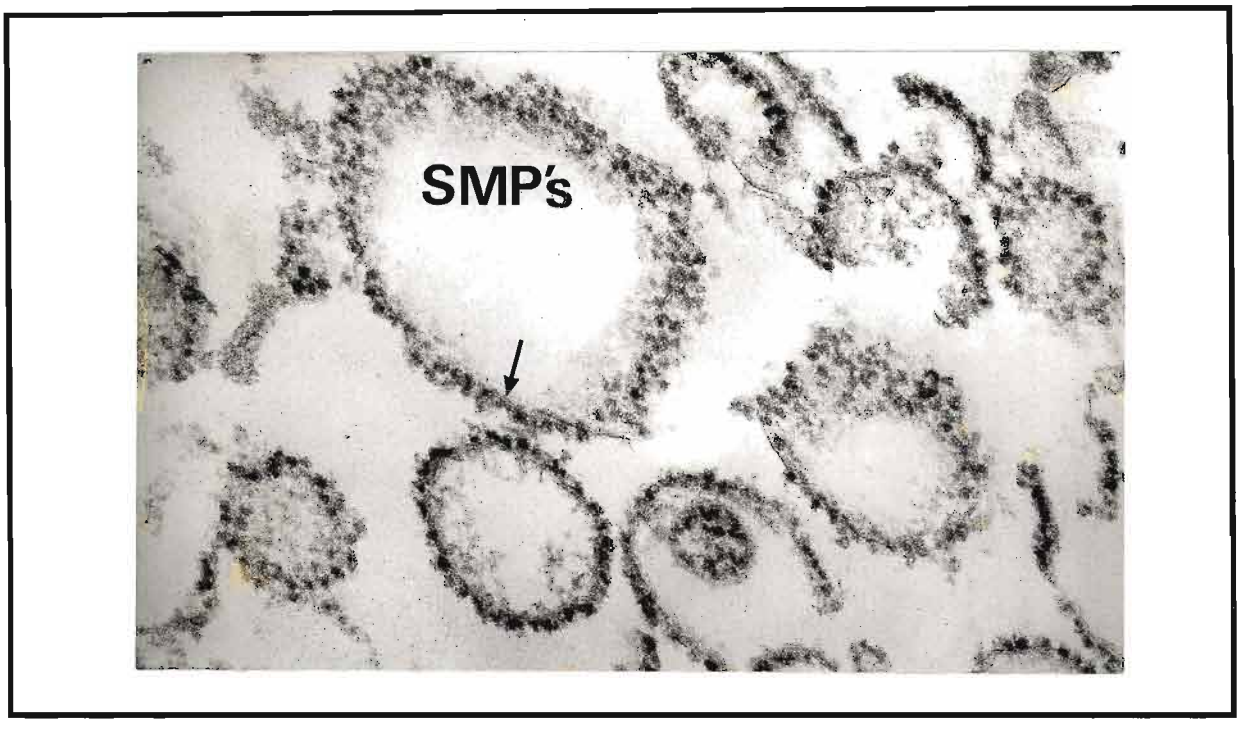


Figure 4.11 Digitonin treated mitochondria (untreated rats), showing several round sub-mitochondrial particles (SMP's). Most of the inner membrane appeared intact (arrow) and with numerous circular particles on the matrix side of the membrane, X50 000.

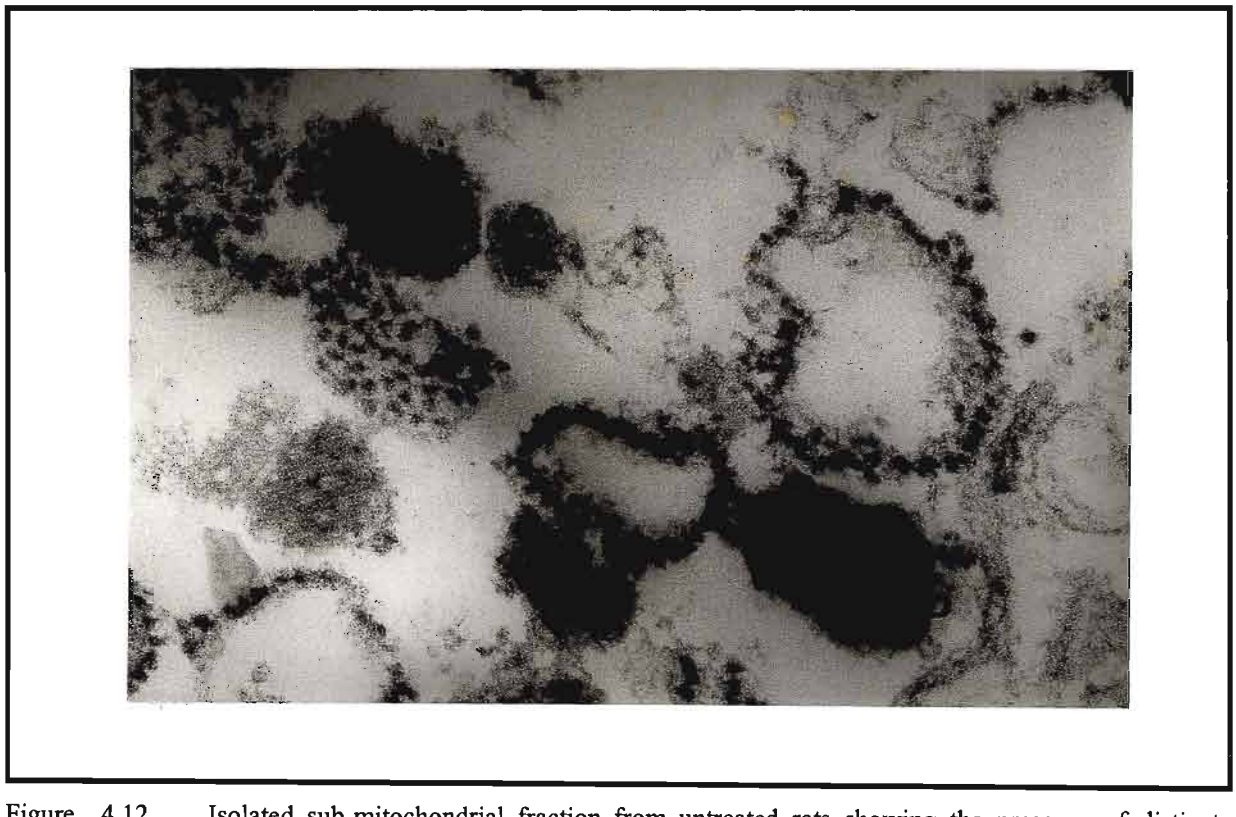

Figure 4.12 Isolated sub-mitochondrial fraction from untreated rats showing the presence of distinct paracrystalline inclusions (P), x50 000.

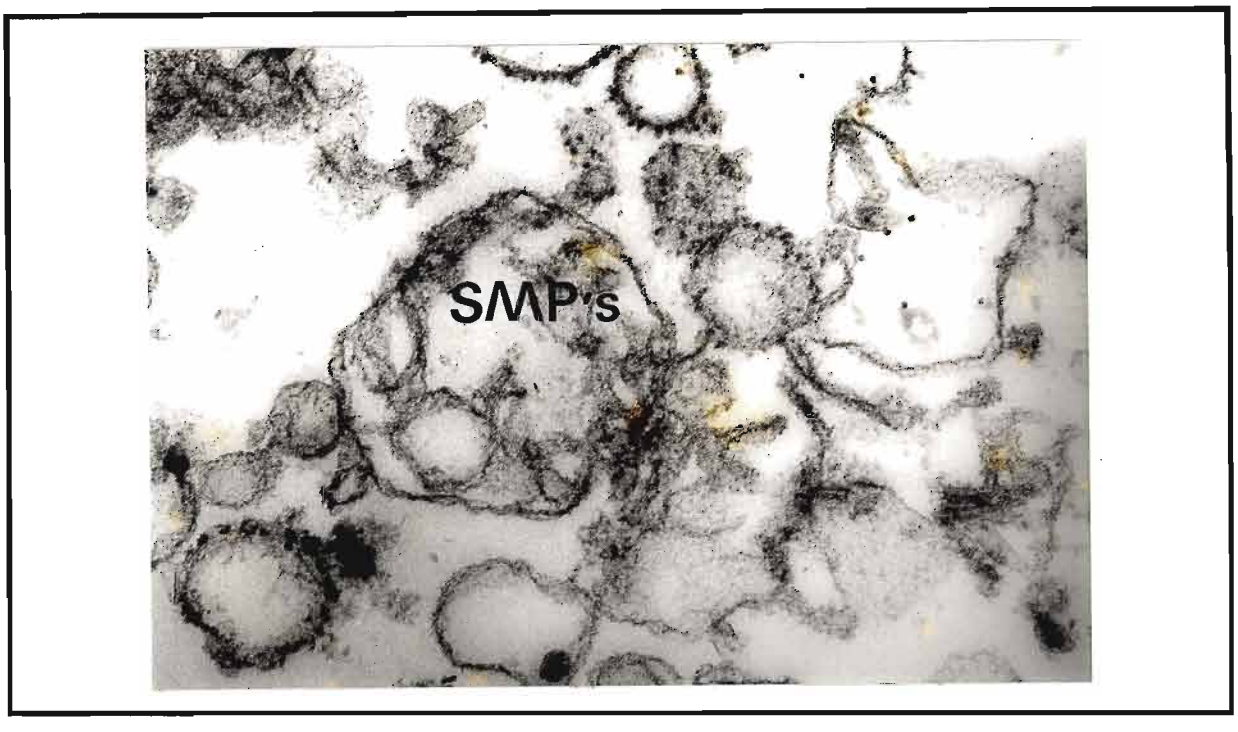


Figure 4.13 Sub-mitochondrial particles from liver tissues of toxin treated rats, showing great disruptions in inner membrane integrity. The particles (SMP's) appear distorted and irregular, X30 000.

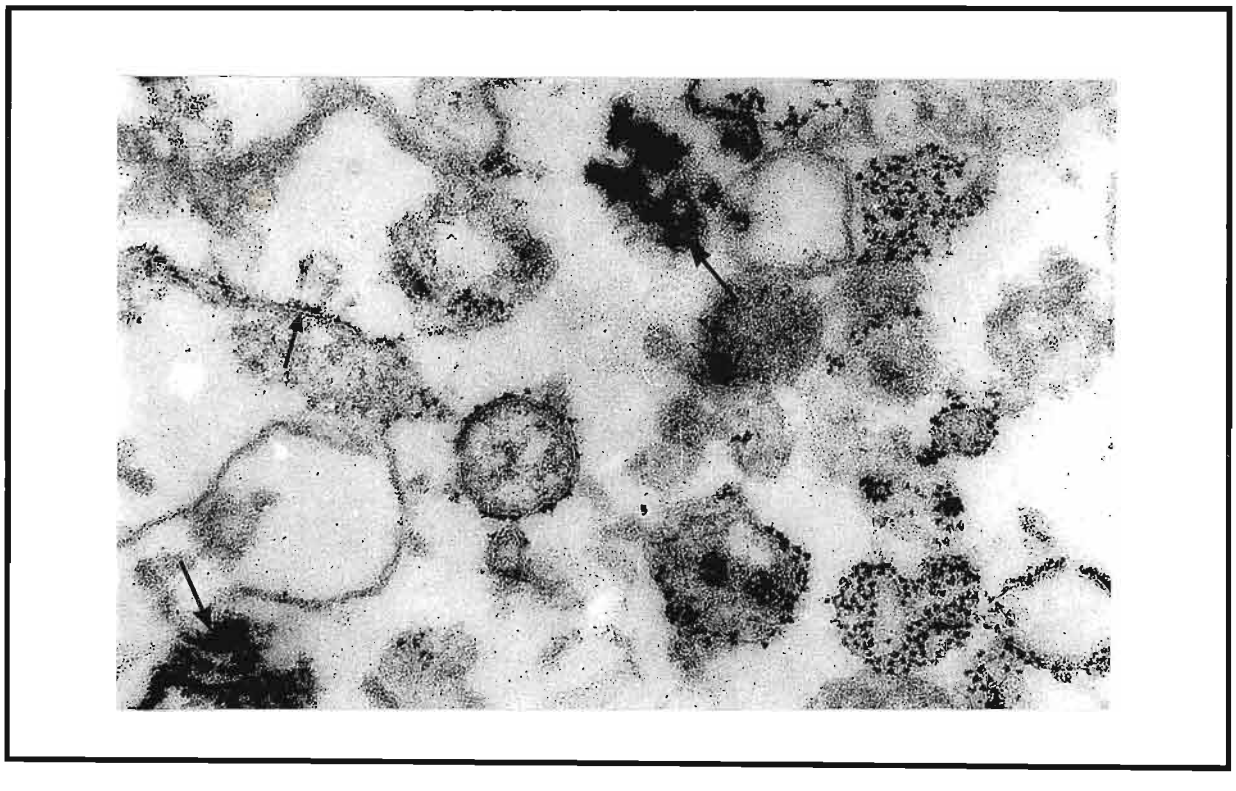

Figure 4.14 Isolated sub-mitochondrial particles from toxin treated rats, with an abundance of damaged fibriller and membranous material (arrows). The particles found in control samples are scarcely present, X40 000.

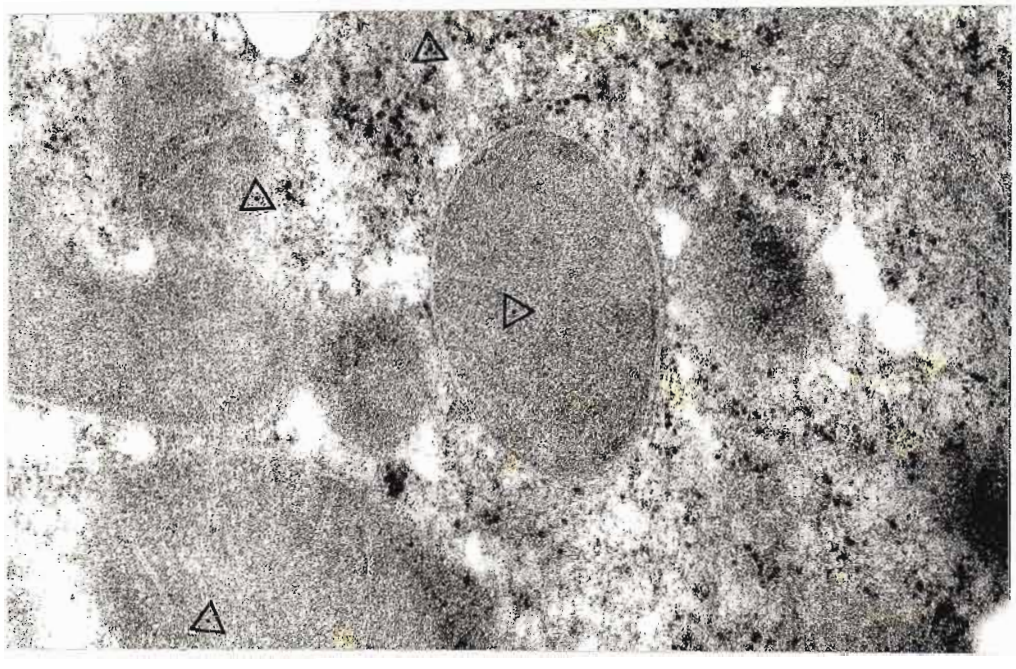

Figure 4.15 ICC electron micrograph of rat liver from treated rats, showing the presence of toxin (triangles) in the mitochondria, X30 000.

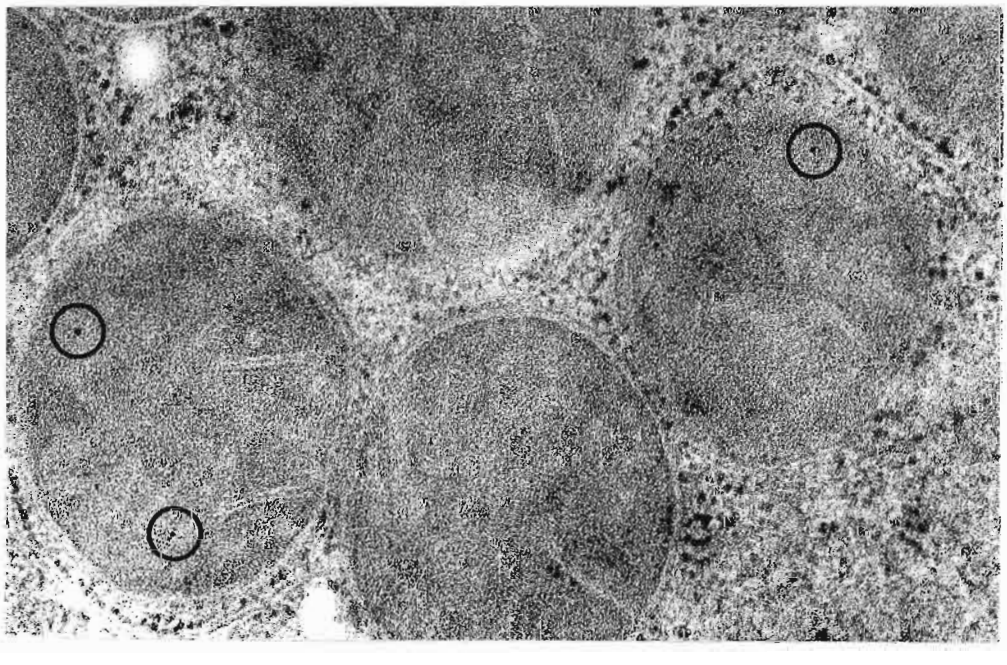

Figure 4.16 ICC electron micrograph of rat liver from treated rats, showing the presence of toxin (circles) in the mitochondria. X40 000.

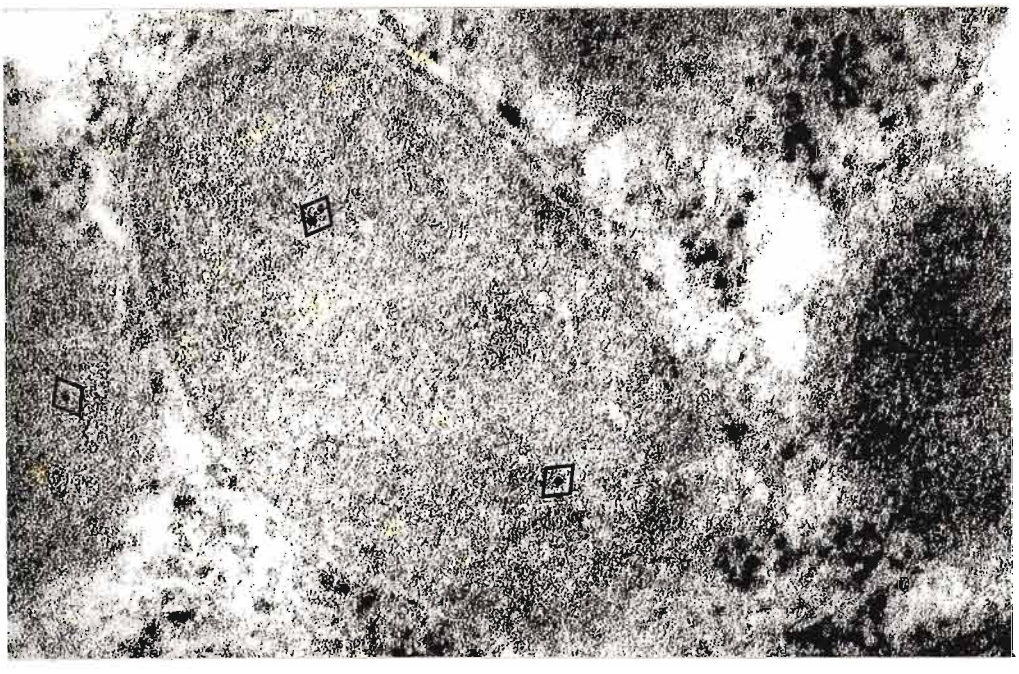

Figure 4.17 ICC electron micrograph of rat liver from treated rats, showing the presence of toxin (triangles) in the mitochondria, X60 000.

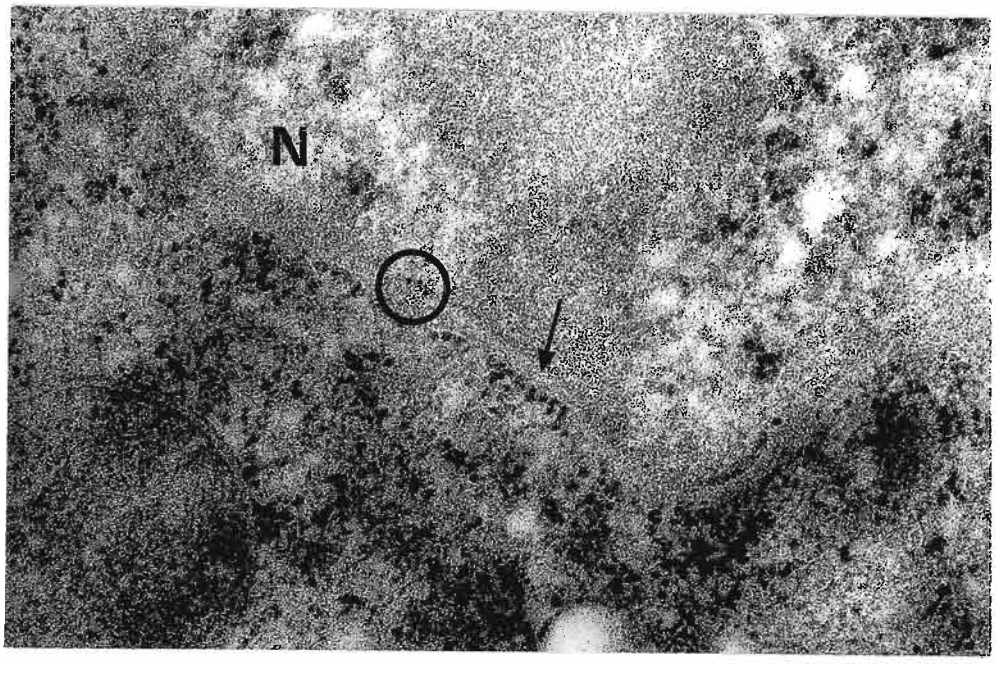


Figure 4.18 An immunocytochemical (ICC) electron micrograph showing the presence of polyclonal gold labelled anti-$AFB_1$ (circle) in the nucleus (N) and along the nuclear membrane (arrow) in a liver cell from a toxin treated rat. X40 000.

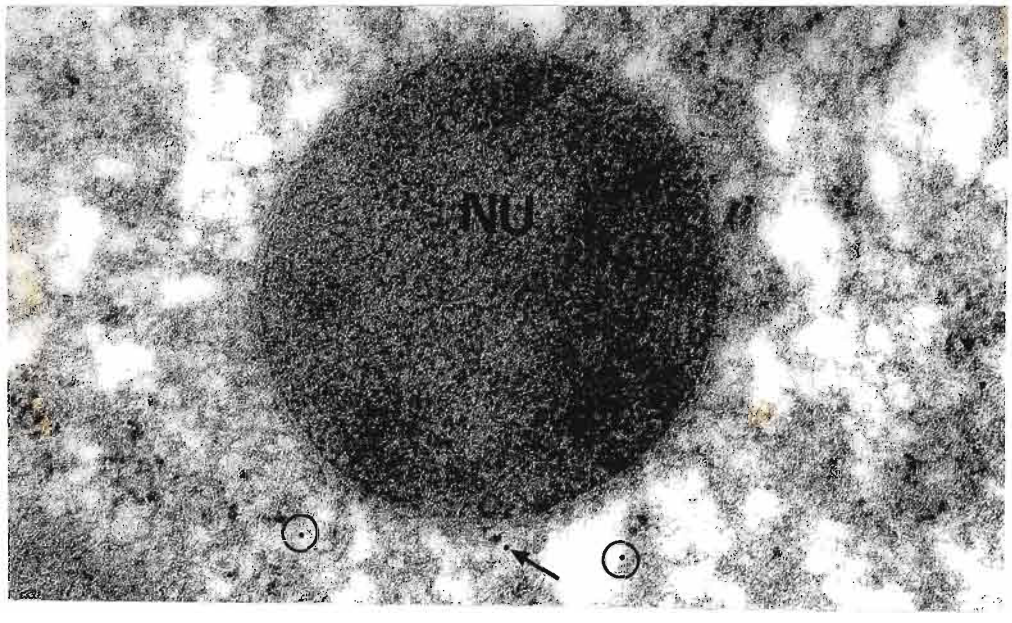


Figure 4.19 ICC electron micrograph showing presence of label (circles) in the nucleouls (NU) and boardering its membranes (arrow) in experimental liver tissues, X40 000.

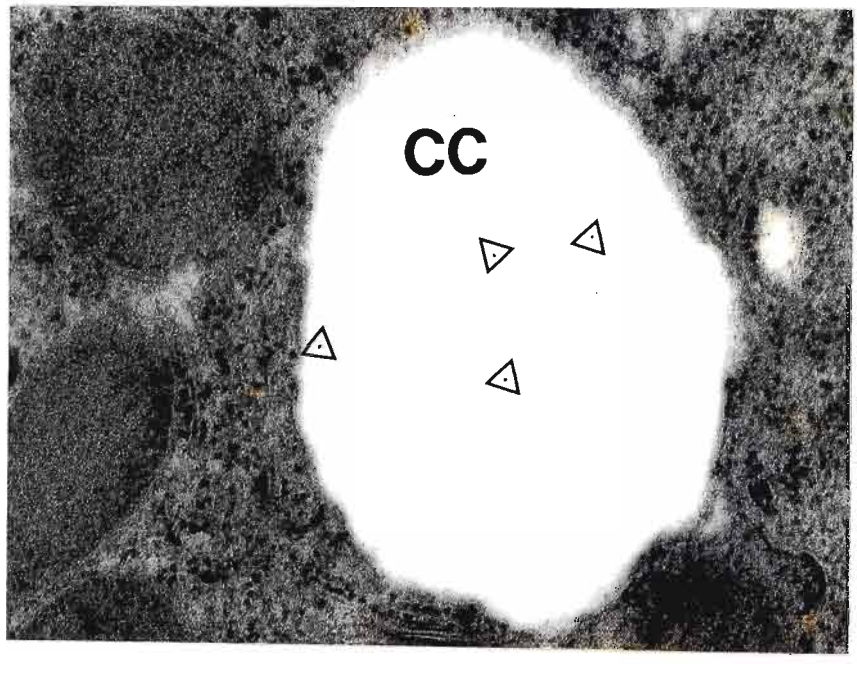


Figure 4.20 ICC electron micrograph showing presence of label (triangles) in areas of cytoplasmic clearing (CC), in experimental liver tissues, X40 000.

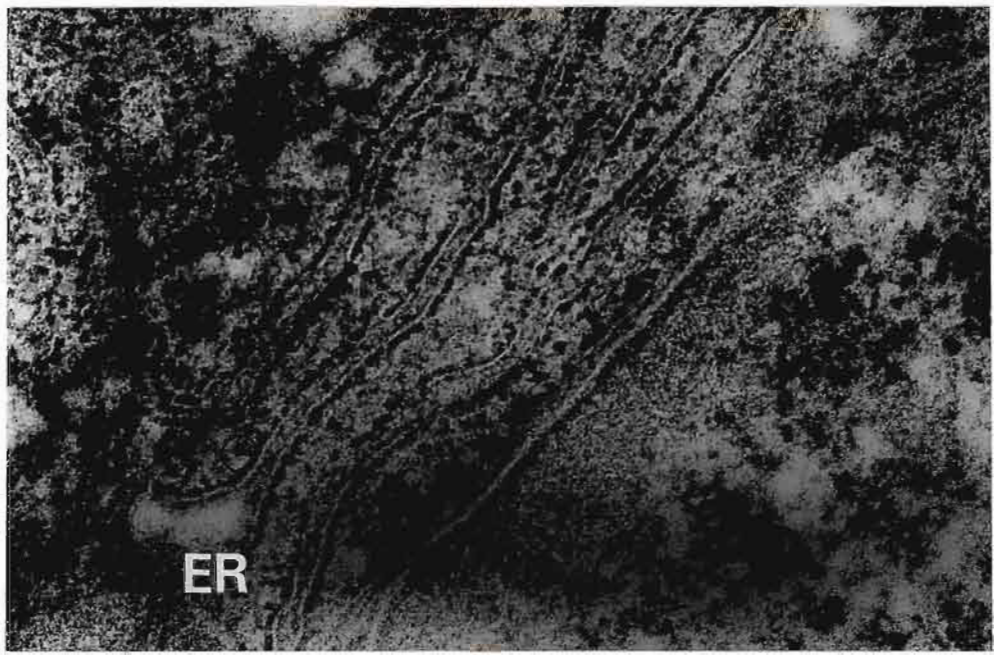


Figure 4.21 An immunocytochemical electron micrograph showing the presence of polyclonal gold labelled toxin (circle) in close association to swollen ER, X30 000

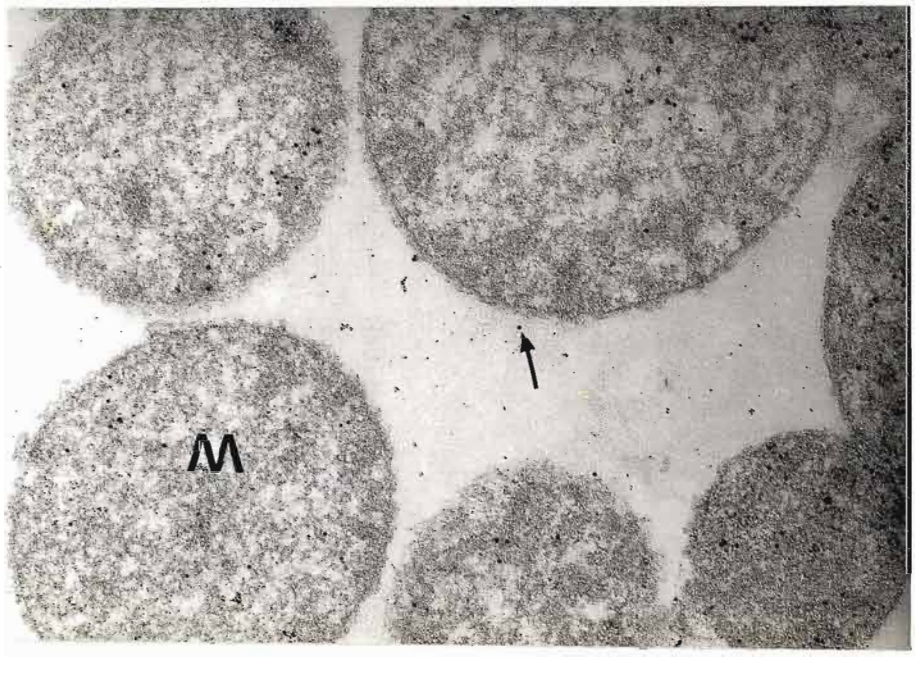


Figure 4.22 Electron micrograph of isolated liver mitochondria from toxin treated rats, showing label within the mitochondria (M). Conjugated gold label was located specifically within the matrix and near the mitochondrial membranes (arrow), X30 000.

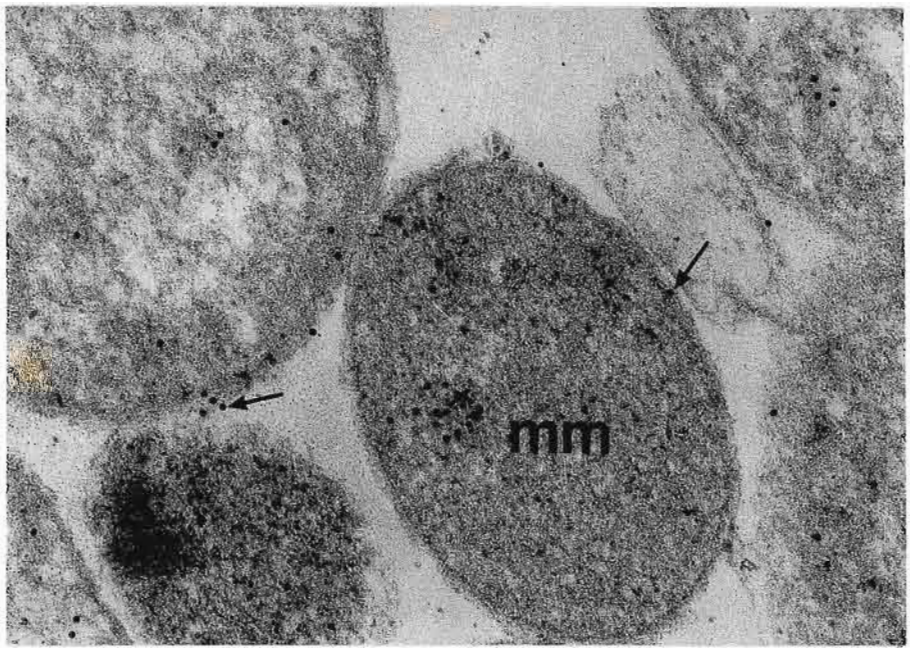


Figure 4.23 Experimental samples showing label within a finely granular mitochondria matrix (MM), and also in areas of the outer membrane (arrows), X50 000.

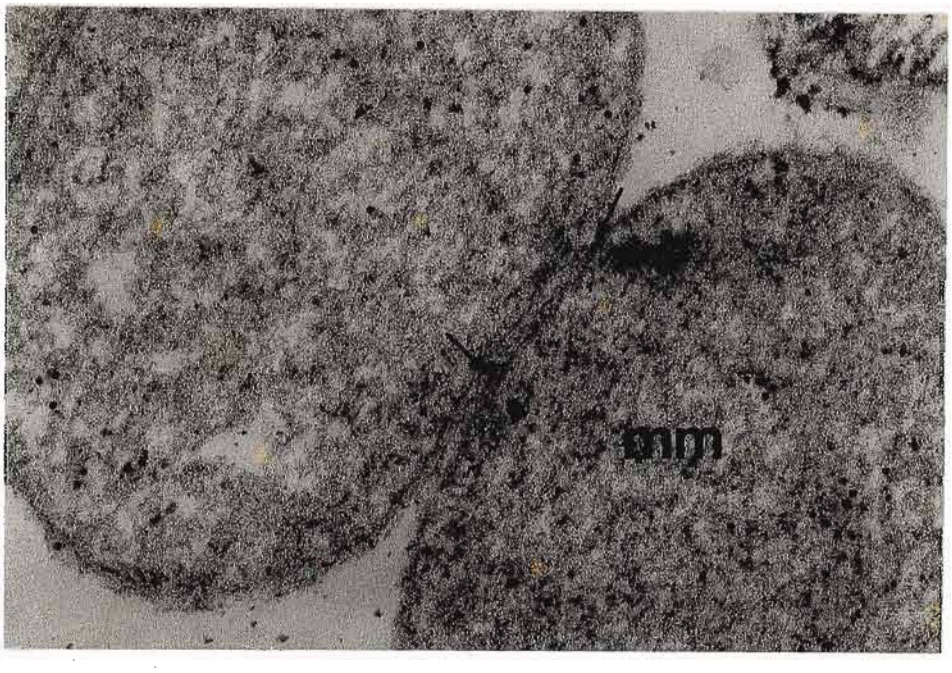


Figure 4.24 Conjugated gold labelled toxin was often found within dividing mitochondria, with toxin in the matrix (MM) and closely associated with the mitochondrial membranes (arrows), X60 000.

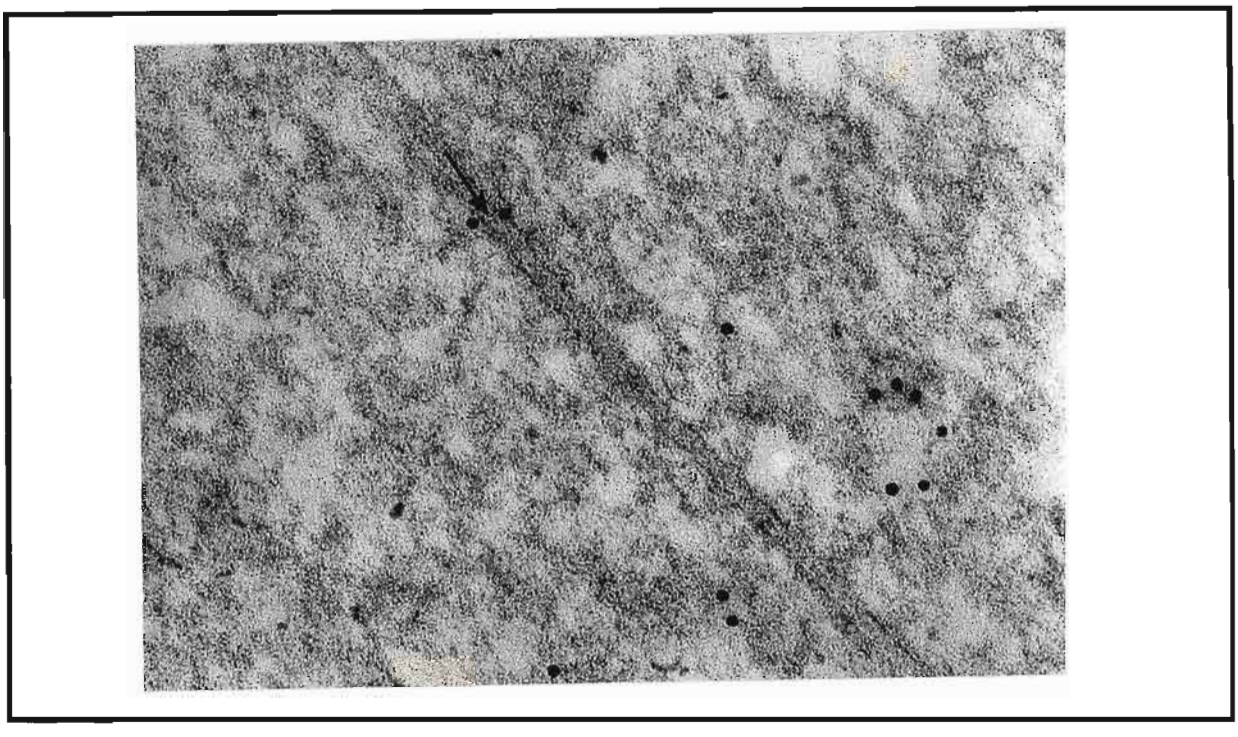

Figure 4.25 ICC electron micrograph showing toxin within the intermembrane space (arrow) and closely associated with areas of the dividing mitochondria (M), X100 000.

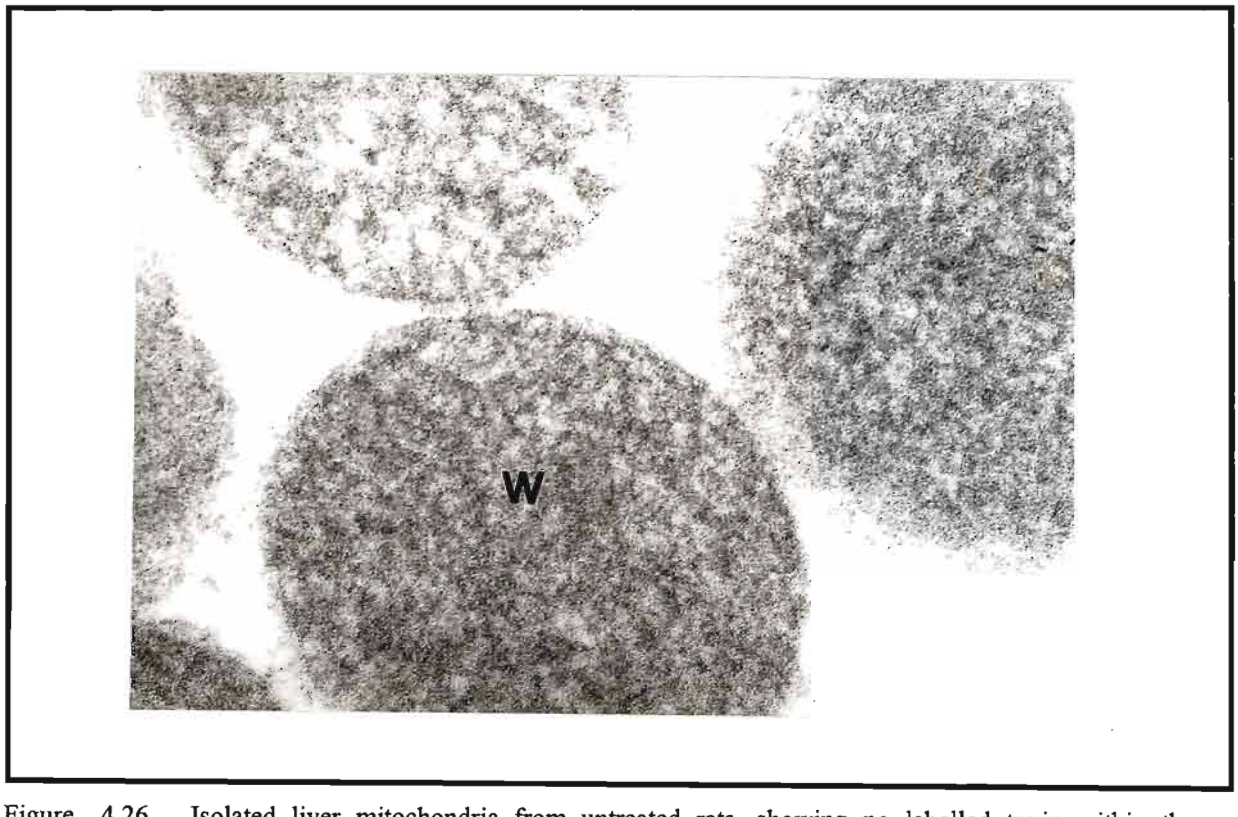


Figure 4.26 Isolated liver mitochondria from untreated rats, showing no labelled toxin within the mitochondria (M), X60 000.

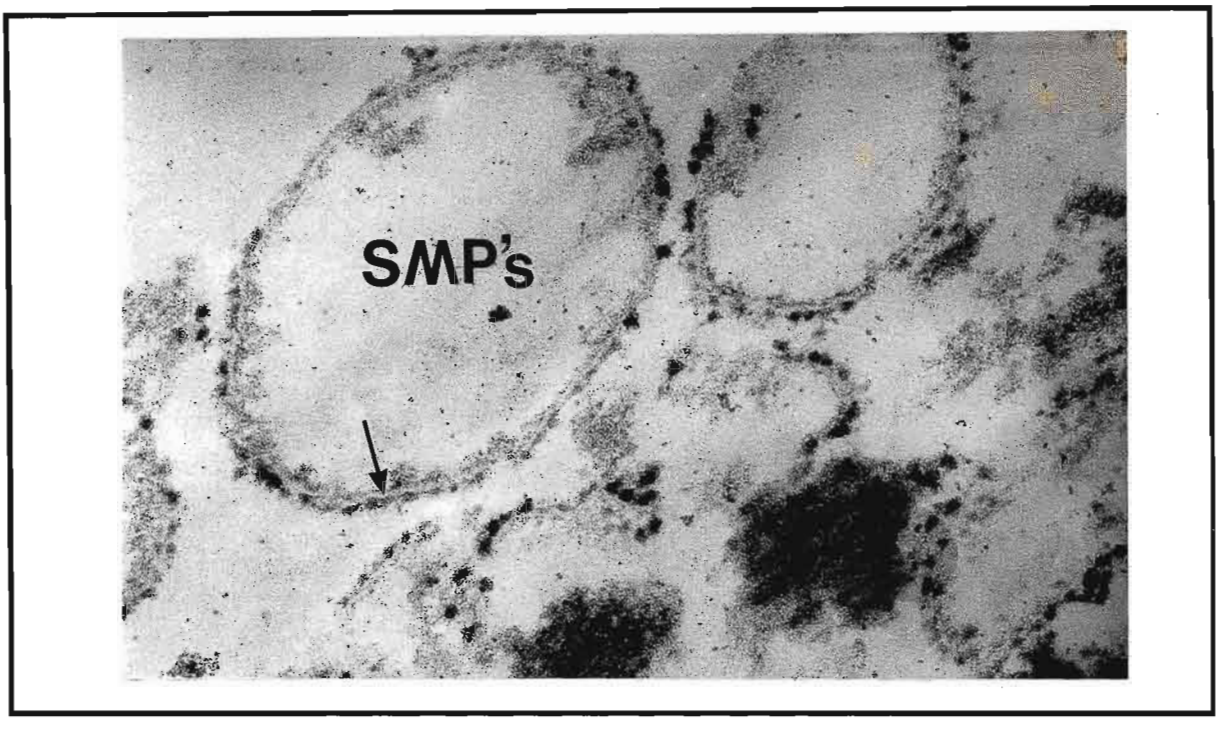


Figure 4.27 ICC electron micrograph of SMP's isolated from untreated rats. No labelled toxin was found in these samples. The particles were well rounded and without any significant alteration to the membranes. The inner membrane was largely intact (arrow), X60 000.

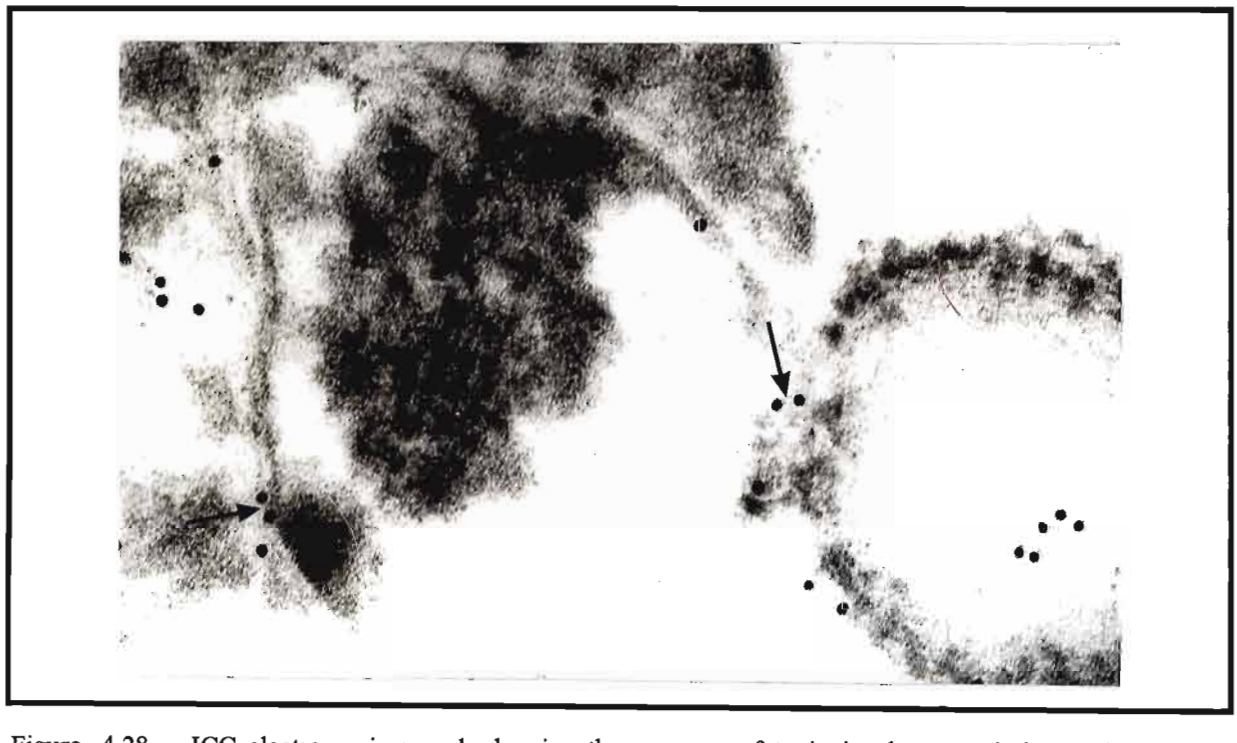

Figure 4.28 ICC electron micrograph showing the presence of toxin in close proximity to damaged membranous regions (arrows) of SMP's isolated from experimental rats, X60 000


Figure 4.29 ICC electron micrograph showing the presence of toxin in definite association with the inner membrane (IM). Portions of the membrane appear dissolved or damaged (arrow), X120 000.

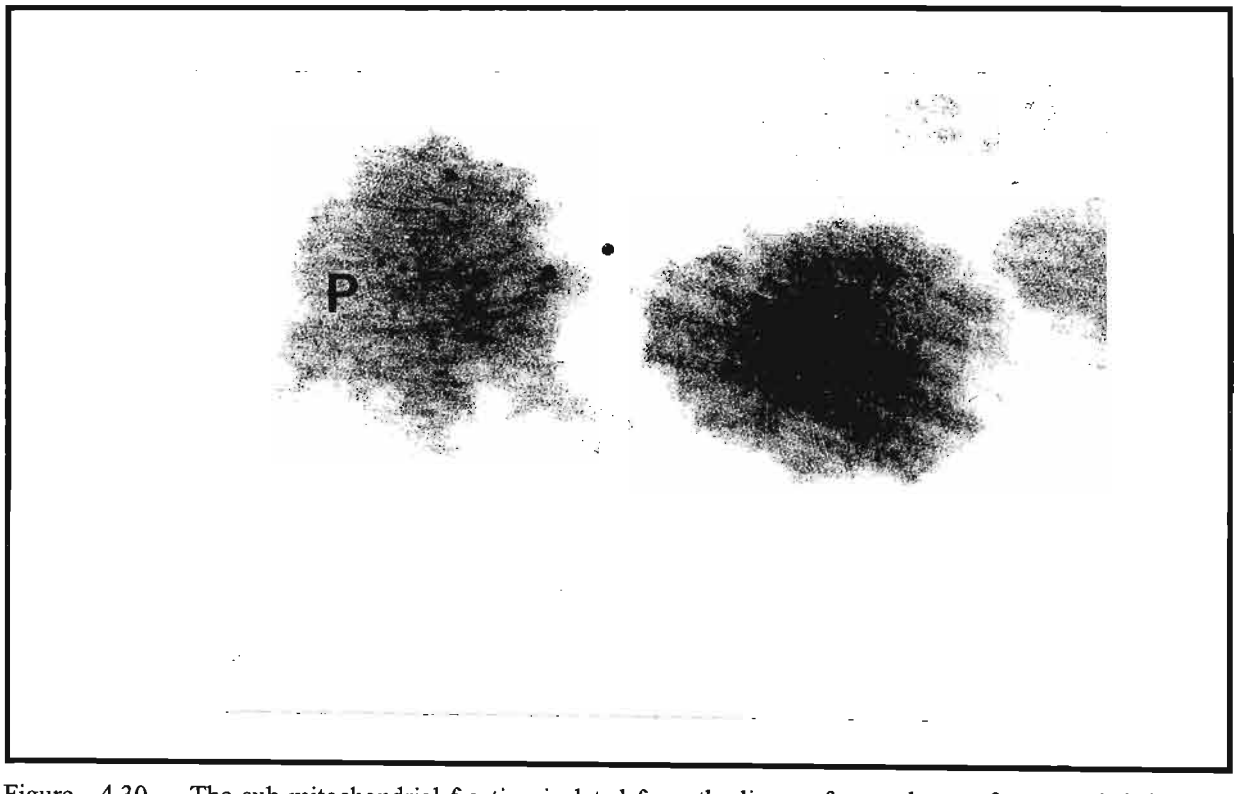


Figure 4.30 The sub-mitochondrial fraction isolated from the livers of treated rats often revealed the presence of conjugated toxin within several paracrystalline inclusion (P), X100 000.

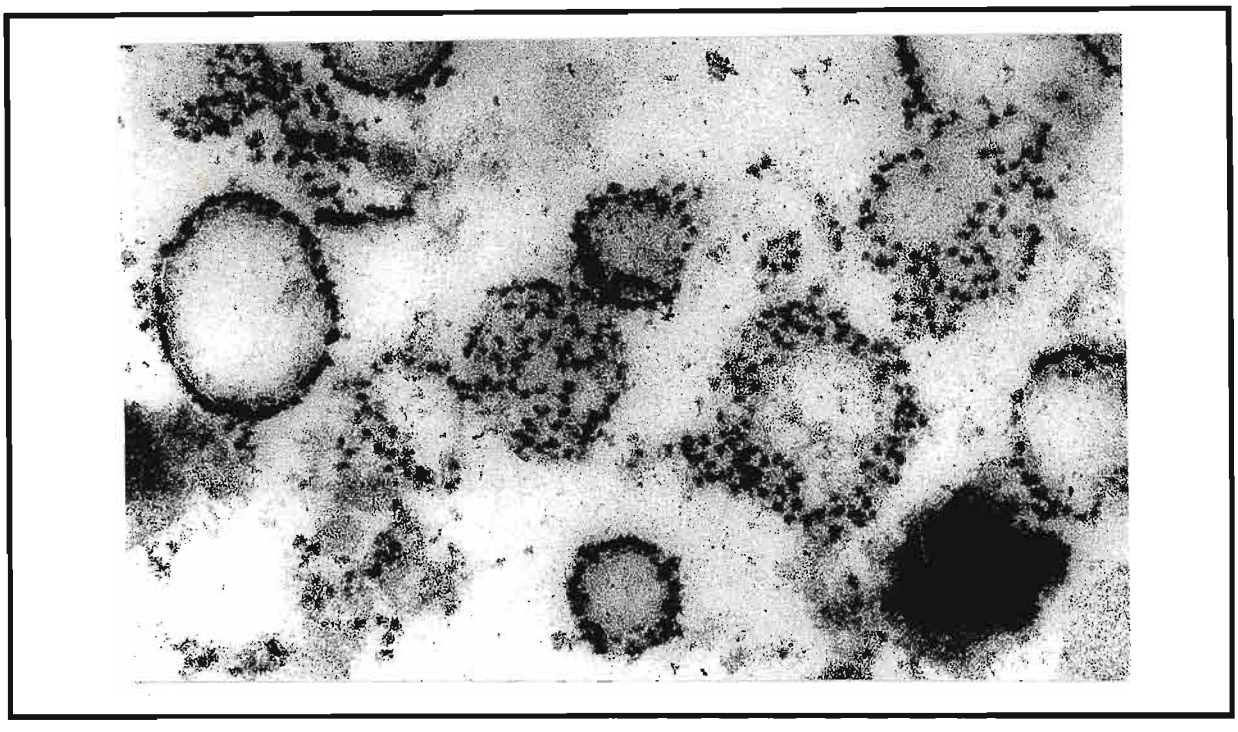

Figure 4.31 ICC electron micrograph showing no presence of label within method controls of SMP's isolated from untreated rats, X40 000.

Figure 4.32 ICC electron micrograph showing no presence of label within method controls of SMP's isolated from treated rats, X30 000.

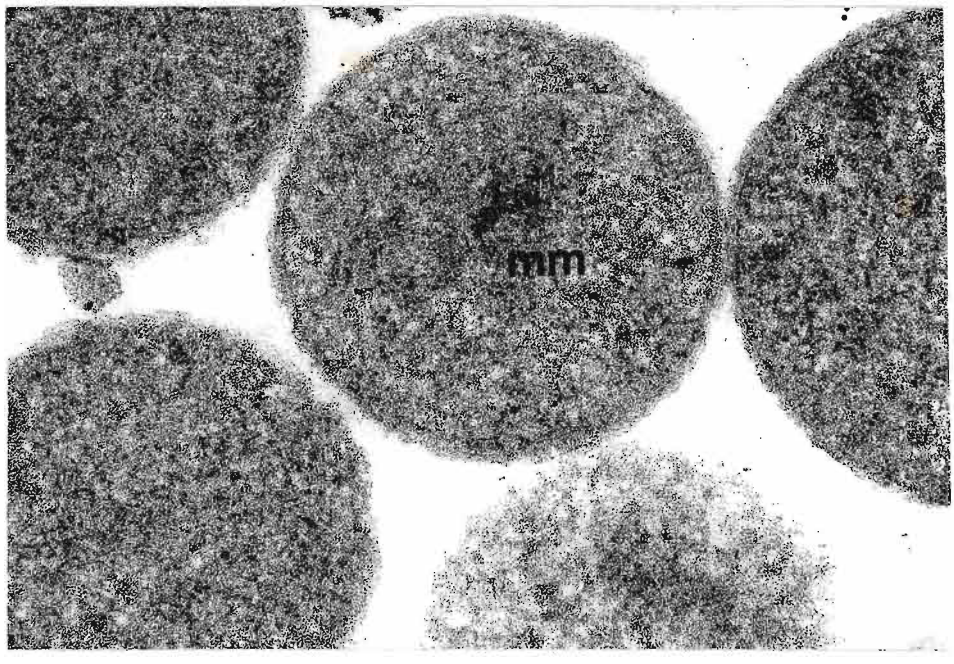


Figure 4.33 Electron micrograph of control mitochondria isolated in 70mM sucrose buffer. The matrix (MM) is finely granular and the cristae are hardly visible, X50 000.

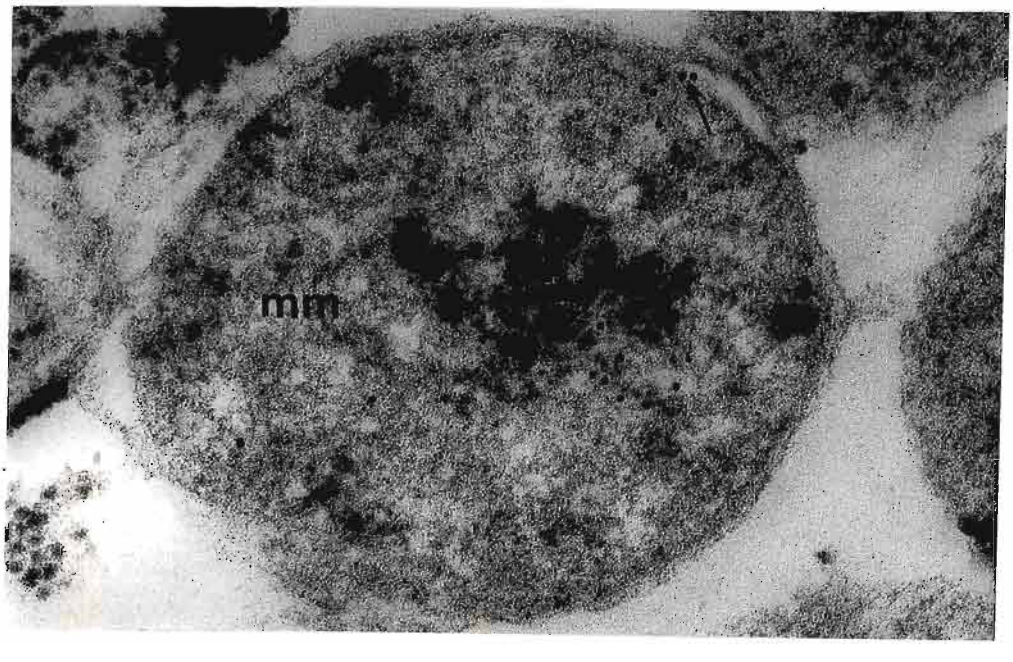


Figure 4.34 ICC electron micrograph of treated mitochondria *(in vitro)*, isolated in 70mM sucrose buffer. Toxin was often found within the mitochondrial matrix (MM) and within the intermembrane fraction (arrow), X60 000.

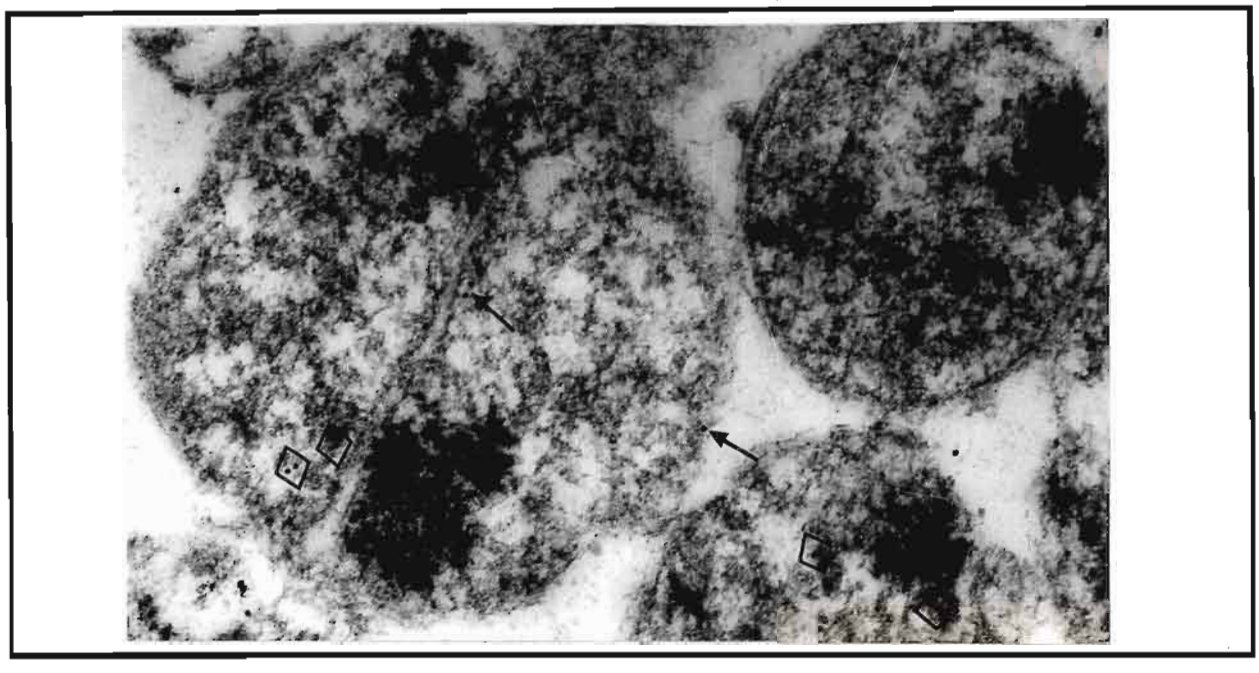

Figure 4.35 ICC electron micrograph of treated mitochondria *(in vitro)*, isolated in 70mM sucrose buffer. Label (diamonds) was also found closely associated with both the outer and inner membranes (arrows) within budding mitochondria, X40 000.

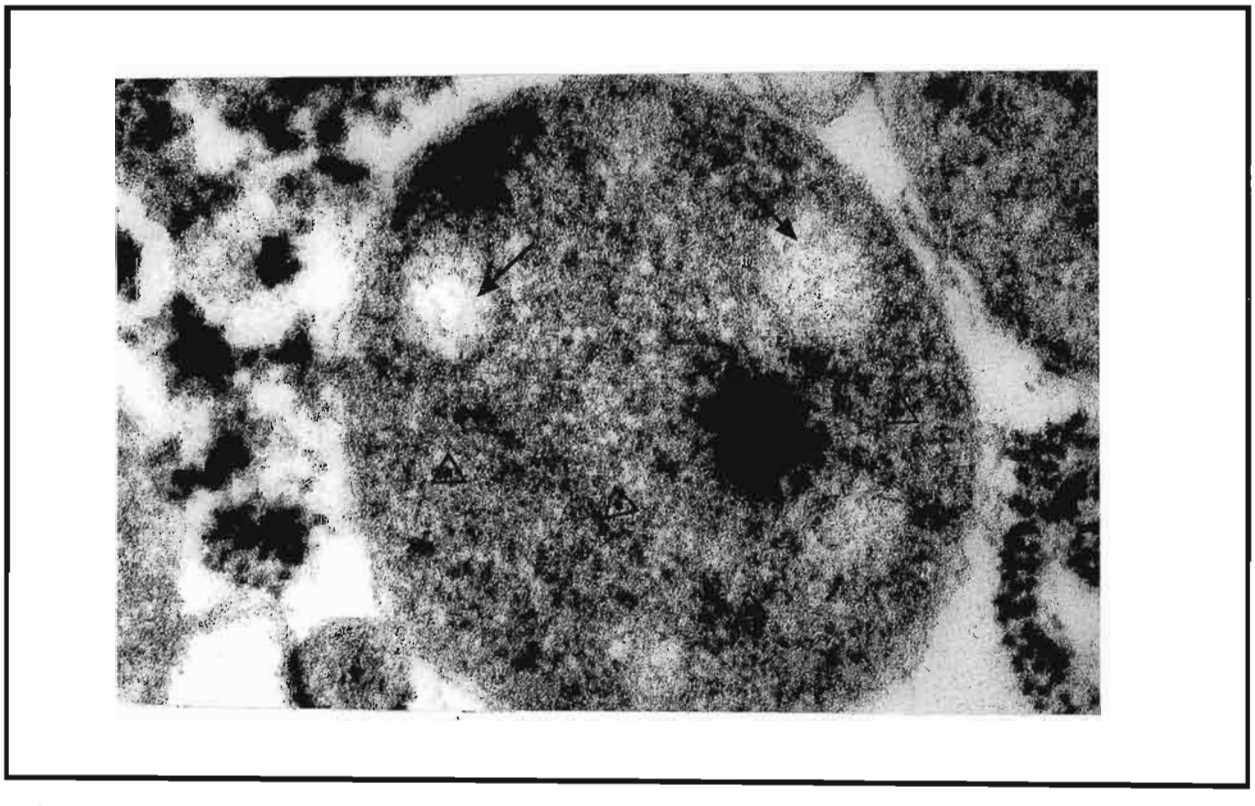

Figure 4.36 ICC electron micrograph of treated mitochondria *(in vitro)*, isolated in 70mM sucrose buffer. Toxin (triangles) was frequently found within mitochondria where matrix clearing (arrows) appeared to be occuring, X60 000.

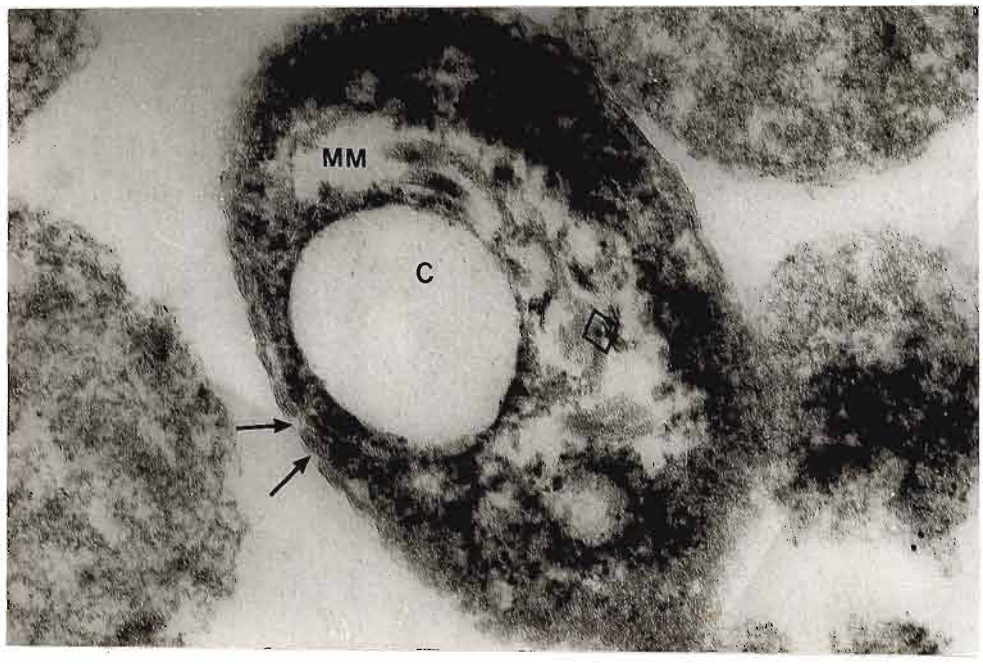


Figure 4.37 ICC electron micrograph of treated mitochondria *(in vitro)*, isolated in 70mM sucrose buffer. Bound toxin (triangles) was located in areas of distinct membrane damage or breaks (arrows), with the associated swelling of cristae (C) and matrix clearing (MM), particulary in areas of localised toxin, X40 000.

Figure 4.38 ICC electron micrograph of treated mitochondria *(in vitro)*, isolated in 70mM sucrose buffer. The appearance of toxin in treated samples appeared to damage the membranes of several mitochondria, allowing the extrusion of the mitochondrial matrix (arrow), X60 000.

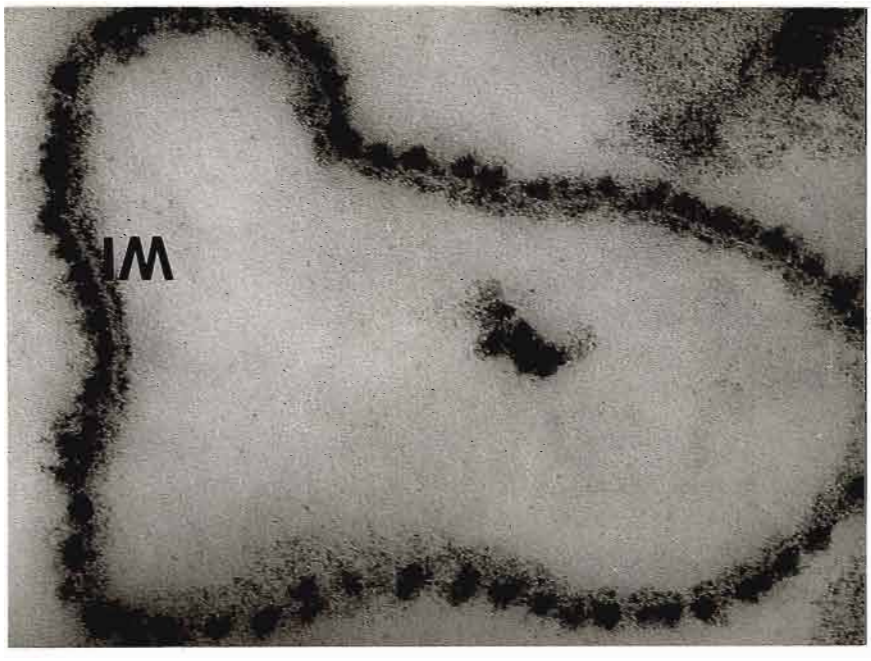


Figure 4.39 ICC electron micrograph of untreated SMP's isolated in 70mM sucrose buffer. No label was found. The inner membrane (IM) is easily visible, with numerous round particles lining the membrane, X 120 000.

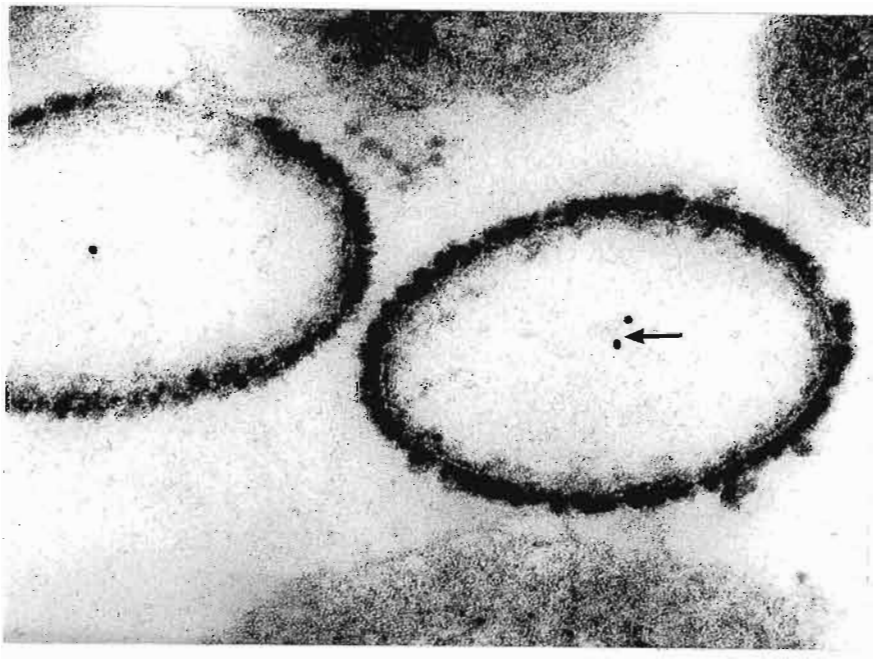

Figure 4.40 ICC electron micrograph of treated SMP'S *(in vitro)*, isolated in 70mM sucrose buffer. Toxin was localised in areas of SMP's (arrow), X60 000.

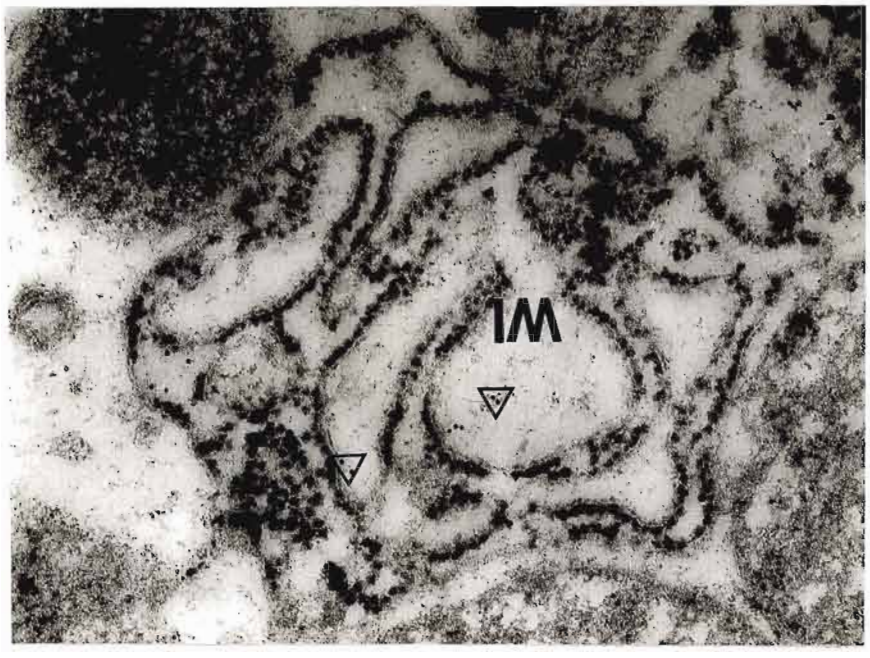


Figure 4.41 ICC electron micrograph of treated SMP's *(in vitro)*, isolated in 70mM sucrose buffer. Gold labelled toxin (triangles) was closely associated with the inner membrane (IM) fragments of SMP's, X30 000.

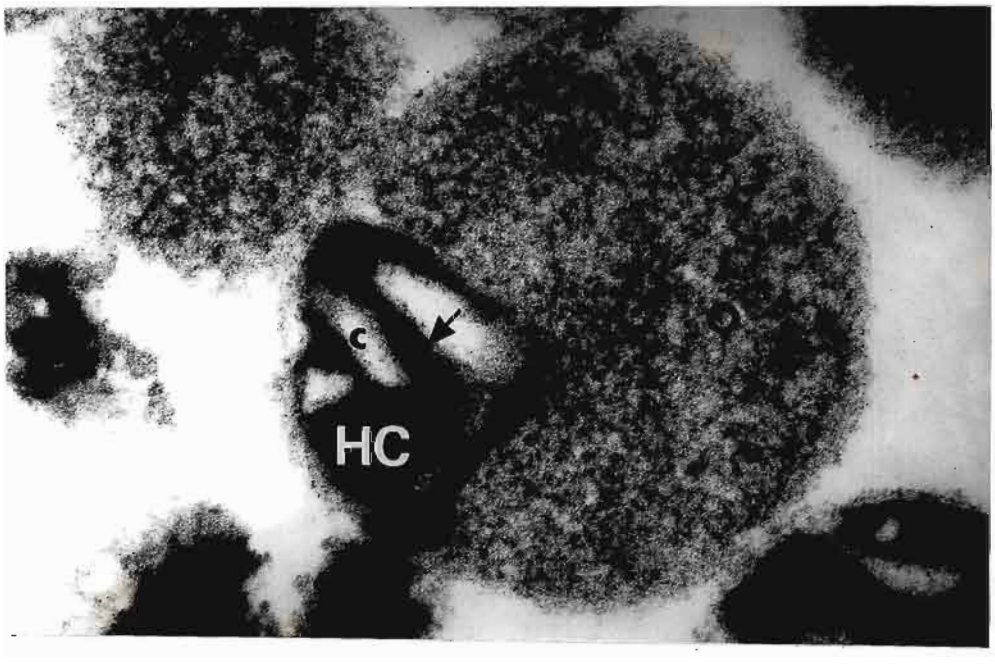


Figure 4.42 Electron micrograph showing untreated mitochondria suspended in 250mM sucrose buffer. The mitochondria revealed a distinct change from an orthodox (O) conformation, to a more highly configured form (HC). Within the configured form, the cristae (C) are easliy visible and the matrix (arrow) is highly condensed, X60 000.

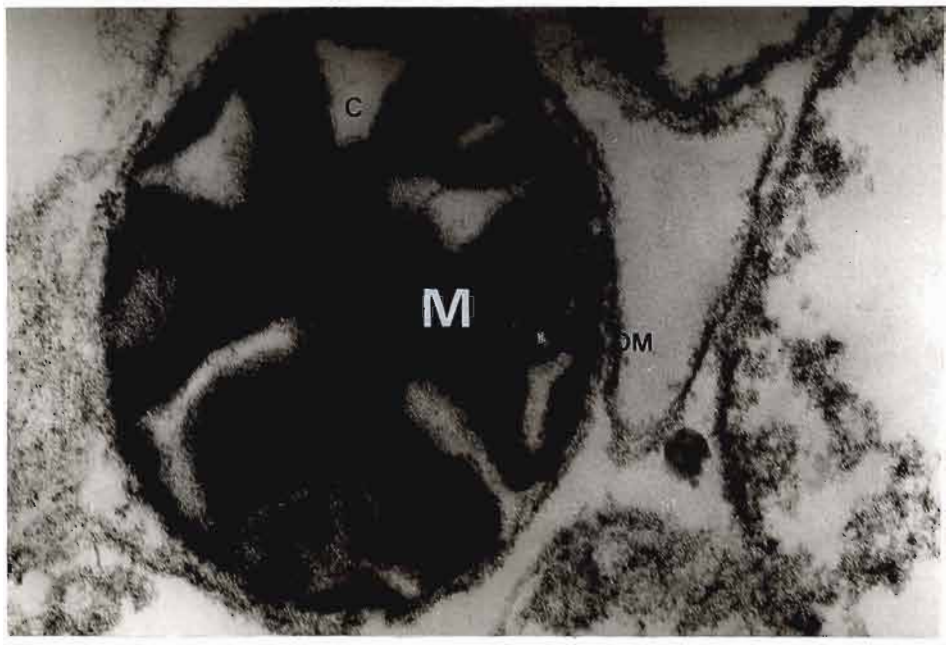


Figure 4.43 ICC electron micrograph of untreated mitochondria suspended in 250mM sucrose buffer. The inner (IM) and outer (OM) membranes are easliy discernible. The cristae (C) and matrix (M) are also easily seen, X60 000.

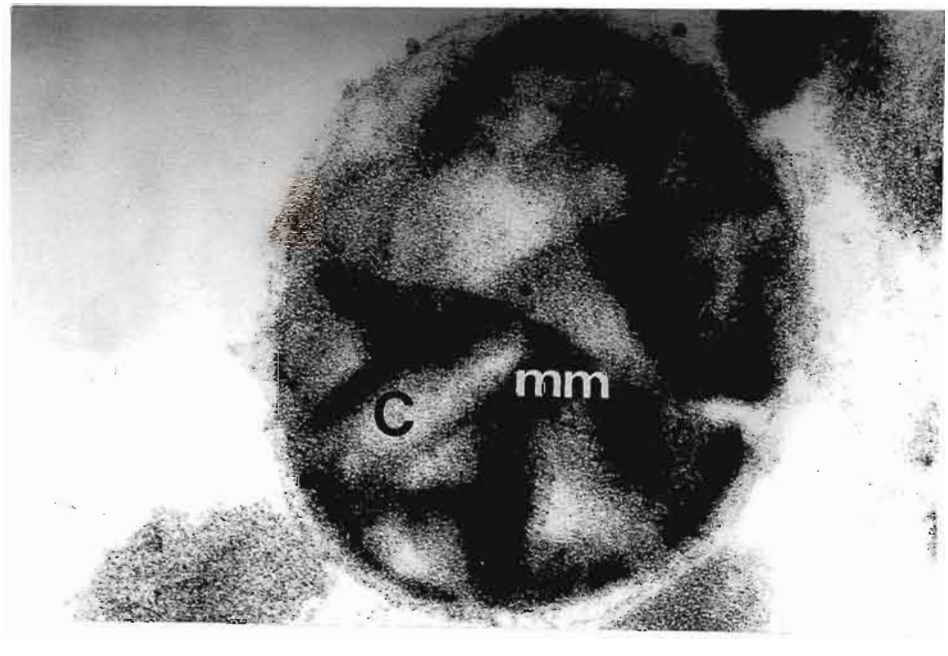


Figure 4.44 ICC electron micrograph of treated mitochondria *(in vitro)*, isolated in 250mM sucrose buffer. Bound toxin was localised within the mitochondrial matrix (MM) and cristae (C), X50 000.

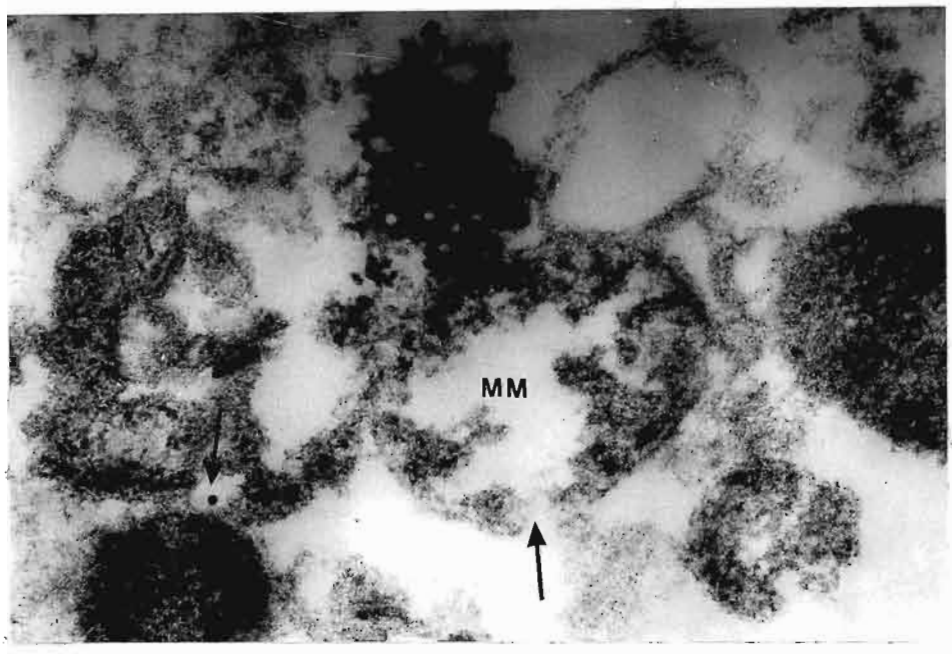


Figure 4.45 ICC electron micrograph of treated mitochondria *(in vitro)*, isolated in 250mM sucrose buffer. Toxin was localised in areas of distinct membrane breaks and membranous damage (arrows), with the associated clearing of mitochondrial matrices (MM), particularly in areas of localised toxin, X60 000.

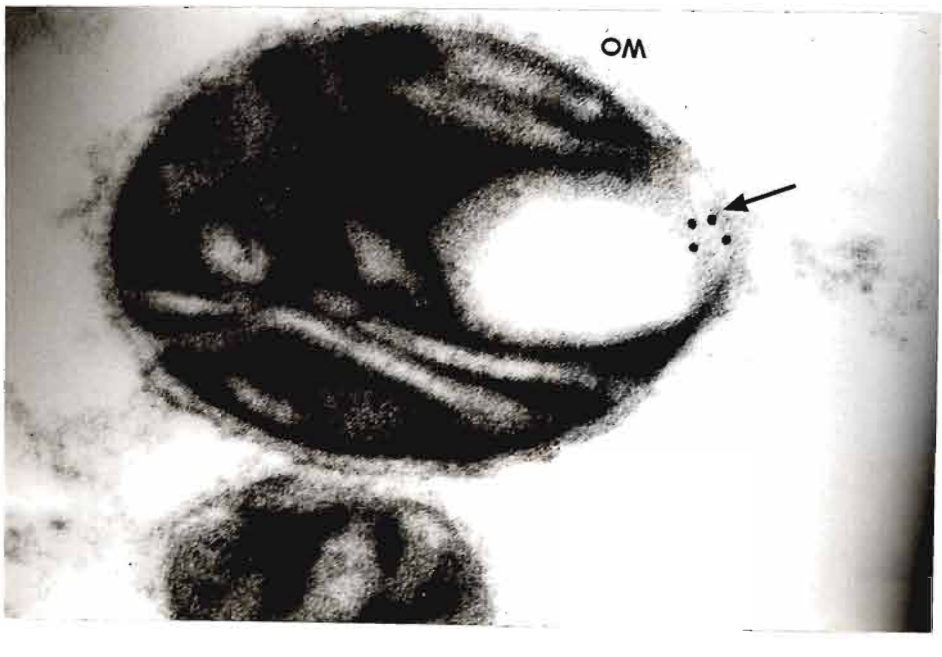


Figure 4.46 ICC electron micrograph of treated mitochondria *(in vitro)*, isolated in 250mM sucrose buffer. Bound toxin was also located in areas of the outer membrane (OM), where the membrane appeared to be dissolved (arrow), and with the associated swelling of the cristae (C) in that region, X60 000.

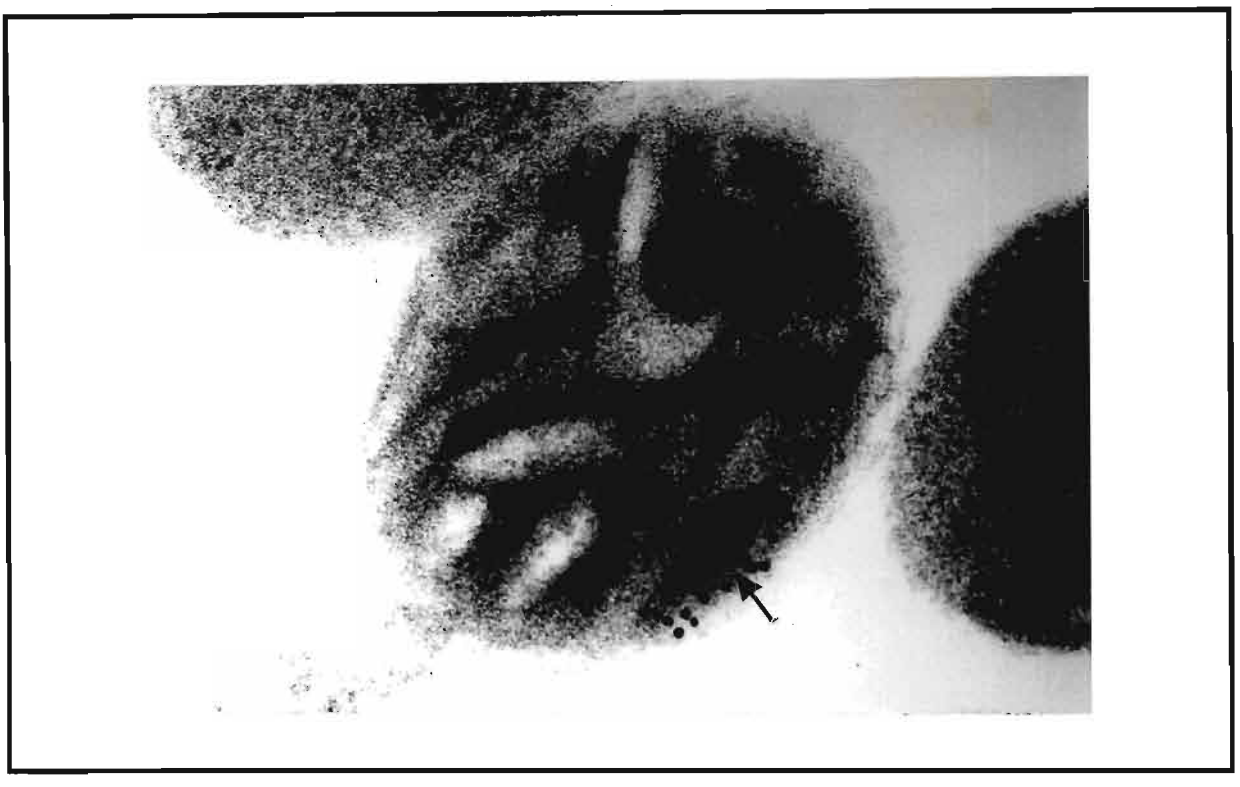

Figure 4.47 ICC electron micrograph of treated mitochondria *(in vitro)*, isolated in 250mM sucrose buffer. Several mitochondria displayed a mass of labelled toxin at the outer membrane (arrow) region of the mitochondria, X50 000.

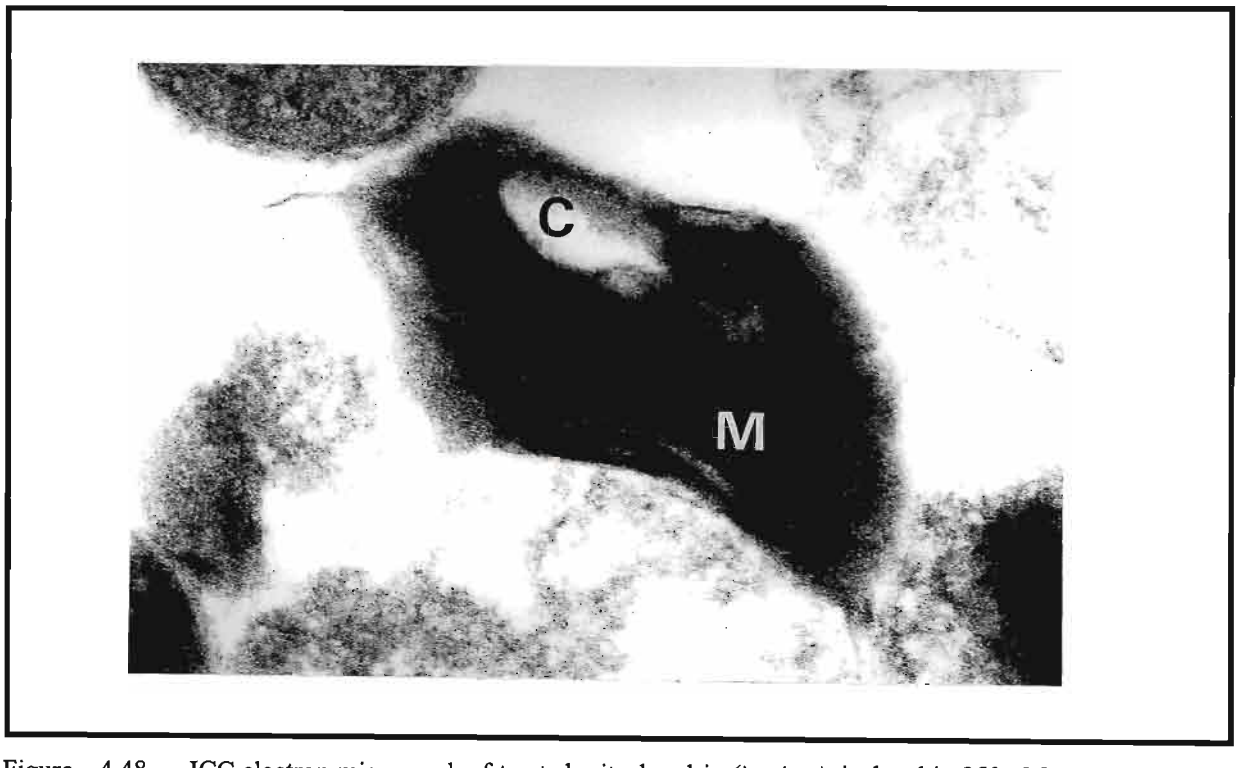


Figure 4.48 ICC electron micrograph of treated mitochondria *(in vitro)*, isolated in 250mM sucrose buffer. Aflatoxin $B_1$ (arrow) was located within distorted mitochondria (M), which displayed swollen cristae (C), X40 000.

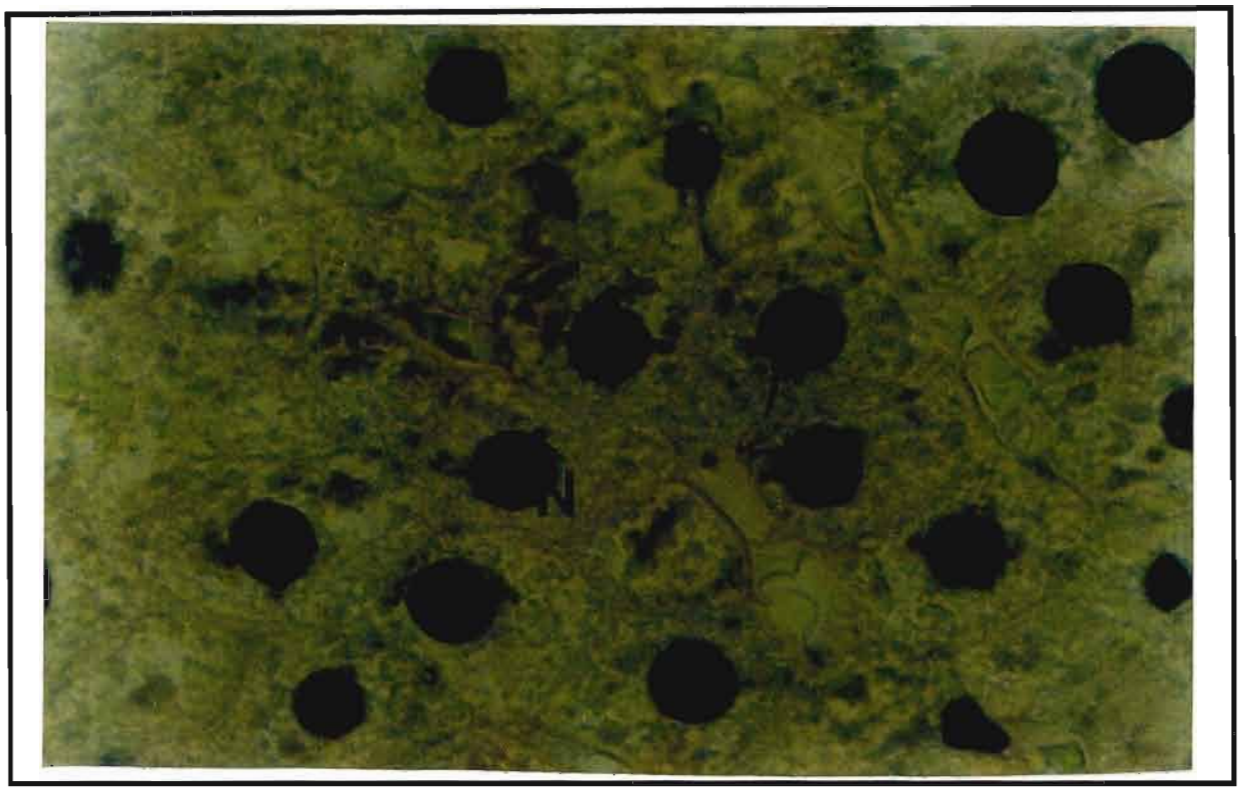

Figure 4.49 Immunohistochemical (IHC) light micrograph of a liver section from untreated rats. No toxin was found in the tissues. The cells were largely intact and the nuclei (N) and nucleolus (arrow) well formed, X5000.

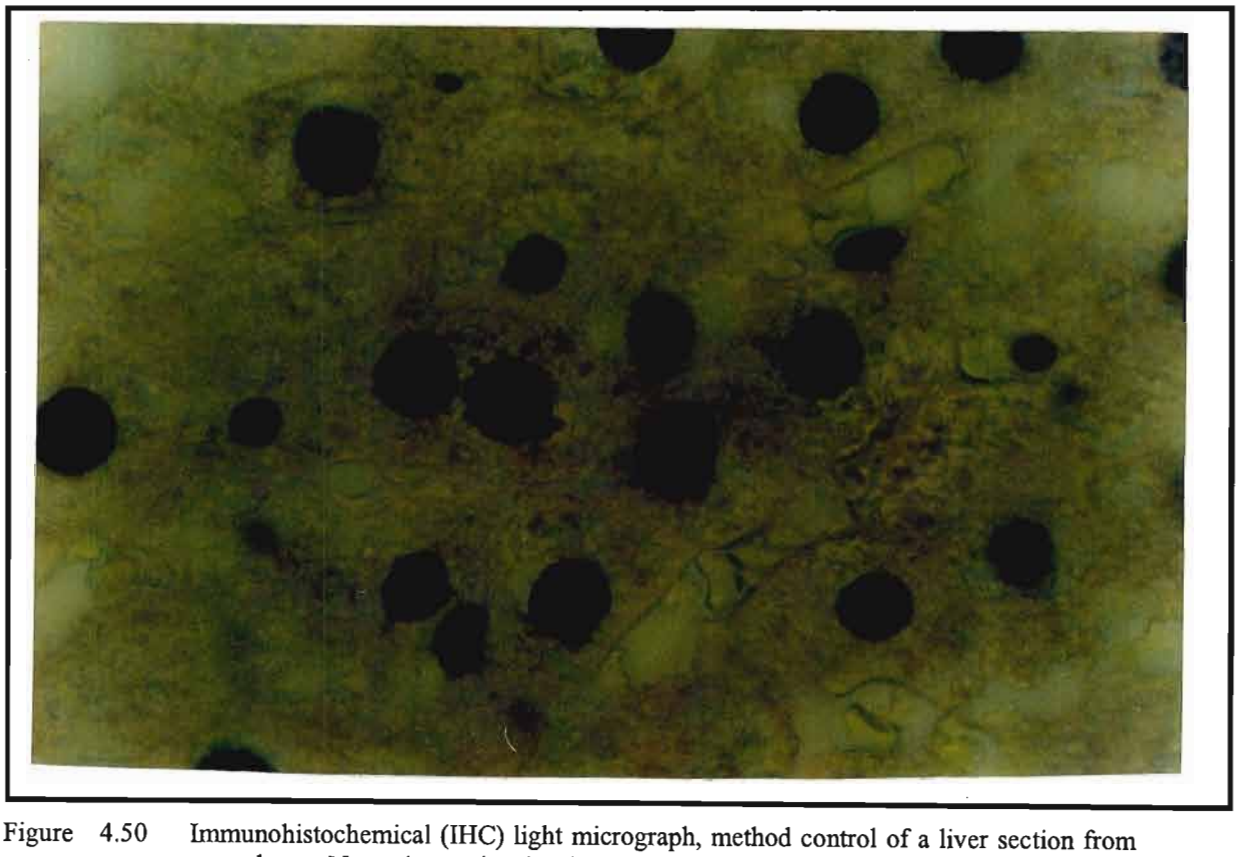

Figure 4.50 Immunohistochemical (IHC) light micrograph, method control of a liver section from treated rats. No toxin was localised within the tissues, X5000.

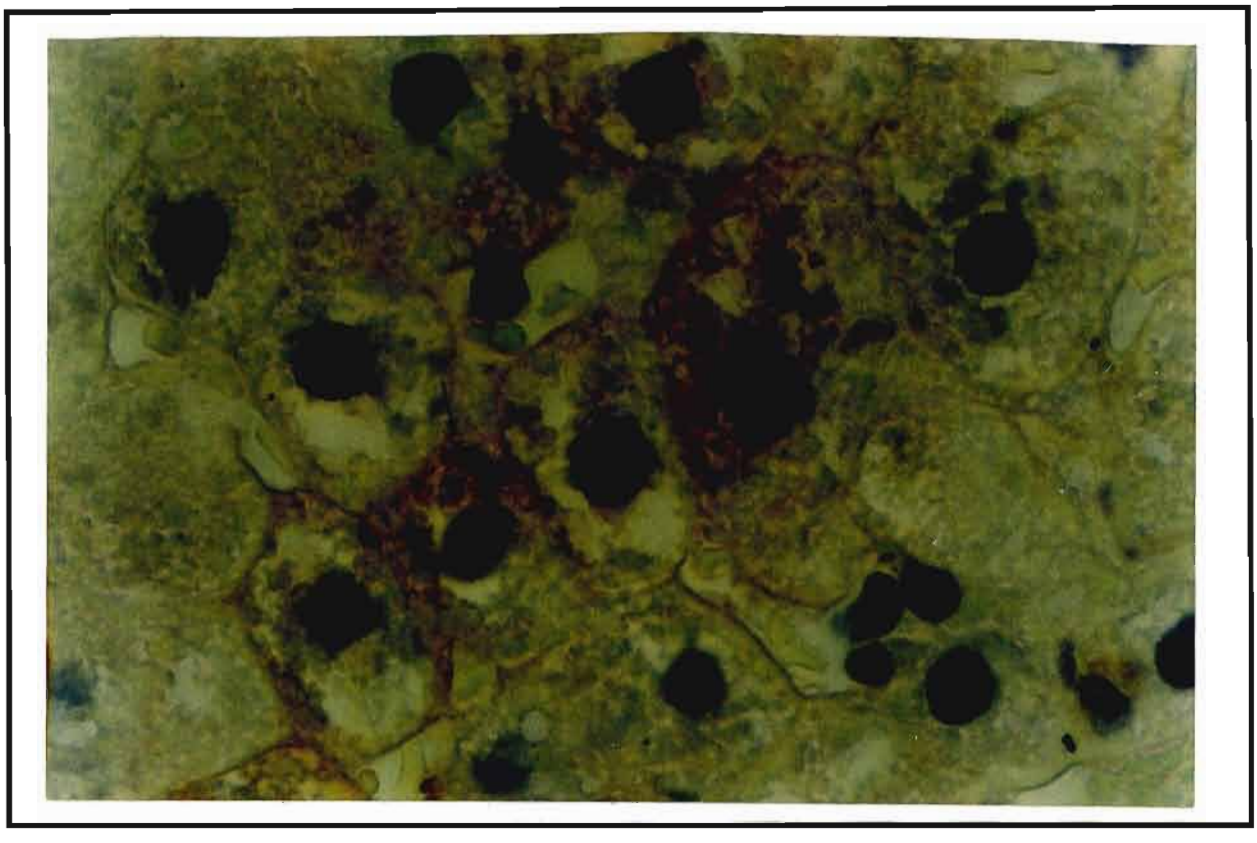

Figure 4.51 Immunohistochemical (IHC) light micrograph of a liver section from treated rats, examined 30 minutes after administration. Toxin was located within the cytoplasm (C) of infected cells. The diaminobenzidine (DAB) chromogenic stain was also found bordering the cell membrane (arrow), X5000.

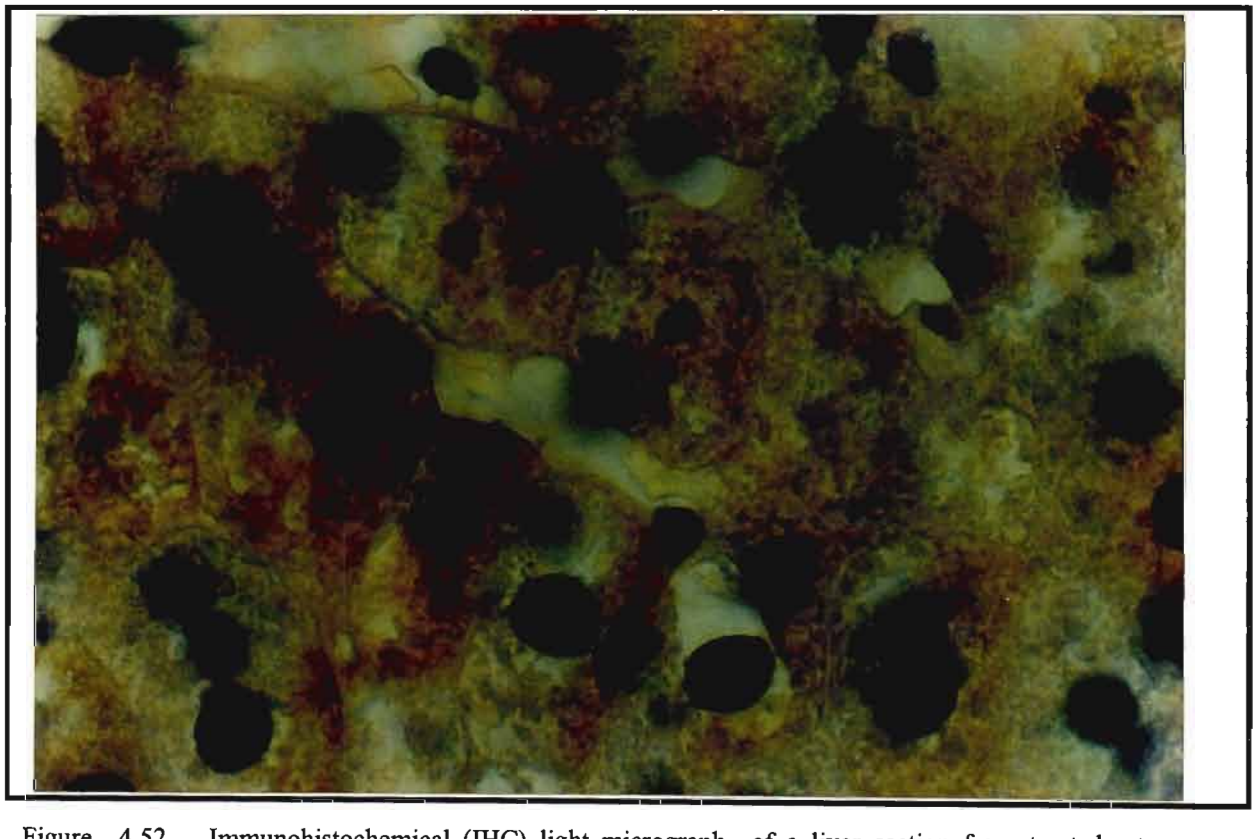

Figure 4.52 Immunohistochemical (IHC) light micrograph of a liver section from treated rats examined 2 hours after toxin administration. The entire cytoplasm (C) and some nuclei (arrow) appeared to be infiltrated with toxin., X5000.

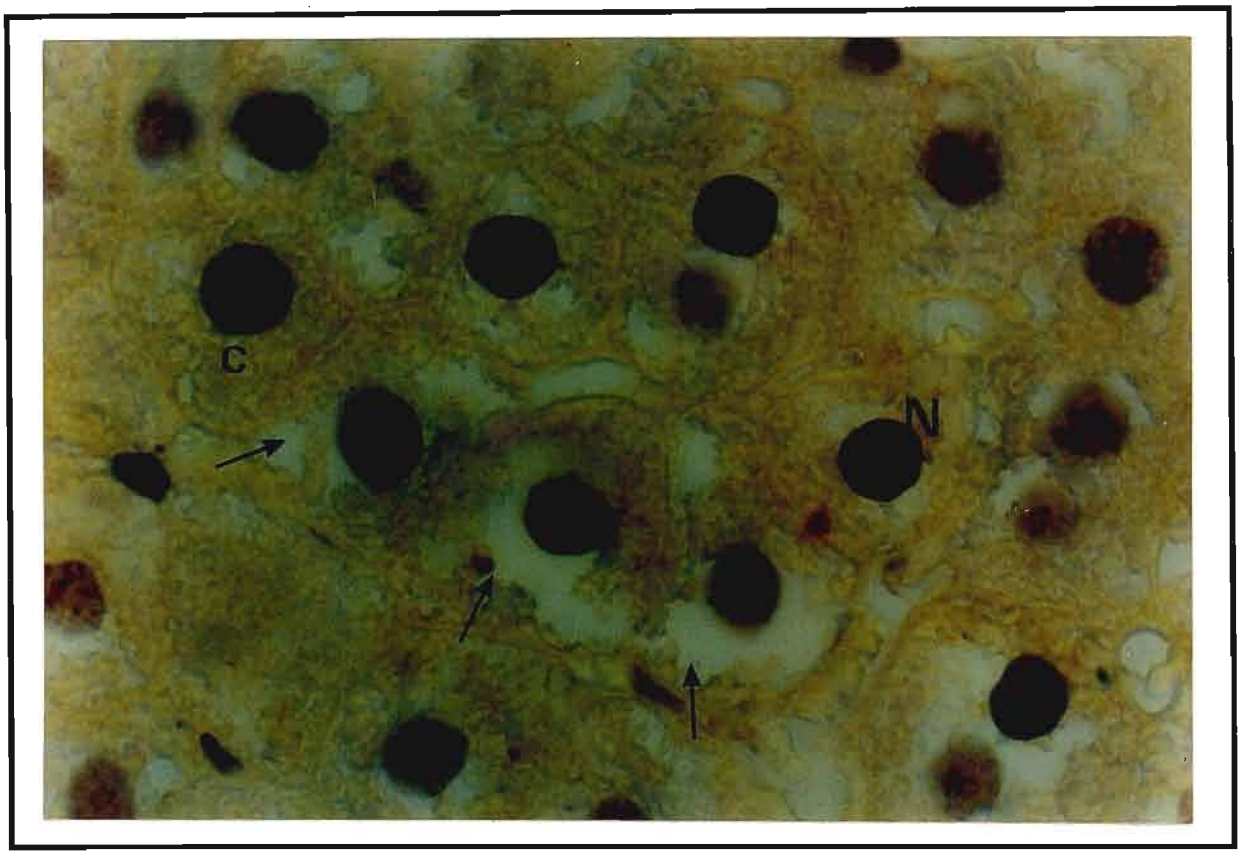


Figure 4.53 Immunohistochemical (IHC) light micrograph of a liver section from untreated rats examined after 24 hours following toxin admistration. The stain was found within the cytoplasm (C), and also within the nuclei (N). The entire tissue appeared to be infected. Several cells showed distinct membrane damage and associated cytoplasmic clearing (arrows), X5000.

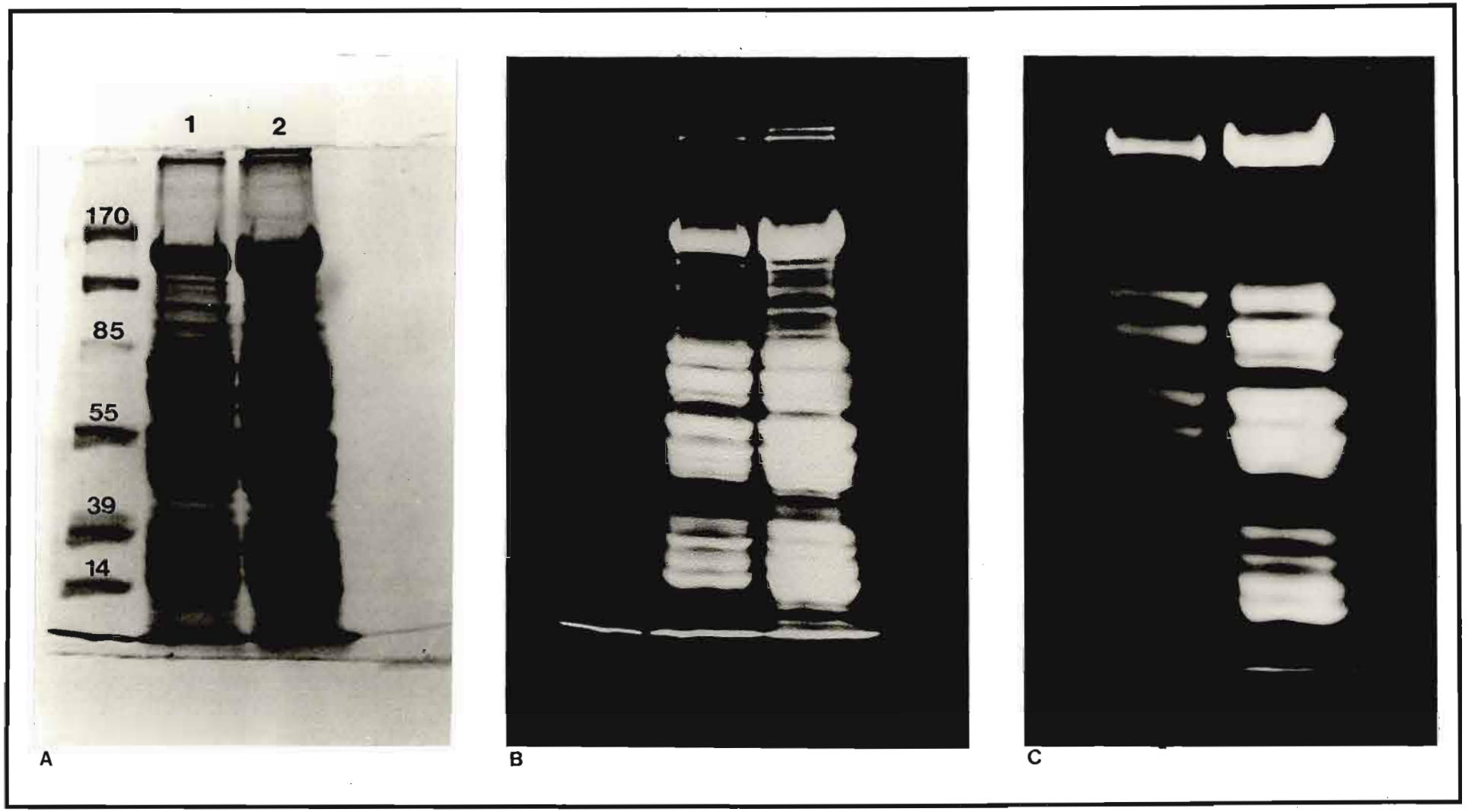


Figure 4.54 Protein concentrations in 10% polyacrylamide gels. A. Normal Coomassie blue stained gel. Lane 1 & 2 represent mitochondria from untreated and treated rats repectively. B. Inverted light image of A., showing a greater density of protein bands in lane 2. C. Inverted light image of A, with a lower light intensity showing the more heavily stained bands in lane 2.

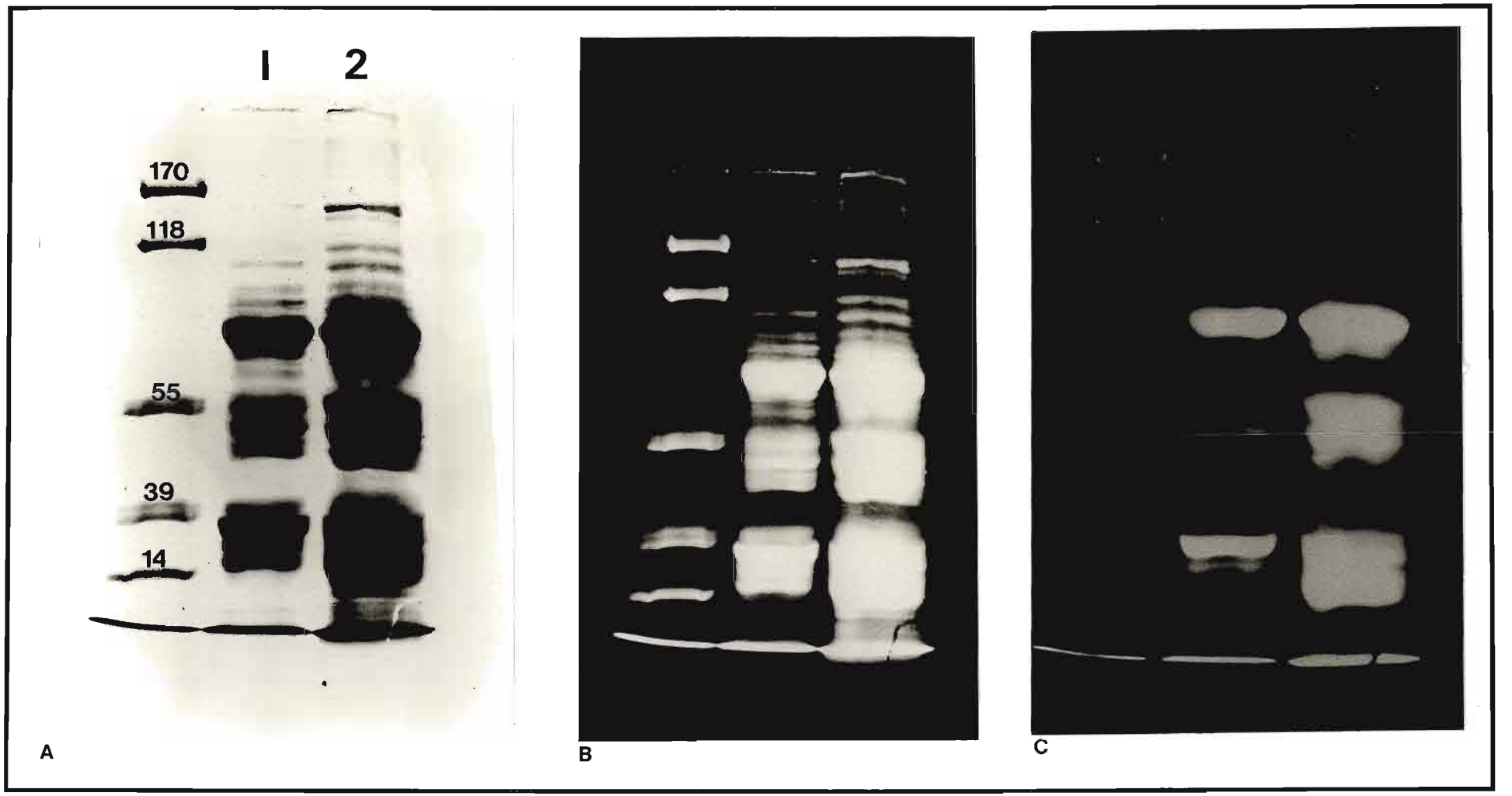


Figure 4.55 Protein concentrations in 10% polyacrylamide gels. A. Normal Coomassie blue stained gel. Lane 1 and 2 represent SMP's from untreated and treated rats repectively. B. Inverted light image of A., showing a greater density of protein bands in lane 2. C. Inverted light image of A, with a lower light intensity showing the more heavily stained bands in lane 2.

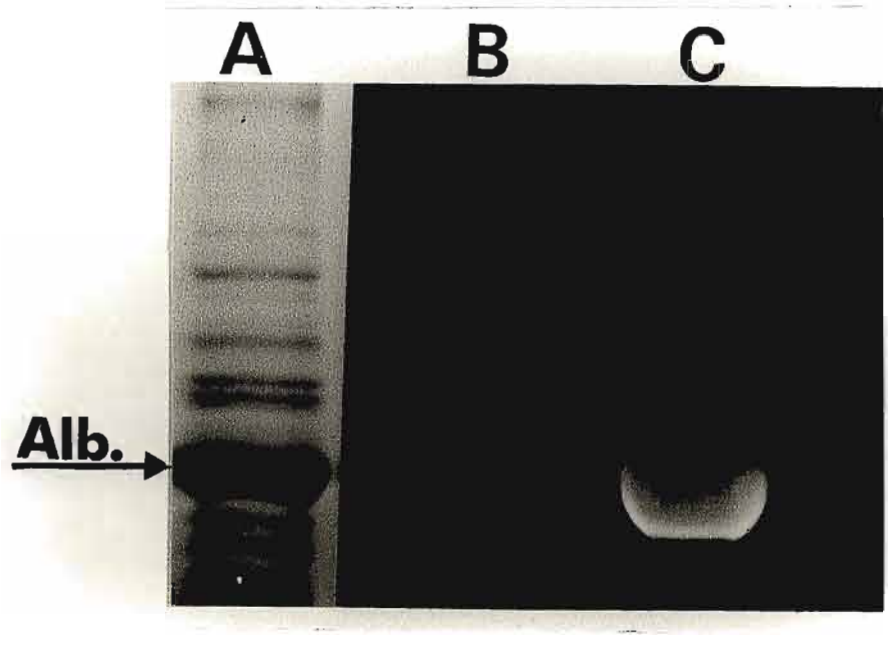


Figure 4.56 Coomaasie blue stained gel, under inverted light intensity showing presence of albumin isolated from untreated rat serum (lane B) and treated rat serum (lane C). Bovine serum albumin marks the first lane of the gel and was used as a standard marker for albumin (lane A).

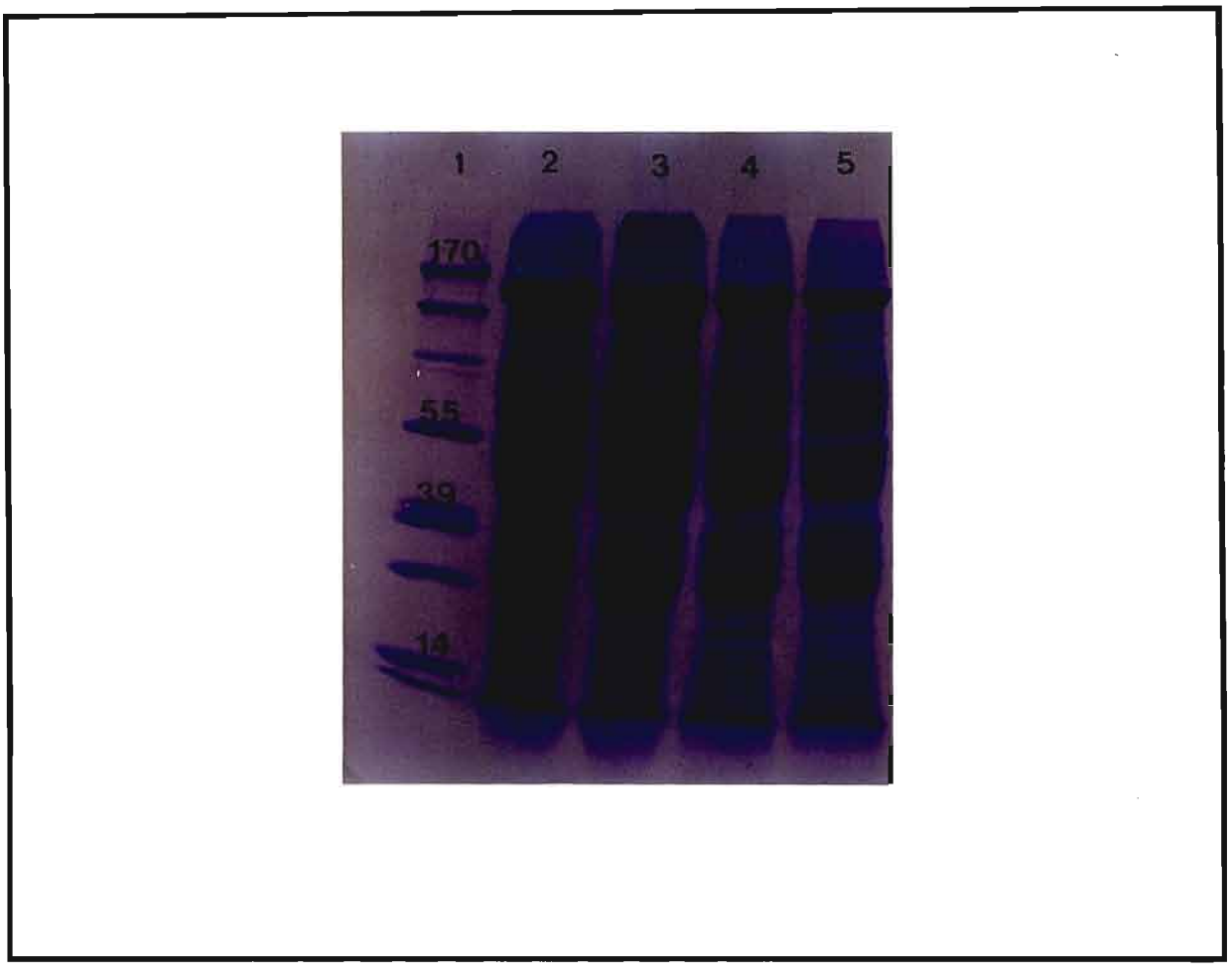


Figure 4.57 Coomassie blue stained gel of rat liver mitochondrial proteins. Lane 1, Molecular weight markers. Lane 2, Mitochondria isolated from untreated rats (*in vivo*). Lane 3, Mitochondria isolated from treated rats (6mg $AFB_1$/kg body weight), (*in vivo*). Lane 4, Isolated mitochondria,untreated, (*in vitro*). Lane 5, Isolated mitochondria treated with aflatoxin $B_1$ (0.5μg AFB1/mg mitochondrial protein), (*in vitro*).

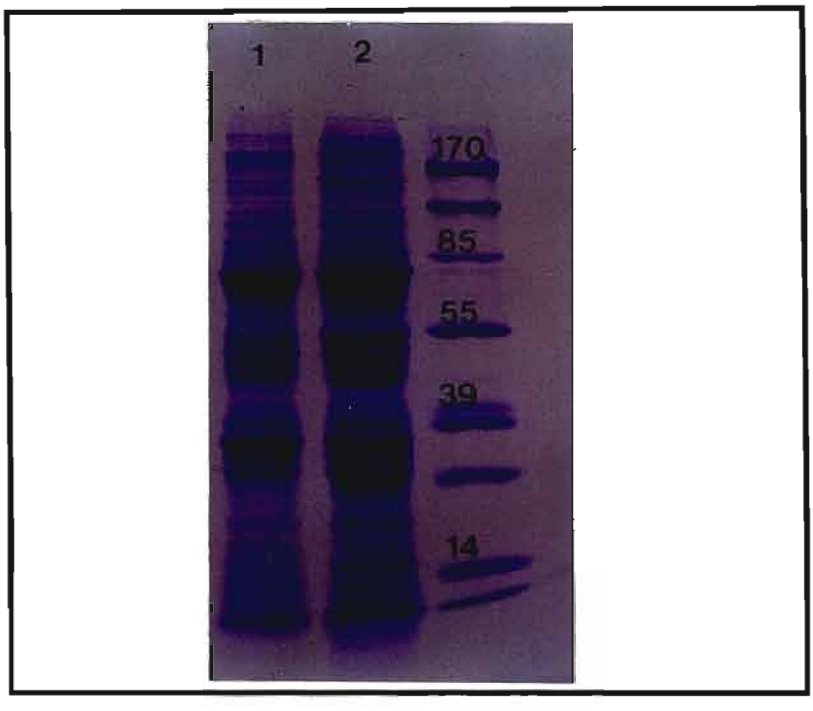


Figure 4.58 Coomassie blue stain polyacrylamide gel showing protein of the inner mitochondrial matrix fraction of rat liver mitochondria. Lane 1, Control sample from untreated rats. Lane 2, Experimental sample from treated rats.

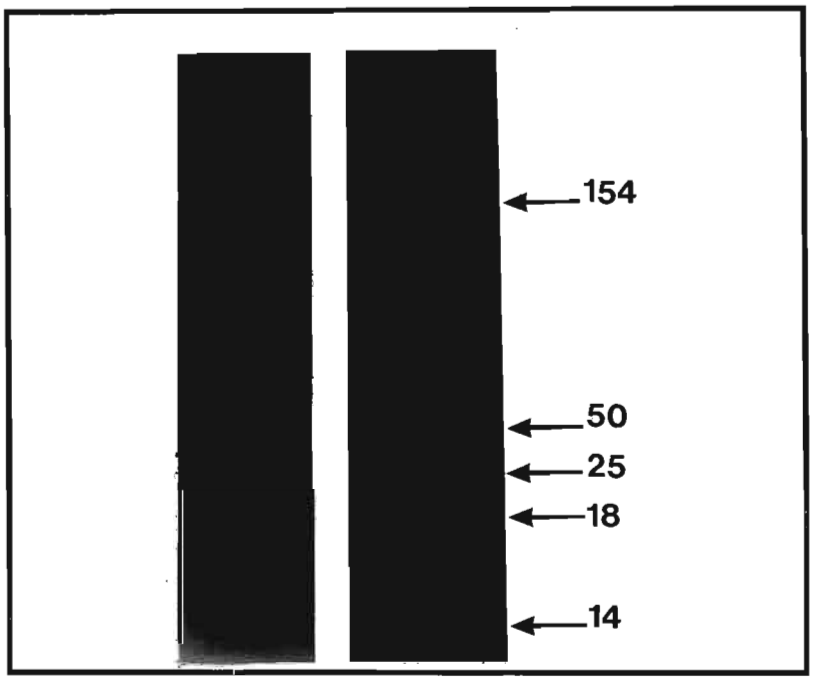


Figure 4.59 Western-immunoblots of the inner mitochondrial-matrix fraction from untreated rats (lane 1) and treated rats (lane 2). Five $AFB_1$-bound protein fragments were identified in the following molecular weight range (154 kDa, 50 kDa, 25 kDa, 18 kDa, 14 kDa).

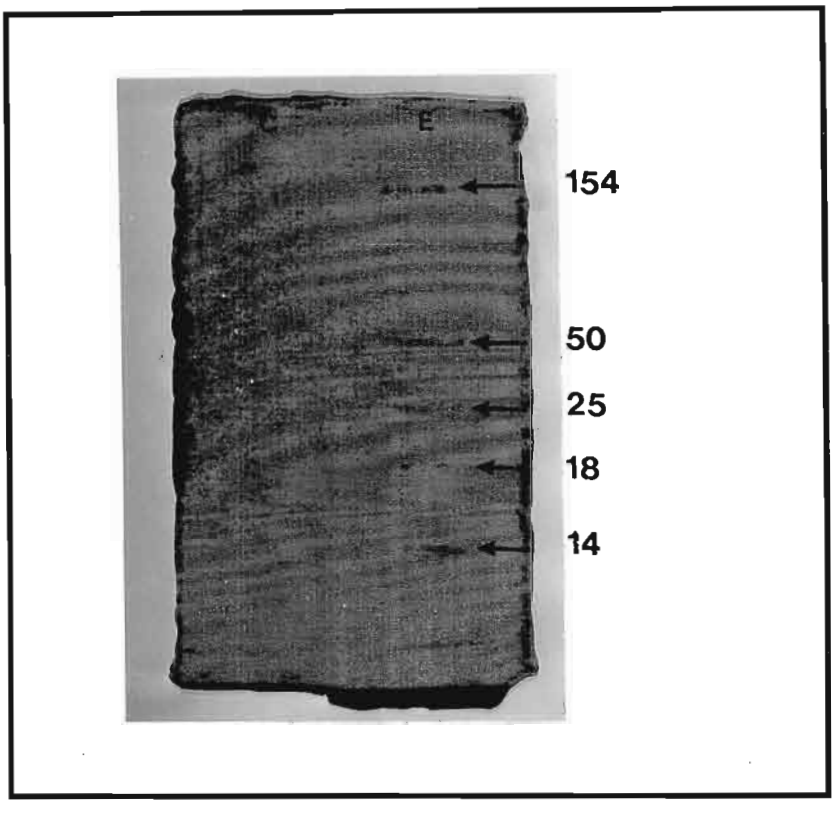


Figure 4.60 Direct immunodetection of $AFB_1$-bound proteins on 10% Polyacrylamide gels. Five $AFB_1$-bound protein fragments were identified in the following molecular weight range (154kDa, 50kDa, 25kDa, 18kDa, 14kDa).

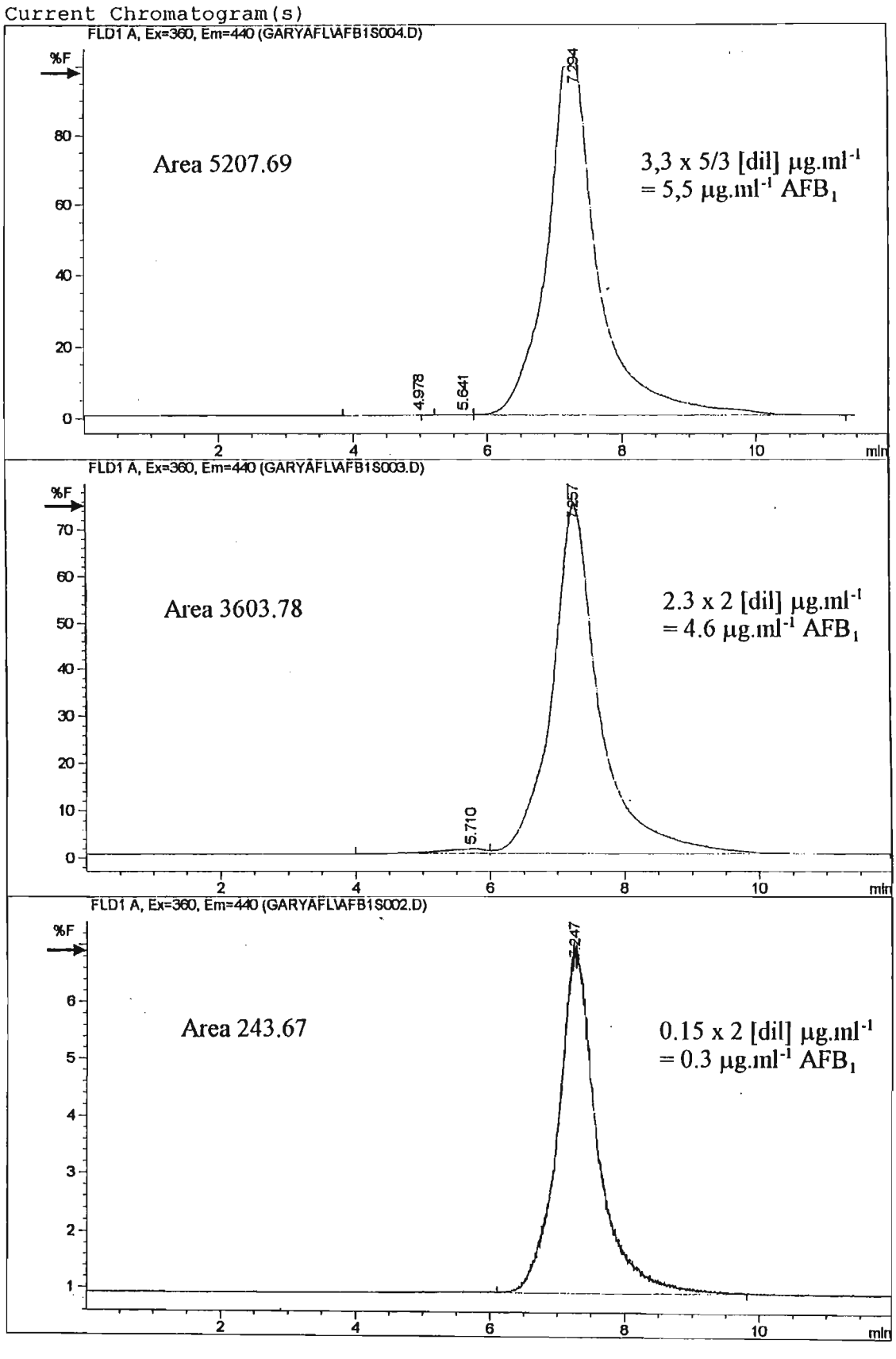


Figure 4.61 Fluorescence chromatograms of aflatoxin $B_1$ standard, 5.5µg.ml$^{-1}$ peak, (A); treated mitochondria pellet fraction, 4.6µg.ml$^{-1}$ peak (B); and supernatant sucrose buffer, 0.3µg.ml$^{-1}$ peak (C).

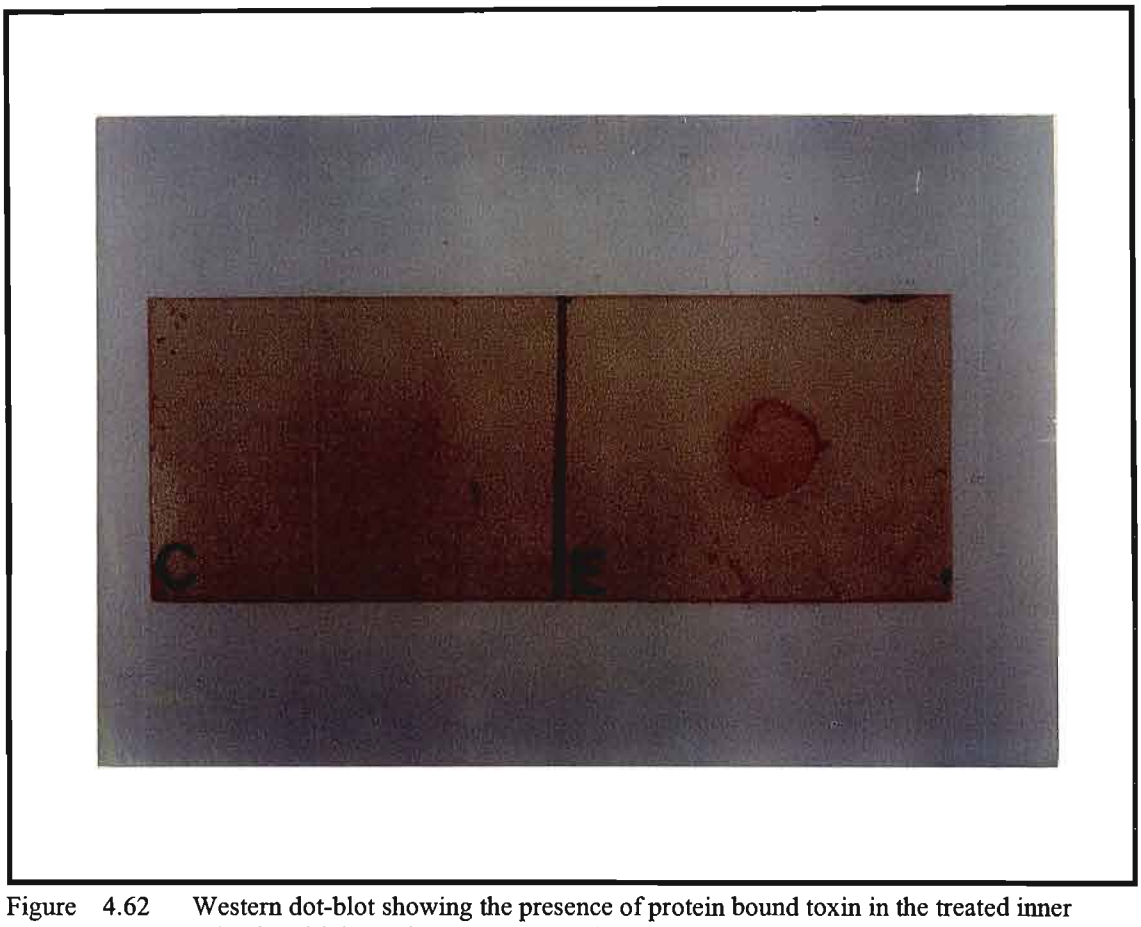


Figure 4.62 Western dot-blot showing the presence of protein bound toxin in the treated inner Mitochondrial membrane fraction (E) analysed by HPLC. No toxin was found in control, untreated mitochondria (C).

# Chapter 5

# DISCUSSION

Cancer of the liver is estimated to be one of the eight most frequent cancers in humans. Biological and chemical factors ($AFB_1$ and other environmental carcinogens) involved in the aetiology of liver cancer in humans have been identified during the latter half of this century, however knowledge of the disease itself extends back into the last century. The first clear demonstration of the chemical induction of hepatomas in rodents was reported by Sasaki and Yoshida (1935). These pioneering studies led to numerous investigations, primarily in rodents; these studies now form an experimental basis on which one can begin to relate the cellular and molecular pathogenesis of chemically induced hepatic neoplasia in animals to the development of the disease in humans.

A great deal obviously remains to be learned about the metabolism of $AFB_1$ by animals and humans. Information on the subject in this thesis further indicates and emphasises the multifaceted mode of action, and diverse metabolic pathways assumed by $AFB_1$ during toxicity. This study indicates that a significant proportion of a single dose of $AFB_1$ is rapidly taken up by the liver and by several organelles within the liver. The treatment gives rise to a persistent array of histologic damage and biological alterations.

These findings imply that a small amount of the toxin or derivatives of it, remain undetected by detoxification processes in the liver, where they can persist in the tissue for prolonged times after dosing, and with the capabilities of interacting with cellular constituents to initiate self-perpetuating biochemical events leading to carcinogenesis and cellular death.

The specificity of uptake and binding of the toxin within the mitochondria, indeed suggests that these organelles play some role in $AFB_1$-mediated toxicity within the liver. Particular interest has been shown in the metabolic fate of the mycotoxin in mammalian hepatocytes, in order to elucidate its toxic and carcinogenic mechanisms. However, the actual transport mechanisms for $AFB_1$ within the cell system is largely unknown. The presence of $AFB_1$ within the several organelles of the liver suggests that the toxin is able to pass across several biological membranes. Aflatoxin $B_1$ is a lipid soluble compound and is capable of dissolving the phospholipid bilayer of the mitochondrial membrane. In this study, membrane damage and extrusion of the matrix was observed in several toxin treated samples (Figures 4.37, 4.38, 4.45), suggesting that the toxin dissolved the membrane at the surface, in order to penetrate the mitochondria. However, this proposed mechanism of $AFB_1$ transport into the mitochondria is not absolute. Several samples of mitochondria isolated from treated rats indicated the presence of toxin within intact mitochondria, the outer and inner membranes completely unaffected by the presence of the toxin (Figure 4.25). In addition, toxin was also located within the inter-membrane fraction in certain mitochondria and also directly on the membrane itself (Figures 4.34, 4.35), together suggesting another mechanism of entry into the mitochondria.

In these cases, it is possible that the toxin may have entered the mitochondria during mitochondrial protein import, through specific protein transport channels or contact sites on the mitochondrial membrane surface.

Moynagh (1995) clearly indicated the presence of several outer and inner membrane proteins involved in a protein translocation complex, that allows preprotein polypeptides to enter the mitochondria (Figure 2.6). It has been proposed therefore that $AFB_1$ may be capable of binding to preprotein and entering the mitochondria via translocation across any one of these contact sites. Aflatoxin $B_1$ can be activated to its reactive epoxide by cytochrome $P_{450}$ in the endoplasmic reticulum and microsomes that are found in the cytoplasm (Eaton and Groopman 1994). The reactive $AFB_1$-8,9-epoxide (AFBO), has been shown to bind to histones and several other proteins including the plasma protein albumin (Iwaki *et al.*, 1993; Sabbioni *et al.*, 1987; Dirr and Schabort, 1986).

Sabbioni *et al.*, (1987) showed that a major serum albumin adduct was formed by $AFB_1$ *in vivo* in rats. They reported that the epoxide formed an adduct by binding with the ε-amino group of lysine, to form a Schiff's base. The Schiff's base undergoes an Amadori rearrangement to an α-amino ketone. Several authors strongly suggest that $AFB_1$-lysine adduct formation is the mechanism of $AFB_1$-protein complex formation (Sabbioni *et al.*, 1987; Iwaki *et al.*, 1993). Although the exact role of $AFB_1$-protein binding remains unclear, their role in $AFB_1$-mediated carcinogenecity and toxicity is slowly being unravelled.

Ch'ih *et al.*, (1993) suggested that the lipophilic nature of $AFB_1$ did not allow it to freely enter the nucleus. They postulated that the toxin might translocate across the nuclear pore as a ligand-protein complex by binding to proteins destined for the nucleus (histones), thus increasing its uptake, activation and damage to DNA. In this study, $AFB_1$ was indeed located in the nucleus and along the nuclear membranes (Figure 4.18, 4.19).

Albumin has been targeted as the major transport protein for $AFB_1$, responsible for toxin binding and translocation, at least in rat blood (Dirr and Schabort, 1986). Interestingly, in this study, albumin concentrations in the blood isolated from rats treated with a single dose of toxin increased by 40% as compared to control albumin samples isolated from untreated rats (Table 8, Figure 4.56). These results strongly suggest that albumin concentrations increased in direct response to the presence of $AFB_1$, and possibly as a means of translocation within the blood to adequate areas of detoxification.

Indeed albumin may be described as the principle binding protein involved in $AFB_1$-mediated toxicity and transport (Wild *et al.*, 1986). However, the presence of other proteins involved in toxin binding have been reported by several authors (Iwaki *et al.*, 1993; Groopman *et al.*, 1980; Mainigi and Sorof, 1977) although their exact roles in $AFB_1$ mediated toxicity are largely unknown.

In can be argued from this study, that $AFB_1$-protein complexes are not necessary for transport into mitochondria, given the results obtained from *in vitro* trials. Aflatoxin $B_1$ was specifically located within mitochondria that were treated directly with a single dose of the toxin.

Toxin was located within the matrix, inner membrane fractions and outer membrane regions (Figure 4.44, 4.45, 4.46), indicating that the native toxin was capable of penetrating the mitochondria, whilst present in an isotonic sucrose buffer.

Several studies have shown that sucrose buffers maintain mitochondrial membrane integrity and function (Munn, 1974; Darley-Usmar *et al.*, 1987), so it is apparent that toxin absorption by the mitochondria did not occur because of a loss in membrane integrity and permeability.

Indeed several studies have shown that rats are very sensitive to $AFB_1$ with high incidence of hepatic tumour, while mice and hamsters were more resistant to the toxins cytotoxic as well as carcinogenic effects (Garner and Martin, 1978; Wogan, 1973). It is well known that the mitochondrial inner membrane presents a barrier to a number of lipophilic and hydrophilic compounds (Pederson, 1978; Munn, 1974). Liposome vesicles have been used for transmembranous delivery of proteins (Racker, 1972).

With the use of this liposome system, Niranjan *et al.*, (1986) showed a severe inhibition of protein synthesis in mouse mitochondria treated with liposome encapsulated $AFB_1$ (0.2μmol of $AFB_1$ per ml), whereas even 4 times this concentration of $AFB_1$ alone, had no effect on protein synthesis by mouse liver mitochondria. Aflatoxin $B_1$ however, inhibited rat liver mitochondrial activity by as much as 80%. The results from the study showed that the hepatic mitochondrial genetic systems in mouse and hamster are protected against injurious effects of $AFB_1$ under both *in vivo* and *in vitro* conditions.

In the case of mouse liver mitochondria, the protection seemed to result from the impermeability of the mitochondrial membrane to the carcinogen. In the case of the hamster liver system, the protective mechanism appears to be more complex and included a permeability barrier and the possible occurrence of a scavenging system. Although the nature of this scavenging system remains unknown, these authors have shown that over 40% of $AFB_1$ associated with hamster liver mitochondria is water soluble, as against no significant water-soluble component in rat liver mitochondria.

If $AFB_1$ is capable of entering rat mitochondria in its native state, by passing freely through the mitochondrial membrane and into the matrix, as is true by the results obtained in this study (Figure 4.34, 4.36, 4.45) the use of toxin-protein complexes for entry would appear unnecessary.

A closer look at the results however shows that a greater amount of label was localised in mitochondria isolated from treated rats (*in vivo*) (Figures 4.22, 4.23), that in isolated mitochondria that were treated with toxin (*in vitro*) (Figures 4.34, 4.46).

One might argue that this result might stem from a concentration effect, considering that the rats received a different dose (6mg $AFB_1$/kg body weight) than the isolated mitochondria (0.5μg/mg mitochondrial protein). However, mitochondria within a cell are more likely to have a higher metabolic activity than mitochondria isolated in sucrose buffer. In this instance, a higher cytochrome $P_{450}$ activity within the mitochondria (*in vivo*) would result in a greater amount of toxin being activated to the $AFB_1$-8,9-epoxide.

Hence one can conclude, that although $AFB_1$ can enter isolated mitochondria in an isotonic sucrose buffer, free of being bound to any protein or polypeptide fragment, and also in an inactivated state, as *in vitro* results imply, there may be some mechanism *in vivo* that greatly enhances entry into mitochondria. Thus, in an *in vivo* system, it is possible that $AFB_1$ can freely enter the mitochondria, where it can then be converted to the reactive AFBO, or it could be activated by microsomal and endoplasmic reticulum cytochrome $P_{450}$ mixed-function oxidases to AFBO. It could then bind to several cytoplasmically synthesised proteins that are destined for the mitochondria.

In this bound form, the toxin may be able to enter the mitochondria through several channels or contact sites involved in protein translocation. Protein profiles of crude mitochondria and inner-membrane matrix fraction from untreated and toxin treated rats, revealed no significant difference in band patterns (Figure 4.57). However it is apparent that protein content in mitochondria isolated from the livers (15g) of treated rats were markedly greater than the protein content in mitochondria isolated from livers (15g) of untreated rats (Table 8, Figure 4.54). Mitochondrial protein content increased by approximately 41.8% following toxin treatment. Interestingly, albumin concentrations in the serum isolated from rats treated with $AFB_1$, also showed an increase of 40%. Bhat *et al.*, (1982) and Niranjan *et al.*, (1986) both showed a marked inhibition of mitochondrial proteins that were imported from the cytoplasm, after 3hrs of toxin treatment. This inhibitory effect appeared to be recovered by 12 hours and the 24 hours pattern compared with the control pattern both qualitatively and quantitatively.

The level of bound $AFB_1$ in the mitochondrial genome also remained nearly constant even up to 24 hours. This is possibly due to the lack of repair in this organelle system. It should also be noted that the number of adducts per $10^7$ daltons mitochondrial DNA is about 3-4 times higher than the level observed for nuclear DNA. Thus the inhibition of mitochondrial activity appears to be largely due to the direct attack on the mitochondrial genetic system.

Considering that the rats were sacrificed 24 hours after toxin administration, any inhibitory effect of mitochondrial protein import from the cytoplasm would be recovered (Bhat *et. al*, 1982). The increase in protein content in treated mitochondria after 24 hrs following toxin treatment, may not therefore be the result of increased protein synthesis, but possibly because of increased protein translocation of $AFB_1$-cytoplasmic protein complexes into the mitochondria, or increased cytoplasmic proteins translocated into the mitochondria because of an increase in mitochondrial biogenesis observed in toxin treated samples (Figures 4.8, 4.9). Increased mitochondrial biogenesis in response to toxin administration has not been reported previously.

The increased mitochondrial protein content could also reflect a repair process to mitochondria that were damaged by the presence of $AFB_1$. Mitochondria in toxin treated samples in this study, however have been shown to undergo several ultrastructural and conformational changes (including a marked increase in division) in response to the presence of the toxin.

Numerous biochemical and autoradiographic studies have indicated that there is a definite turnover of mitochondrial components (e.g. proteins, lipids, and cytochrome *c*) in response to various pathological situations (Fletcher and Sanadi, 1961; Beattie *et al.*, 1967; Gold and Menzies, 1968). Morphological evidence supporting the idea of a molecular repair and replacement of mitochondrial components is lacking, but there is a great deal of evidence that mitochondria can divide and multiply as a means of removal of what would appear to be old, effete or damaged mitochondria.

Hence the greater frequency of such changes in pathological states (during $AFB_1$-mitochondrial toxicity for example), may be looked upon as an activation of normal mechanisms geared to the removal of organelles damaged by such noxious influences. Mitochondrial swelling has at times been regarded as another possible fate that might befall effete mitochondria (Rouiller, 1960). Ghadially (1980) reported that mitochondrial swelling occurs in virtually every mitochondrion. Ghadially (1982) and Rouiller (1960) further reported that in certain cases, one may occasionally find one or two grossly swollen mitochondria in company with other normal-looking mitochondria in a variety of experimental and other situations. Here there is clearly no general derangement of osmotic forces within the cell.

The primary defect lies in the swollen mitochondria itself, and this could well be regarded as an effete or damaged organelle about to suffer dissolution. Several toxin treated samples in this study showed mitochondria in this form (Figure 4.7).

Swollen mitochondria or even swollen mitochondrial components have been observed in almost every type of tissue subjected to a variety of pathological influences. It is so common a manifestation of cell injury that it would be impossible to list every situation in which this change has been noted. David (1964) has listed the following conditions in which mitochondrial swelling has been seen in the liver : kwashiorkor, choline deficiency, vitamin $B_1$ deficiency, hepatitis, diphtheria toxin, and cirrhosis. By far the commonest form of swelling, is that due to the involvement of the matrix or inner chamber. In early stages of induced swelling, there is only a modest increase in the size of the mitochondria, with the dilution of the matrix, as evidenced by decreased density, just visible.

Loss of matrix density increases and this is also associated with the loss of matrix substance (Ghadially, 1980). These results by Ghadially (1980) were found in the mitochondria from the liver of a rat bearing a carcinogen-induced subcutaneous sarcoma, and are consistent with findings in this study. Several samples showed treated mitochondria with markedly swollen cristae (Figures 4.37, 4.45, 4.46). The matrix sometimes appeared patchy (Figures 4.36, 4.37), and several breaks were evident in the mitochondrial limiting membranes (Figure 4.37). The mitochondria found in tumours (Ghadially, 1980) are frequently disrupted owing to a flooding of the matrix chamber with water. In this study, disrupted membranes were a common feature associated with the presence of toxin (Figures 4.37, 4.45). In addition the mitochondria in toxin treated cells, particularly in areas of the nucleus were markedly swollen (often referred to as cloudy swelling) and well contrasted (Figure 4.1), from the more normal looking mitochondria in the same area, in untreated rats (Figure 4.2).

Another common feature, often found in neoplastic tissues, are mitochondria with swollen or ballooned cristae and a relatively dense matrix, as evidenced by mitochondria from cells infected with the Herpesvirus (Ghadially, 1982).

In certain pathological situations this type of ballooning may be accompanied by the separation of the inner and outer membranes (Ghadially, 1982). In this study a distinct separation of the outer and inner membranes were visible in toxin treated samples (Figures 4.10), and this was sometimes coupled with the mitochondrial division (Figure 4.9), and swollen cristae (Figure 4.45).

Mitochondrial inclusions (Figure 4.12), found in isolated mitochondria from toxin treated rats, of filamentous or crystalline nature have been reported in a number of cell types such as hepatic cells. These intramitochondrial paracrystalline inclusions have been reported in various normal and pathological tissues. Little is known about the chemistry or significance of these crystals. These inclusion have also been shown to be closely associated with the inner mitochondrial membrane and cristae (Ollerich, 1968). Several investigators have shown that these mitochondrial inclusions in liver cells under different pathological conditions represented a non-specific degenerative phenomenon in the mitochondrion (Ghadially, 1982). Interestingly a large proportion of these inclusions in this study were observed, closely associated with the inner-mitochondria membrane fraction from untreated control samples (Figure 4.12). There were hardly any inclusions in the experimental samples (Figure 4.13, 4.14). Ollerich (1968) indicated that these crystals might represent a form of protein storage or energy reserve (often found in hibernating animals and oocytes).

If this were the case within the mitochondria found in this study, it would adequately explain a greater concentration of these "energy storage" crystals in mitochondria isolated form untreated rats. It is possible that during $AFB_1$-toxicity, the mitochondria may effectively utilise these stored forms of energy. This energy would be needed during mitochondrial repair processes and mitochondrial division.

Other studies have indicated that these crystals might represent crystallised mitochondrial proteins. Although there is little to support or refute such assumptions, the presence of label within these inclusions (Figure 4.30), could further suggest $AFB_1$-protein binding within these inclusions. In addition to the various altered mitochondrial morphology associated with the presence of $AFB_1$, several other ultrastructural abnormalities were found in experimental tissues.

The endoplasmic reticulum in several samples from treated tissues appear to be slightly swollen (Figure 4.21). Conjugated toxin was also closely associated with the endoplasmic reticulum membranes (Figure 4.21). According to Ghadially (1982) morphological features of necrosis and often neoplasia include familiar cytoplasmic changes, such as dilation or swelling of the endoplasmic reticulum and mitochondrial swelling, and often includes chromatin margination. Margination of chromatin (Figure 4.1) in toxin treated tissues as compared to control-untreated tissues (Figure 4.2) appears to be a fairly early change that occurs in the nucleus after irreversible injury leading to cell death (Trump *et al.*, 1963).

The evidence describing the specific attack of the mitochondrial system by $AFB_1$ in this study becomes more compelling, given the vast cellular alterations and ultrastructural abnormalities associated with the presence of the toxin.

Western immunoblots and direct detection on polyacrylamide gels, used for the localisation of $AFB_1$-bound proteins within the mitochondria further confirmed a possible role of mitochondrial proteins in $AFB_1$-mediated toxicity (Figures 4.59, 4.60). There have been a number of studies on the macromolecular binding of labelled carcinogens to macromolecules. Several of these researchers have indicated that nucleic acid binding is of greater importance for tumour initiation. This opinion has been largely based on the fact that nucleic acid binding is greater on a per molecule basis than protein binding (Garner and Wright, 1975). In addition, it is a well established fact that AFBO reacts with liver DNA forming aflatoxin-$N^7$-guanine adducts, leading ultimately to cellular mutations and carcinogenesis.

Garner and Wright (1975) showed that 6 hours after toxin administration to rats, for every molecule of protein reacted with carcinogen, there were 400 molecules of DNA with bound carcinogen. These studies greatly emphasise the importance of $AFB_1$-DNA binding in induced carcinogenesis. At the same time, the role of $AFB_1$-protein binding may often be taken for granted as a secondary or insignificant process. This study however is the first to show that in an *in vitro* system, a significantly large proportion (84%) of a single dose of toxin remains bound to mitochondrial protein (Figures 4.61, 4.62). These HPLC results further suggested that $AFB_1$-bound protein binding plays an important role in aflatoxin mediated carcinogenesis.

Hence, although $AFB_1$-DNA binding may still remain the ultimate step in tumour initiation, $AFB_1$-protein binding may also play just as important or crucial role in $AFB_1$-induced cellular toxicity through metabolism, modulation of DNA-adduct formation or transport. No $AFB_1$-protein complexes were found in the outer and intermembrane fractions that were blotted and immunoprobed. Five specific proteins (Figures 4.59, 4.60), however, indicated the presence of bound toxin in the inner-mitochondrial matrix fraction.

This indicated that the toxin may have specifically targeted the electron transport chain, which is found in this fraction. It should be noted that $AFB_1$ inhibits the electron transport chain at complex III (the cytochrome *c* oxidase complex), by inhibiting the activity all the enzymes of the complex (Ramachandra *et al.*, 1975; Doherty and Cambell, 1973).

This complex has been shown to contain several subunits. Some of these subunits include core protein (49kDa), core protein II (45kDa), cytochrome *b* (34kDa), cytochrome *c* (29kDa), iron sulphur protein (24kDa), (Ragan *et al.*, 1987). Most other cytochrome *c* polypeptides (many are unidentified) have molecular weights in the region of 8-54kDa (Darley-Usmar *et al.*, 1987). Fasman (1976) reported that of all the amino acids comprising cytohrome *c* in humans and animals, lysine appeared to be the most concentrated (comprising 17% of the total amount of amino acids). Other amino acids for example were found in much smaller percentages of the total amount of amino acids viz. arginine, 1.92%; histidine, 1.82; asparagine, 7.69%; threonine, 6.73%; serine, 1.92%; glutamine, 9.62%, proline, 3.85%; glycine, 12.5%; alanine, 5.77%; cysteine, 1.92; valine, 2.88%; methionine, 2.88%; isoleucine, 7.69%; leucine, 5.77%; tyrosine, 4.81; phenylalanine, 2.88%; tryptophan, 0.96% (Fasman, 1976).

Given aflatoxin $B_1$ inhibition of the electron transport chain at Complex III, and considering the large amount of lysine residues in polypeptides comprising the complex, plus the fact that most of the inner-membrane matrix proteins found bound to $AFB_1$ in this study do fall within the molecular weight regions (50kDa, 25kDa, 18kDa, 14kDa), of the polypeptides of Complex III (8-56kDa, Ragan *et al.*, 1987), it would be safe to suggest that the some of the $AFB_1$-bound proteins may be part of the polypeptides subunits of Complex III.

Although largely unproved at this stage, this assumption may be likely when considering the exact role of mitochondria in $AFB_1$ mediated toxicity. Niranjan *et al.*, (1984) reported a unique hepatic mitochondrial cytochrome $P_{450}$ enzyme system involved in the bioactivation of $AFB_1$.

Interestingly, this system is located in mitochondria, exclusively in the same inner-membrane matrix fraction. The same fraction that houses Complex III and the $AFB_1$-bound proteins found in this study. One theory for the presence and significance of $AFB_1$-bound proteins within mitochondria from the livers of rats treated with a single dose of $AFB_1$ could be the following :

*In the cytoplasm of liver tissues, Aflatoxin $B_1$ may bind non-covalently to selective cytoplasmically sythesized proteins destined for the mitochondrial inner-membrane matrix fraction (electron transport chain). In this way, the protein-toxin conjugate could pass freely through several channels or contact sites of the mitochondria membranes during mitochondrial protein import and biogenesis.*

*The toxin will therefore be transported to the inner mitochondrial matrix, where a unique cytochrome $P_{450}$ enzyme system would convert it to the highly carcinogenic and reactive AFBO. The epoxide (AFBO) could then bind to mtDNA, mtRNA and proteins resulting in the inhibition of oxidative phosphorylation, protein synthesis and ultimately lead to mitochondrial injury, cellular death, mutation and eventually carcinogenesis.*

*Alternatively $AFB_1$ may enter the mitochondria in its native state (being lipid soluble it would be able to cross the phospholipid bilayer). Once within the inner-mitochondrial matrix it would be activated by mitochondrial cytochrome $P_{450}$ to its reactive epoxide. The epoxide would then be capable of binding to proteins, mt DNA, and mt RNA.*

*Aflatoxin $B_1$ can also be activated by microsomal and endoplasmic reticulum cytochrome $P_{450}$ enzymes to AFBO. The epoxide (AFBO) could then enter the mitochondria or the nucleus, resulting in impaired activity and mutation, and eventually cellular death and carcinogenesis.*

## CHAPTER 6

# CONCLUSION

Primary liver cancer is one of the leading causes of cancer mortality in Asia and Africa. $AFB_1$-induced carcinogenesis is of primary interest since the toxin is widely distributed as a human and animal food contaminant and its ingestion has been associated with high primary liver cancer incidence in several parts of the world.

The exact mechanism of $AFB_1$-induced carcinogenesis and cellular toxicity remains to be elucidated. The toxin appears to have a multifaceted mode of attack on several organelle systems within liver tissues. Hence $AFB_1$-toxicity may involve several metabolic pathways that ultimately lead to toxin activation and eventually cellular death.

Involvement of the mitochondrial system in cancer has been a subject of argument ever since Warburg's (1935) discovery on altered mitochondrial oxidative metabolism in tumour cells. Over the years a number of studies have demonstrated differential properties of mitochondria in tumour cells with respect to membrane structure, function and biogenesis. Experimental carcinogenesis and chemotherapy studies have shown that significant levels of nitrosamine and nitrogen mustard (Niranjan and Avadhani, 1980) are transported to mitochondrial compartments where they form adducts with mitochondrial DNA.

Similarly, it has been proposed that $AFB_1$ administration leads to inhibition of mitochondrial oxidative phosphorylation and also DNA biosynthesis. The results of this thesis show that in rats treated with a single dose of aflatoxin, the mitochondria appear as direct targets for attack by the carcinogen. In addition, incubation of the toxin with isolated mitochondria and sub-mitochondrial particles revealed a significant specificity of the toxin to enter and bind to components of the mitochondria.

This is the first study to specifically show the selective uptake and immunolocalisation of aflatoxin $B_1$ in rat liver mitochondria *in vivo* and *in vitro*. In addition, this study also emphasises for the first time that a significant proportion of administered toxin binds to protein found in the mitochondria, and thus suggests that $AFB_1$-protein binding forms a major part of $AFB_1$-induced toxicity in liver mitochondria and tissues. The identification of several $AFB_1$- bound proteins found within the inner membrane fraction of treated mitochondria, reveals that the electron-transport chain is a specific target of $AFB_1$. To clarify the roles and cellular localisation of the several $AFB_1$-proteins found in this study, purification and characterisation of the individual proteins in necessary.

**These results taken together confirm that mitochondria are indeed direct and perhaps preferential targets for attack by $AFB_1$. Mitochondria therefore appear to play a significant role in $AFB_1$ mediated toxicity and carcinogenesis.**

# REFERENCES

**Bai NJ, Ramachandra Pai M & Venkitasubramanian TA.** Mitochondrial function in aflatoxin toxicity. Ind. J. Biochem. 1977; 14: 347-349.

**Bailey GS.** Role of Aflatoxin-DNA adducts in the cancer process. In: Eaton DL and Groopman JD, eds. The Toxicology of Aflatoxins, Human health, Veterinary, and Agricultural significance. United Kingdom, Academic Press Inc., 1994: 137-149.

**Backer JM & Weinstein IB.** Mitochondrial DNA is a major cellular target for dihydrodiol-epoxide derivative of benzo(α)pyrene. Science 1980; 209: 297-299.

**Beattie DS, Basford RE & Koritz SB.** The turnover of the protein components of mitochondria from rat liver, kidney, and brain. J. Biol. Chem. 1967; 242: 4584-4597.

**Bhat NK, Emeh JK, Niranjan BG & Avadhani NG.** Inhibition of mitochondrial protein synthesis during early stages of aflatoxin $B_1$-induced hepatogenesis. Cancer Res. 1982; 42: 1876-1880.

**Bohni PC, Daum G & Schatz G.** A matrix-localised mitochondrial protease processing cytoplasmically made precursors to mitochondrial proteins. In: Kroon AM and Saccone C, eds. The Organisation and Expression of the Mitochondrial Genome. Holland, Elsevier, 1983: 423-433.

**Bradford M.** A rapid and sensitive method for the quantitation of microgram quantities of protein utilising the principle of protein-dye binding. Anal. Biochem. 1976; 72: 248-254.

**Butler WH & Barnes JM.** Carcinoma of the glandular stomach in rats given diets containing aflatoxin. Nature 1966; 206: 90-96.

**Cain K & Skilleter DN.** Isolation of rat liver mitochondria. In: Snell K and Mullock B, eds. Biochemical Toxicology, a practical approach. Oxford, IRL Press, 1987: 109-113.

**Cederbaum AI, Becker FF & Rubin E.** Ethanol metabolism by transplantable hepatocellular carcinoma. Role of microsomes and mitochondria. J. Biol. Chem. 1976; 251: 5366-5374.

**Clifford JI & Rees KR.** The action of aflatoxin $B_1$ on the rat liver. Biochemistry 1967; 102: 65-75.

**Croy RG & Wogan GN.** Temporal patterns of covalent DNA adducts in rat liver after single and multiple doses of aflatoxin $B_1$. Cancer Res. 1981; 41: 197-203.

**Ch'ih JJ, Ewaskiewicz JI, Taggart P, & Devlin TM.** Nuclear translocation of aflatoxin $B_1$ - protein complex. Biochem. Biophsy. Res. Commun. 1993; 190: 186-191.

**Cole KE, Jones TW, Lipsky MM, Trump BF & Hsu IC.** In vitro binding of aflatoxin $B_1$ and 2-acetylaminofluorene to rat, mouse, and human hepatocyte DNA: The relationship of DNA binding to carcinogenecity. Carcinogenesis 1988; 9; 711-716.

**Darley-Usmar VM, Capaldi RA, Takamiya S, Millet F, Wilson MT, Malatesta F & Sarti P.** Reconstitution and molecular analysis of the respiratory chain. In: Darley-Usmar VM, Rickwood D, and Wilson MT, eds. Mitochondria. Washington, IRL Press: 1987.

**David H.** Submicroscopic Ortho- and Pathomorphology of the liver. Translated by Epstein HG. Oxford, Pergamon Press: 1964.

**De Recondo AM, Frayssinet C, Lafarge C & Le Breton E.** Inhibition de la synthese du DNA par l'aflatoxine $B_1$ au cours de l'hypertrophie compensatrice du foie chez le rat. Compt. Rend. Acad. Sci. 1965; 261: 1409-1412.

**Detroy RW, Lilliehoj EB & Ciegler A.** Aflatoxin and related compounds. In: Ciegler A, Kadis S, and Aji SJ, eds. Microbial Toxins. New York, Academic Press Inc., 1971: 3-178.

**Dirr HW & Schabort JC.** Aflatoxin $B_1$ transport in rat blood plasma. Binding to albumin *in vivo* and *in vitro* and spectrofluorimetric studies into the nature of the interaction. Biochim. Biophys. Acta. 1986; 881: 383-390.

**Doherty WP & Cambell TC.** Inhibition of rat liver mitochondria. Chem-Biol. Interact. 1973; 7: 63-77.

**Eaton DL & Groopman JD.** Eds. The Toxicology of Aflatoxins: Human Health, Veterinary, and Agricultural Significance. United Kingdom, Academic Press: 1994.

**Emeh JK, Niranjan BG, Bhat NK & Avadhani NG.** Modulation of hepatic transcription and translation during early stages of aflatoxin $B_1$ carcinogenesis. Carcinogenesis 1981; 2: 373-378.

**Epstein M, Bartus B & Farber E.** Renal epithelium neoplasms induced in male Wistar rats by oral aflatoxin $B_1$. Cancer Res. 1969; 29: 1045-1050.

**Fasman GD.** Handbook of biochemistry and molecular biology: Proteins, Vol. III. CRC Press, Ohio: 1976.

**Feo F, Bonelli G, Canuto RA & Garcia R.** Further observations on the effects of trypsin on the volume and functions of mitochondria isolated from normal liver and AH-130 Yoshida ascites hepatoma. Cancer Res. 1973; 33: 1804-1812.

**Fletcher MJ & Sanadi DR.** Turnover of rat-liver mitochondria. Biochim. Biophys. Acta 1961; 51: 356-364.

**Friedman MA, Bailey W & van Tuyle GC.** Inhibition of mitochondrial DNA synthesis by aflatoxin $B_1$ and dimethyl-nitrosamine. Res. Commun. Chem. Pathol. Pharmacol. 1978; 21: 281-293.

**Garner RC & Martin CN.** Fungal toxins, aflatoxins, and nucleic acids. In: Grover PL ed. Chemical Carcinogenesis and DNA. Boca Raton, CRC Press 1978; 1: 187-216.

**Garner RC, Miller EC & Miller JA.** Liver microsomal metabolism of aflatoxin $B_1$ to a reactive derivative toxic to *Salmonella typhimurium* TA 1530. Cancer Res. 1972; 32: 2058-2063.

**Garner RC & Wright CM.** Binding of [$^{14}$C]Aflatoxin $B_1$ to cellular macromolecules in the rat and hamster. Chem.-Biol. Interact. 1975; 11: 123-131.

**Ghadially FN.** Diagnostic electron microscopy of tumours. London, Butterworths: 1980.

**Ghadially FN.** Ultrastructural pathology of the cell and matrix. London, Butterworths: 1982.

**Gelboin HV, Wortham JS, Wilson RG, Friedman MA & Wogan GN.** Rapid and marked inhibition of rat liver RNA polymerase by aflatoxin $B_1$ . Science 1966; 154: 1205-1206.

**Gold PH & Menzies RA.** Mitochondrial turnover in several tissues of the rat. Fed. Proc. 1968; 27: 832-833.

**Greenawalt JW.** Biomembranes : The isolation of outer and inner mitochondrial membranes. Methods Enzymol. 1974; 31: 311-321.

**Groopman JD, Busby WF & Wogan GN.** Interaction of aflatoxin with rat liver DNA and histones *in vivo.* Cancer Res. 1980; 40: 4343-4351.

**Hackenbrock CR, Rehen RG, Weinbach EC & Lemaster JJ.** Oxidative phosphorylation and ultrastructural transformations in mitochondria in intact ascites tumor cells. J. Cell Biol. 1971; 51: 123-137.

**Hartl FU & Neupert W.** Import of proteins into various submitochondrial compartments. Journal of Cell Sci. Suppl. 1989; 11: 187-198.

**Hartl FU, Pfanner N, Nicholson DW & Neupert W.** Mitochondrial protein import. Biochim. Biophys. Acta. 1989; 988: 1-45.

**Hay R, Bohni P & Gasser S.** How mitochondria import proteins. Biochim. Biophys. Acta. 1984; 779: 65-87.

**Hayes JD, Judah DJ, Mclellan LI & Neal GE.** Contribution of the glutathione *S*-transferases to the mechanisms of resistance to aflatoxin $B_1$. Pharmacol. Ther. 1991; 50: 443-472.

**Heathcote JG & Hibbert JR.** Aflatoxins: Chemical and biological aspects. New York, Elsevier Science: 1978.

**Hinke PC.** Mitochondria. In: Arias, IM, Boyer, JL, Fausto N. eds. The Liver : Biology and Pathology, Third Edition. New York, Raven, 1994: 309-316.

**Holeski CJ, Eaton DL, Monroe DH & Bellamy GM.** Effects of Phenobarbital on the biliary excretion of aflatoxin $P_1$ -glucuronide and aflatoxin $B_1$-S-glutathione in the rat. Xenobiotica 1987; 17: 139-153.

**Howatson AF & Ham AW.** Electron Microscopy study of sections of two rat liver tumours. Cancer Res. 1955; 15; 62-69.

**Hsieh DPH, Cullen JM & Ruebner BH.** Comparative hepatocarcinogenecity of aflatoxin $B_1$ and $M_1$ in the rat. Food Chem. Toxicol. 1984; 22: 1027-1028.

**International Agency for Research on Cancer.** Aflatoxins. In: IARC monograph on the evaluation of carcinogenic risks to humans 1976; 10: 55-64.

**International Agency for Research on Cancer.** Aflatoxins. In: IARC monograph on the evaluation of carcinogenic risks to humans 1987; 7: 83-87.

**Iwaki M, Kumagi S, Akamatsu Y & Kitagawa, T.** Aflatoxin $B_1$-binding proteins in primary cultured hepatocytes of chicken embryo: studies *in vivo* and *in vitro*. Biochim. Biopsy. Acta. 1993; 1225: 83-88.

**Kensler TW, Davis EF & Bolton MG.** Strategies for chemoprotection against aflatoxin-induced liver cancer. In: Eaton DL and Groopman JD, eds. The Toxicology of Aflatoxins, Human health, Veterinary, and Agricultural significance. United Kingdom, Academic Press Inc., 1994 : 281-301.

**Kumagai S.** Intestinal absorption and excretion of aflatoxins in rats. Toxicol. Appl. Pharmacol. 1989; 97: 88-97.

**Kushel S. & Ralston D.** Schaum's Outline Series : Biochemistry. New York, Academic Press Inc., 1988.

**Lafarge C, Frayssinet C & Simard R.** Inhibition preferentielle des syntheses de RNA nucleolaire provoquee par l'aflatoxine dan les cellules hepatiques du rat. Compt. Rend. Acad. Sci. (1969); 263: 1011-1014.

**Laemmli UK.** Cleavage of structural proteins during the assembly of the head of bacteriophage $T_4$. Nature 1970; 227: 680-685.

**Lancaster CM, Jenkins FP & Philip P.** Toxicity associated with certain samples of groundnuts. Nature 1961; 192: 1095-1096.

**Lijinsky W, Lee KY & Gallagher CH.** Interaction of aflatoxins $B_1$ and $G_1$ within tissues of the rat. Cancer Res. 1970; 30: 2280-2283.

**Liu L & Massey TE.** Bioactivation of aflatoxin $B_1$ by lipoxygenases, prostaglandin-H synthetase and cytochrome-P450 monooxygenase in guinea-pig tissues. Carcinogenesis 1992; 13: 533-539.

**Lowry OH, Rosebrough NJ, Farr AL & Randall RL.** Protein measurement with the Folin phenol reagent. J. Biol. Chem. 1951; 193: 265-275.

**Mainigi KD & Sorof S.** Carcinogen-protein complexes in liver during hepato-carcinogenesis by aflatoxin $B_1$. Cancer Res. 1977; 37: 4304-4312.

**Malik VS.** Genetics and biochemistry of secondary fungal metabolites. Adv. Appl. Microbiol. 1982; 28: 27-116.

**Massey TE, Stewart RK, Daniels JM & Liu, L.** Biochemical and molecular aspects of mammalian susceptibility to aflatoxin carcinogenecity. Proc. Soc. Exp. Biol. Med. 1995: 213-227.

**McAda PC & Douglas MG.** A neutral metallo-endoprotease involved in the processing of an $F_1$ATPase subunit precursor in mitochondria. J. Biol. Chem. 1982; 257: 3177-3182.

**Mclean M & Dutton MF.** Cellular interactions and metabolism of aflatoxin: An update. Pharmac. Ther. 1995; 65: 163-192.

**Monroe DH & Eaton DL.** Comparative effects of butylated hydroxyanisole on hepatic *in vivo* DNA binding and *in vitro* biotransformation of aflatoxin $B_1$ in the rat and mouse. Toxicol. Appl. Pharmacol. 1987; 90: 401-409.

**Moynagh PN.** Contact sites and transport in mitochondria. In: Apps DK and Tipton KF, eds. Essays in Biochemistry 1995; 30: 1-14.

**Munn EA.** The structure of mitochondria. London, Academic Press Inc. 1974.

**Newborne PM & Butler WH.** Acute and chronic effects of aflatoxin on the liver of domestic and laboratory animals: A review. Cancer Res. 1969; 29: 236-250.

**Newberne PM & Wogan GN.** Sequential morphological changes in aflatoxin $B_1$ carcinogenesis in the rat. Cancer Res. 1968; 28: 770-781.

**Niranjan BG, Wilson N, Jefcoate C & Avadhani NG.** Hepatic mitochondrial cytochrome P-450 system: Distinctive features of cytochrome P-450 involved in the activation of $AFB_1$ and benzo(α)pyrene. J. Biol. Chem. 1984; 259: 12495-12501.

**Niranjan BG & Avadhani NG.** Activation of aflatoxin $B_1$ by a monooxygenase system localised in rat liver mitochondria. Journal of Biol. Chem. 1980; 255; 6575-6578.

**Niranjan BG, Schaefer H, Ritter C & Avadhani NG.** Protection of mitochondrial genetic system against aflatoxin $B_1$ binding in animals resistant to aflatoxicosis. Cancer Res. 1986; 46: 3637-3641.

**Obidoa O.** Aflatoxin inhibition of rat liver mitochondrial cytochrome oxidase activity. Biochem. Med. Metab. Biol. 1986; 35: 302-307.

**Obidoa O & Siddiqui HT.** Aflatoxin inhibition of avian hepatic mitochondria. Biochem. Pharmacol. 1978; 27: 547-550.

**Olden K & Yamada KM.** Direct detection of antigens in sodium dodecyl sulphate-polyacrylamide gels. Anal. Biochem. 1970; 78: 483-490.

**Ollerich DA.** An intramitochondrial crystalloid in element III of rat chorioallantoic placenta. J. Cell Biol. 1968; 37: 188-191.

**Pederson PL.** Tumor mitochondria and the bioenergetics of cancer cells. Prog. Exp. Tumor. Res. 1978; 22: 190-274.

**Polak JM & van Noorden S.** Immunocytochemistry: Modern methods and applications (2nd edition). 1983: 161-172.

**Pon LA, Vestweber D, Yang M & Gottfried S.** Interaction between mitochondria and the nucleus. J. Cell Science 1989; 11: 1-11.

**Pfaller R, Steger HF, Rassow J, Pfanner N & Neupert W.** Import pathways of precursor proteins into mitochondria: multiple receptor sites are followed by a common membrane insertion site. J. Cell Biol. 1988; 107: 2483-2490.

**Pfanner N, Hartl FU, Guird B & Neupert W.** Mitochondrial precursor proteins are imported through a hydrophilic membrane environment. Eur. J. Biochem. 1987; 169: 289-293.

**Quinn BA, Crane TL, Kocal TE, Best SJ, Cameron RG, Rushmore TH, Farber E & Hayes MA.** Protective activity of different hepatic cytosolic glutathione *S*-transferases against DNA-binding metabolites of aflatoxin $B_1$. Toxicol. Appl. Pharmacol. 1990; 105: 351-363.

**Racker E.** Reconstitution of a calcium pump with phospholipids and a purified $Ca^{++}$-adenosine triphosphatase from sarcoplasmic reticulum. J. Biol. Chem. 1972; 247: 8198-8200.

**Ragan CI, Wilson MT, Darley-Usmar VM & Lowe PN.** Sub-fractionation of mitochondria and isolation of the proteins of oxidative phosphorylation. In: Darley-Usmar VM, Rickwood D, and Wilson MT, eds. Mitochondria. Washington, IRL Press 1987: 70-112.

**Ramachandra Pai M, Bai JN & Venkitasubramanian TA.** Effect of aflatoxin on oxidative phosphorylation by rat liver mitochondria. Chem.-Biol. Interact. 1975; 10: 123-131.

**Ramsdell HS & Eaton DL.** Mouse liver glutathione *S* transferase isoenzyme activity toward aflatoxin $B_1$-8,9-epoxide and benzo(a)pyrene-7,8-dihydrodiol-9,10-epoxide. Toxicol. Appl. Pharmacol. 1990; 105: 216-225.

**Raney KD, Shimada T, Kim DH, Groopman JD, Harris TM & Guengerich FP.** Oxidation of aflatoxins and sterigomatocystin by human liver microsomes: Significance of aflatoxin-$Q_1$ as a detoxification product of aflatoxin $B_1$. Chem. Res. Toxicol. 1992; 5: 202-210.

**Reynolds ES.** The use of lead citrate at high pH as an electron opaque stain in electron microscopy. J. Cell Biol. 1963; 17: 208-212.

**Rouiller C.** Physiological and pathological changes in mitochondrial morphology. Int. Rev. Cytol. 1960; 9: 227-235.

**Sabbioni G, Skipper PL, Buchi G & Tannenbaum, SR.** Isolation and characterisation of the major serum albumin adduct formed by aflatoxin $B_1$ *in vivo* in rats. carcinogenesis 1987; 8: 819-824.

**Santella RM, Zhang Y, Chen C, Hsieh L, Lee C, Haghighi, Yang G, Wang L & Feitelson M.** Immunohistochemical detection of aflatoxin $B_1$-DNA adducts and hepatitus B virus antigens in hepatocellular carcinoma and nontumorous liver. Environmental Health Perspectives 1993; 99: 199-202.

**Sasaki T & Yoshida T.** Experimentelle Erzeugung des Lebercarcinoms durch Futterung mito-Amidoazotoluol. Virchows Arch [A] 1935; 295: 175-200.

**Schleyer M & Neupert W.** Transport of proteins into mitochondria: Translocation intermediates spanning contact sites between outer and inner membranes. Cell 1985; 43: 339-350.

**Schnaitman C & Greenawalt JW.** Enzymatic properties of the inner and outer membranes of rat liver mitochondria. J. Cell Biol. 1968; 38: 158-175.

**Shank RC.** Environmental toxicosis in humans. In: Shank RC ed. Mycotoxins and N-Nitroso-Compounds: Environmental Risks. Florida, CRC Press, 1981: 107-140.

**Snyman C.** An introduction to immunocytochemistry. South Africa, University of Natal Press, 1993.

**Svoboda D, Grady HJ & Higginson J.** Aflatoxin $B_1$ injury in rat and monkey liver. Am. J. Pathol. 1966; 49: 1023-1029.

**Swenson DH, Miller EC & Miller JA.** Aflatoxin $B_1$-2-3-oxide: Evidence for its formation in rat liver *in vivo* and by human liver microsomes *in vitro*. Biochim. Biophys. Res. Commun. 1974; 60: 1036-1043.

**Swenson DH, Lin JK, Miller EC & Miller JA.** Aflatoxin $B_1$-2-3-oxide as a probable intermediate in the covalent binding of aflatoxin $B_1$ and $B_2$. Cancer Res. 1977; 37: 172-181.

**Theron JJ.** Acute liver injury in ducklings as a result of aflatoxin poisoning. Lab. Invest. 1965; 14: 1586-1603.

**Towbin H, Staehelin T & Gordon J.** Electrophoretic transfer of proteins from polyacrylamide gels to nitro-cellulose sheets: Procedure and some applications. Proc. Natl. Acad. Sci. USA. 1979; 76: 4350-4354.

**Trump BF, Goldblatt PJ & Stowell RE.** Nuclear and cytoplasmic changes during necrosis *in vitro* : an electron microscopic study. Am. J. Path. 1963; 43: 23-30.

**Wong ZA & Hsieh DPH.** The comparative metabolism and toxikinetics of aflatoxin $B_1$ in the monkey, rat, and mouse. Toxicol. Appl. Pharmacol. 1980; 55: 115-125.

**Wu PC, Lai CL & Liddel RH.** Quantitative morphology of mitochondria in hepatocellular carcinoma and chronic liver disease. Arch. Pathol. Lab. Med. 1984; 108: 914-916.

**Yeh FS, Yu MC, Mo CC, Luo S, Tong MJ & Henderson BE.** Hepatitis B virus, aflatoxins and hepatocellular carcinoma in southern Guangxi, China. Cancer Res. 1989; 31: 1936-1942.

# APPENDICES

## APPENDIX 1

**THE BRADFORD ASSAY :** A rapid and sensitive method for the quantitation of microgram quantities of protein utilising the principle of protein-dye binding (Bradford, 1976). Laboratory practise in protein purification often requires a rapid and sensitive method for the quantitation of protein. Several methods are available but most partially fulfil the requirement for this type of quantitation. The standard Lowry (1951) procedure is subject to interference by compounds such as potassium ions, magnesium ions, EDTA, Tris and carbohydrates (Bradford, 1976). The relatively insensitive Biuret reaction is also subject to interference by Tris, ammonia and glycerol (Bradford, 1976). The Bradford assay eliminates most of these problems, and is easily utilised for a large number of samples.

**Preparation of the Bradford reagent :** Coomassie Brilliant Blue G-250 (100mg) was slowly dissolved in 50ml 95% ethanol. To this solution 100ml 85% (w/v) phosphoric acid was added. The resulting solution was diluted to a final volume of 1 litre. Final concentrations in the reagent were 0.01% (w/v) Coomassie Brilliant Blue G-250, 4.7% (w/v) ethanol, and 85% (w/v) phosphoric acid.

**Protein Assay (Standard method) :** Six protein solutions (albumin standards) containing 0 to 100µg protein in a volume up to 100µl were pipetted into three sets of 6 x 100mm test tubes (Table $A_1$ and $A_2$). The volume in the test tube was adjusted to 100µl with the appropriate buffer (distilled water). Five millilitres of protein reagent was then added to each test tube and the contents were then mixed by inversion or vortexing. The absorbance at 595nm was then measured after 2 minutes and before 1 hour in 3ml cuvettes (using a Spectronic 3000 Array Spectrophotometer, Milton Roy, USA), against a reagent blank prepared from 0.1ml distilled water and 5ml protein reagent. he weight of protein was plotted against the corresponding absorbance resulting in a standard curve used to determine the protein in unknown samples (Figure $^1$A).

**Protein assay (unknown sample) :** Twenty microlitres of the unknown mitochondrial sample was first diluted to 1ml in distilled water (Dilution 1:50). Ten microlitres of this diluted sample was then transferred to a new, clean test tube. Five millilitres of reagent was then added and the absorbance measured as described above.

The absorbance obtained and the protein determined from the standard graph was indicative of the protein content in 10 µl of the diluted 1ml mitochondrial sample (designated B). The protein content in 20 µl of mitochondrial suspension was therefore 10 times the protein content (B) obtained above. This would indicate the protein content in 20ul of mitochondrial suspension. Hence the amount of protein per ml of mitochondria was calculated as follows :

| | | |
|---|---|---|
| **Concentration of mitochondrial protein** | **=** | **mg protein (x-axis) X 10 X 50** |
| | **=** | **mg protein/ml mitochondrial sample** |

**Table $A_1$ Preparation of a standard calibration curve**

| **Standard albumin, µl (1 mg/ml)** | 0 | 20 | 40 | 60 | 80 | 100 |
|---|---|---|---|---|---|---|
| **Distilled water, µl** | 100 | 80 | 60 | 40 | 20 | 0 |
| **Corresponding to the following mg protein per 100µl sample** | 0 | 0.02 | 0.04 | 0.06 | 0.08 | 0.1 |

**Table $A_2$ Absorbance (595 nm) of standard albumin samples**

| **STANDARD ALBUMIN (mg)** | **ABSORBANCE (595nm)** | | | |
|---|---|---|---|---|
| | **Duplicate 1** | **Duplicate 2** | **Duplicate 3** | **Mean** |
| Blank | 0.00 | 0.00 | 0.00 | 0.00 |
| 0.02 | 0.22 | 0.20 | 0.19 | 0.20 |
| 0.04 | 0.48 | 0.46 | 0.29 | 0.41 |
| 0.06 | 0.62 | 0.76 | 0.63 | 0.67 |
| 0.08 | 0.83 | 0.87 | 0.85 | 0.85 |
| 0.10 | 0.99 | 0.99 | 0.98 | 0.99 |

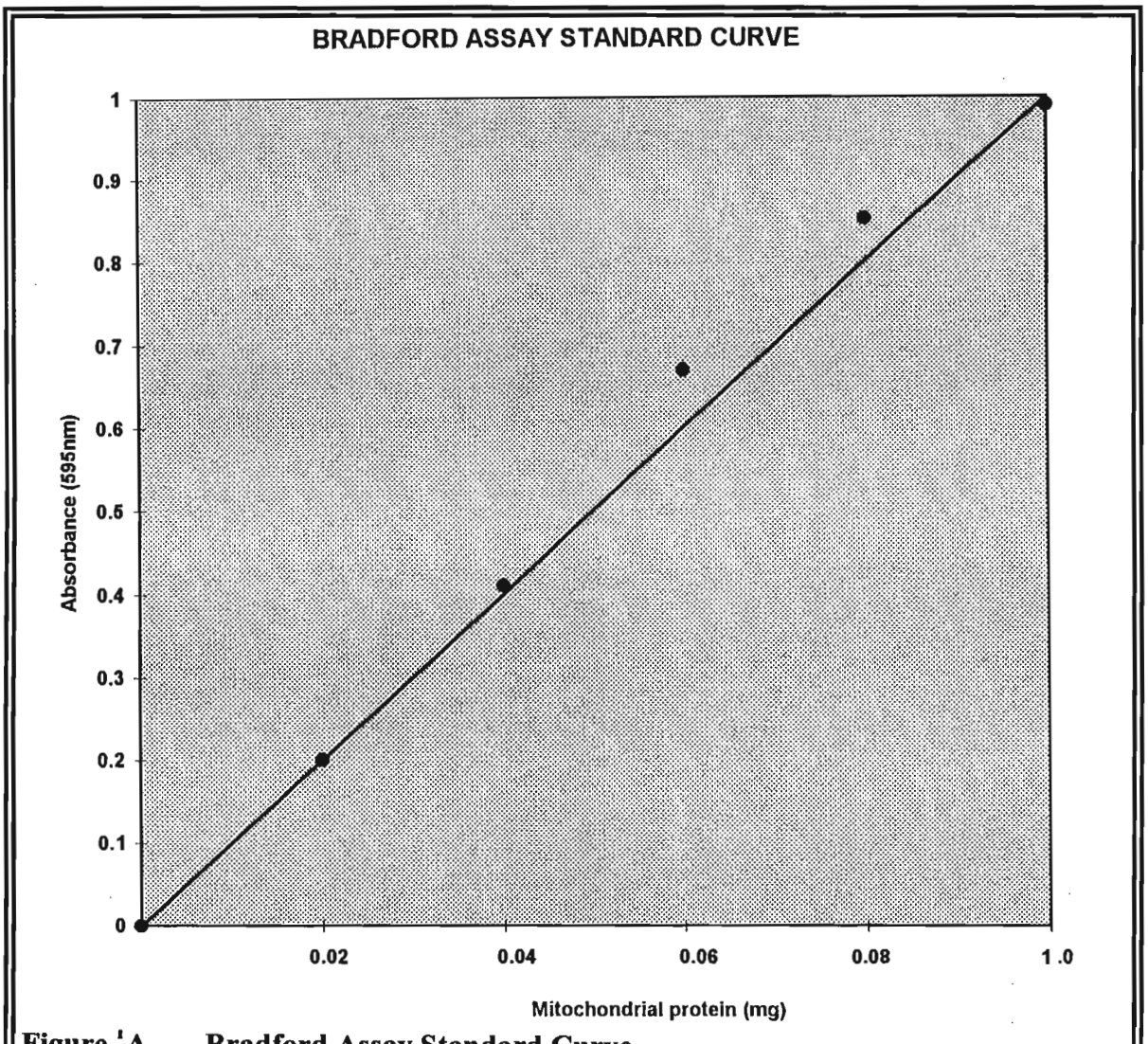


**Figure 'A. Bradford Assay Standard Curve**

## APPENDIX 2

## PAGE AND WESTERN BLOT REAGENTS

STOCK SOLUTIONS (All solution were filtered)

**1 Monomer solution (30%T; 2.7% C)**

| | | |
|---|---|---|
| *Acrylamide | 58.40 | g |
| Bis | 1.60 | g |
| $H_2O$ | 200.00 | ml |

Stored at 4° C in the dark

* **Acrylamide is neurotoxic and must be handled with extreme care.**

**2 Resolving Gel Buffer (1.5 M Tris-Cl, pH 8.8)**

| | | |
|---|---|---|
| Tris | 36.30 | g |
| $H_2O$ | 200.00 | ml |

**3 Stacking Gel Buffer (0.5 M Tris-Cl, pH 6.8)**

| | | |
|---|---|---|
| Tris | 3.00 | g |
| $H_2O$ | 50.00 | ml |

**4 10% Sodium dodecyl sulphate (SDS)**

| | | |
|---|---|---|
| SDS | 50.00 | g |
| $H_2O$ | 500.00 | ml |

**5 Initiator (10% Ammonium persulphate)**

| | | |
|---|---|---|
| Ammonium persulphate | 0.50 | g |
| $H_2O$ | 5.00 | ml |

**6 Resolving Gel Overlay (0.375M Tris-Cl, pH 8.8; 0.1% SDS)**

| | | | |
|---|---|---|---|
| Tris | 25.00 | ml | (Solution 3) |
| SDS | 4.00 | ml | (Solution 5) |
| $H_2O$ | 100.00 | ml | |

**7 2x Treatment Buffer (0.125M Tris-Cl, pH 6.8; 4% SDS; 20% glycerol; 10% 2-mercaptoethanol)**

| | | | |
|---|---|---|---|
| Tris | 2.50 | ml | (Solution 3) |
| SDS | 4.00 | ml | (Solution 5) |
| Glycerol | 2.00 | ml | |
| 2-mercaptoethanol | 1.00 | ml | |
| $H_2O$ | 10.00 | ml | |

**Divided into aliquots and frozen**

**8 Tank Buffer (0.025 M Tris, pH 8.3; 0.1% SDS; 0.192 M glycine)**

| | | | |
|---|---|---|---|
| Tris | 12.00 | g | |
| Glycine | 57.60 | g | |
| SDS | 40.00 | ml | (Solution 5) |
| $H_2O$ | 4.00 | litres | |

The pH of this solution need not be checked, hence large volumes (up to 16 litres can be made up at one time and stored in 4 litre reagent bottles until needed).

**9 Stain Stock (1% Coomassie Brilliant Blue R-250)**

| | | |
|---|---|---|
| Coomassie Blue R-250 | 2.00 | g |
| $H_2O$ | 200.00 | ml |

**10 Stain (0.125% Coomassie Blue R-250; 50% methanol; 10% acetic acid)**

| | | | |
|---|---|---|---|
| Coomassie blue R-250 | 62.50 | ml | (Solution 9) |
| Methanol | 250.00 | ml | |
| Acetic acid | 50.00 | ml | |

**11 Destaining Solution 1 (50% methanol; 10% acetic acid)**

| | | |
|---|---|---|
| Methanol | 500.00 | ml |
| Acetic acid | 100.00 | ml |
| $H_2O$ to 1 litre | | |

**12 Destaining Solution 2 (7% methanol; 5% acetic acid)**

| | | |
|---|---|---|
| Methanol | 700.00 | ml |
| Acetic acid | 500.00 | ml |
| $H_2O$ to 10 litres | | |

**13 Ponceau S Stock solution**

| | | |
|---|---|---|
| Ponceau S | 2.00 | g |
| Trichloroacetic acid | 30.00 | g |
| Sulphosalicylic acid | 30.00 | g |
| $H_2O$ to 100 ml | | |

Dilute 10 ml of stock solution with 90 ml $H_2O$ to make a working solution of Ponceau S.

**14 Diaminobenzidine (DAB)**

| | | |
|---|---|---|
| *DAB | 18.00 | mg |
| Tris-Cl (0.01M, pH 7.6) | 9.00 | ml |
| Copper chloride (0.5% $CoCl_2$) | 3.00 | ml |

The solution is then mixed by vortexing and filtered and used immediately.
***DAB is toxic and must be handled with extreme caution.**